THE INFLUENCE OF TIRE PROPERTIES ON PASSENGER VEHICLE HANDLING VOL. III - APPENDICES A THRU E

EDC Library Ref. No. 1020

DISCLAIMER

These materials are available in the public domain and are not copyrighted. Engineering Dynamics Corporation (EDC) copies and distributes these materials to provide a source of information to the accident investigation community. EDC makes no claims as to their accuracy and assume no liability for the contents or use thereof.

DOT HS-801 325

THE INFLUENCE OF TIRE PROPERTIES ON PASSENGER VEHICLE HANDLING Volume III - Appendices A-E

Contract No. DOT-HS-053-3-727
January 1975
Final Report

PREPARED FOR:
U.S. DEPARTMENT OF TRANSPORTATION
NATIONAL HIGHWAY TRAFFIC SAFETY ADMINISTRATION
WASHINGTON, D.C. 20590

TECHNICAL REPORT STANDARD TITLE PAGE

1. Report No.	2. Government Accession No.	3. Recipient's Catalog No.
DOT HS-801 325		

4. Title and Subtitle	5. Report Date
The Influence of Tire Properties on Passenger Vehicle Handling Volume III - Appendices A-E	January 1975
	6. Performing Organization Code
7. Author(s)	8. Performing Organization Report No.
D. J. Schuring, D. T. Kunkel, D. E. Massing, R. D. Roland	ZM-5350-K-3
9. Performing Organization Name and Address	10. Work Unit No.
Calspan Corporation	11. Contract or Grant No. DOT-HS-053-3-727
12. Sponsoring Agency Name and Address	13. Type of Report and Period Covered
National Highway Traffic Safety Administration U. S. Department of Transportation Washington, D. C. 20590	Final Report 30 June 1973 - 30 June 1974
	14. Sponsoring Agency Code

15. Supplementary Notes

16. Abstract

The overall objectives of this research program were to identify the properties of tires that affect vehicle dynamic response and to describe those effects in quantitative terms and to evaluate the degree to which the various tire parameters affect vehicle dynamic response, and to assess their relative importance.

This volume contains several appendices which include: (A) a literature review and annotated bibliography of publications related to tire construction properties and performance parameters, (B) a discussion of the development of mathematical functions of aligning torque and overturning moment and the development of automatic computation techniques for obtaining simulation tire model coefficients from measured tire data, (C) a discussion of the vehicle test procedures employed in the study modifications of these procedures for testing in the wet, and the automatic computation techniques used to process the vehicle test data, (D) complete simulation data sets for the four test vehicles used in this study, (E) a discussion of a preliminary test program to evaluate the performance of a three component vehicle wheel force sensor.

17. Key Words	18. Distribution Statement
Tire properties, tire parameters, tire modeling, vehicle test procedures, vehicle characteristics, wheel force measurement	

19. Security Classif. (of this report)	20. Security Classif. (of this page)	21. No. of Pages	22. Price
Unlimited	Unlimited	148	

Form DOT F 1700.7 (8-69)

FOREWORD

The work reported herein was performed by Calspan Corporation for the National Highway Traffic Safety Administration (NHTSA) under Contract No. DOT-HS-053-3-727 during the period 30 June 1973 to 30 June 1974. The NHTSA contract technical manager was Mr. Edward Kakaley of the Office of Operating Systems Research. The project engineer was Mr. R. Douglas Roland of the Transportation Safety Department of Calspan.

The complete project is reported in the following separate volumes:

Volume I	-	Summary Report
Volume II	-	Technical Report
Volumes III and IV	-	Appendices
Volume V	-	Measured Tire Performance Data

This is Volume III which contains five appendices authored by various members of the project staff.

TABLE OF CONTENTS

		Page
FOREWORD		iv
INTRODUCTION		vi
APPENDIX A:	LITERATURE SURVEY AND ANNOTATED BIBLIOGRAPHY	A-1
B:	TIRE MODELING AND TIRE DATA REDUCTION TECHNIQUES	B-1
C:	VEHICLE TEST PROCEDURES AND DATA REDUCTION TECHNIQUES	C-1
D:	MEASURED VEHICLE CHARACTERISTICS	D-1
E:	MEASUREMENT OF VEHICLE WHEEL FORCES	E-1

INTRODUCTION

The overall objectives of this research program were to identify the properties of tires that affect vehicle dynamic response and to describe those effects in quantitative terms and to evaluate the degree to which the various tire parameters affect vehicle dynamic response, and to assess their relative importance.

This volume contains five appendices primarily devoted to discussions of interesting or significant developments or techniques that were employed during the study.

Appendix A is a thorough review of over 80 publications which were selected from about 120 pertinent reports and papers related to tire construction properties and performance parameters. Appendix B discusses the development of mathematical functions of aligning torque and overturning moment and the development of automatic computation techniques for obtaining simulation tire model coefficients from measured tire data. Appendix C discusses the vehicle test procedures, modifications of these procedures for testing in the wet, and the automatic computation techniques used to process the vehicle test data. Appendix D contains complete simulation data sets for the four test vehicles used in this study. Two sets of inertia parameters are given for each vehicle corresponding to the automatic controller and driver controlled configurations. Appendix E discusses a preliminary test program to evaluate the performance of a three component vehicle wheel force sensor.

APPENDIX A

LITERATURE SURVEY AND ANNOTATED BIBLIOGRAPHY

by

D. J. Schuring

INTRODUCTION AND SUMMARY

In order to facilitate the selection of important tire properties and parameters for this program, a literature search was undertaken with the objective of (1) identifying significant relations between tire construction and performance data, and (2) isolating construction-performance relations that are not covered in the open literature and therefore need experimental attention.

From about 120 pertinent references, 75 were reviewed in detail and then grouped into seven subject areas:

- General information on construction-performance relations
- Effect of tire construction type on performance
- Effect of tread geometry on performance
- Effect of tread compound on performance
- Effect of road wheel dimensions on performance
- Effect of aspect ratio on performance
- Effect of cord material on performance

The selected references are arranged in alphabetical order according to the first author's name; pertinent subject areas are noted as keywords.

The literature search revealed that the effects on tire performance of tire construction type, tread geometry, and tread compound are well investigated although certain questions remained unanswered (for instance,

the effect of tread geometry on dry braking traction). The effects of road wheel dimensions, aspect ratio, and cord material were less well covered. The scarcity of studies in these fields was unexpected.

The major findings in each of the subject areas, as they pertain to the selection of tires for the contemplated test program, are summarized under the respective subject headings, together with tentative conclusions. Briefly, the performances of cross-ply, bias-belted, and radial-ply tires are sufficiently different to consider the construction type a principal parameter of the test program. The same is true for tread geometry although its influence on performance is less pronounced on dry surfaces than it is on wet surfaces. The effect of tread compound appears not to surpass $\pm$ 10% (in general). The effects of road wheel dimensions, aspect ratio and cord material are uncertain, as already pointed out.

Effect of Tire Construction Type

The performance differences of cross-ply (also called: cross-bias, bias-ply, crossed-ply, bias), bias-belted (belted-bias, belted-bias-ply), and radial-ply (belted-radial, radial-belted, radial) tires are rather well investigated and documented. Of the many data presented in the referenced literature, we will point out only those that have a significant bearing upon the proposed experimental program.

Thieme and Pacejka (1971) presented spring rate data on non-rolling cross-ply and radial-ply tires. The spring rates presented in Table 1 were considered important for the study of tire response to road disturbances and other transient inputs. In all cases, the radial-ply tire showed markedly lower stiffnesses than the cross-ply tire.

Elliot, Klamp, and Kraemer (1971) determined the rolling resistance of eighty tires. Their findings are presented in Figure 1. At speeds up to 60 mph, cross-ply tires develop a 37% higher rolling resistance than radial-ply tires. The resistance of bias-belted tires is 24% higher. At speeds beyond 90 mph, cross-over occurs, and the radial-ply tire shows a higher rolling resistance than the two other types.

Differences in braking traction due to tire construction are insignificant. Figure 2 shows peak and slide braking coefficients for radial-ply and cross-ply tires, both equipped with winter tread pattern (Figure 2a) or sipes (Figure 2b) and operating on wet, fine cold asphalt. The results are almost identical for both tire types. These findings are corroborated by Kelley (1968), who measured stopping traction of cross-ply and radial-ply tires on two wet surfaces, one with very low coefficient of friction ($\mu = 0.1$) and one with high coefficient ($\mu = 0.7$). On both surfaces, both tire types produced approximately the same stopping distance. Similar results were arrived at by Meades (1967).

The difference in cornering, camber, and aligning torque coefficients due to differences in tire construction data are generally significantly large. Peterson and Rasmussen (1973) published a table (Table 2) with pertinent data for bias-belted and radial-ply tires. In the average, radial-ply tires had a 20% higher cornering coefficient than bias-belted tires; their camber coefficient, however, was 60% smaller, and

Spring Rate	Cross-Ply	Radial-Ply	
Tangential (longitudinal)	12400	7500	kgf/rad
Lateral	11.4	8.4	kgf/mm
Torsional	250	190	m kgf/rad
Vertical	20	17	kgf/mm

TABLE 1

Spring Rates of Non-Rolling Cross-Ply and Radial-Ply Tires

(At Small Deflections)

Tires: Cross-Ply 175 S14, 22 psi
Radial-Ply 175 SR14, 27 psi

Vertical Load: 335 kgf

Extracted from Thieme and Pacejka (1971)

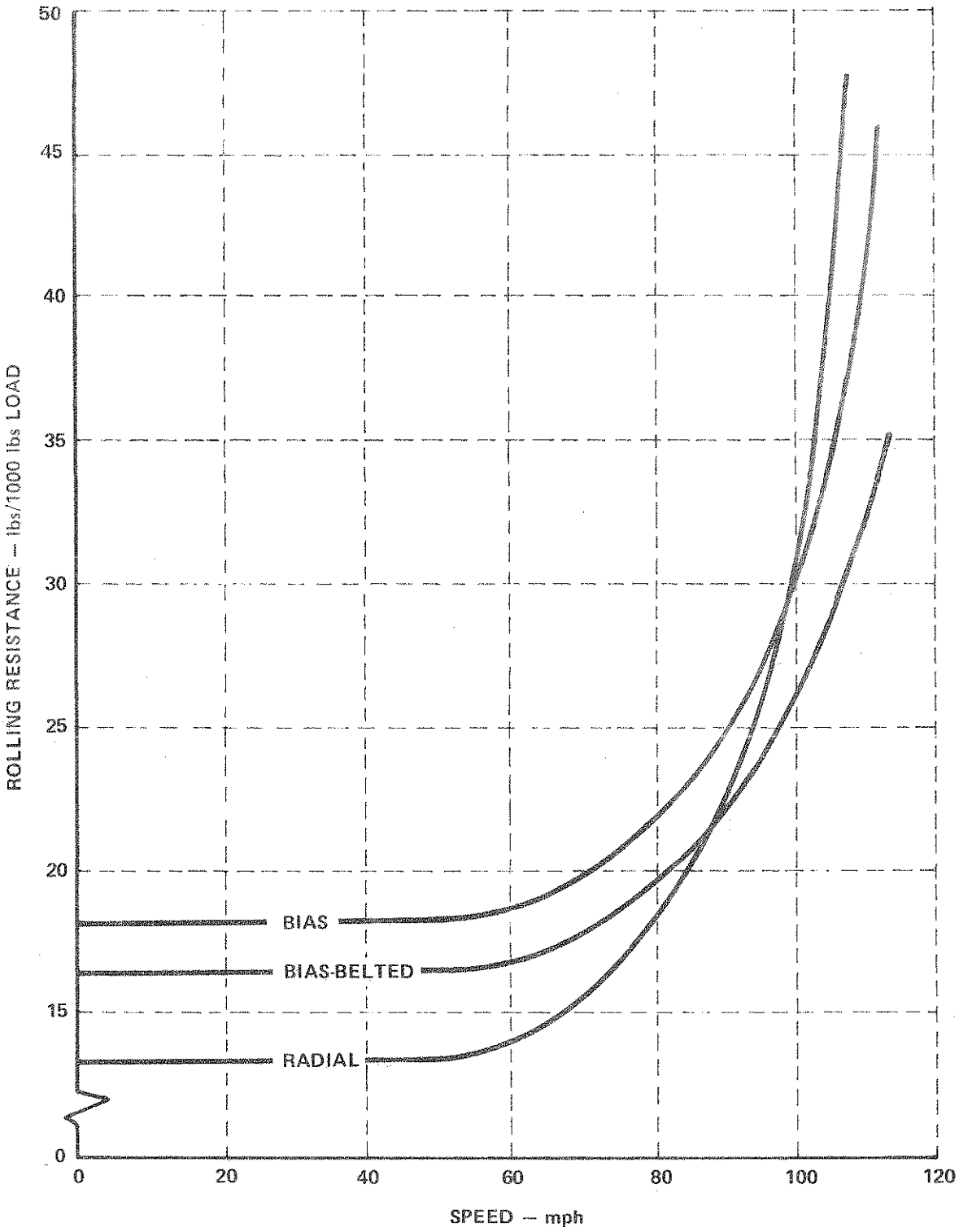

Figure 1 AVERAGE ROLLING RESISTANCE OF BIAS, BIAS-BELTED, AND RADIAL TIRES, AS FUNCTION OF SPEED

From Elliot, Klamp, and Kraemer (1971)

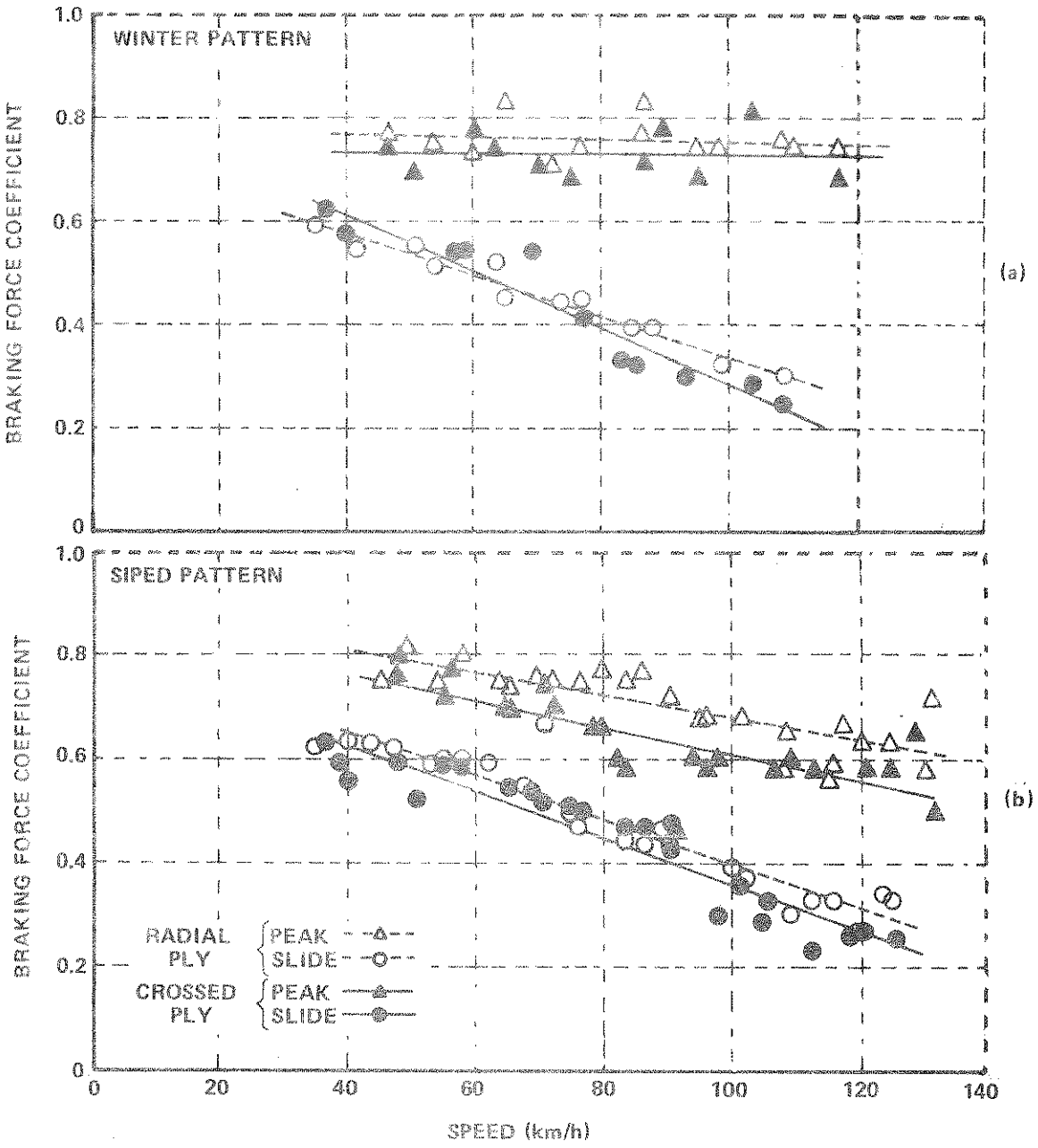

From Meades (1969)

Figure 2 PEAK AND SLIDE (LOCKED) BRAKING COEFFICIENT (AS FUNCTION OF SPEED) OF RADIAL-PLY AND CROSS-PLY TIRES, ON FINE COLD ASPHALT, WET CROSS-PLY — 5.90-14
RADIAL-PLY — 165-14

	Cornering Coefficient		Camber Coefficient		Aligning Torque Coefficient	
	Mean	Standard Deviation	Mean	Standard Deviation	Mean	Standard Deviation
Bias-belted (N = 9)	0.129	0.014	0.021	0.004	0.031	0.003
Radial (N = 12)	0.156	0.019	0.008	0.001	0.025	0.001

TABLE 2

Typical Force and Moment Coefficients
of Bias-Belted and Radial-Ply Tires

From Peterson and Rasmussen (1973)

their aligning torque coefficient 20% smaller than the respective coefficients of the bias-belted tires. A comparison of cornering and camber coefficients of cross-ply and radial-ply tires is presented in Figure 3. Compared with data given in Table 2, Figure 3 suggests that camber and cornering stiffnesses of bias-belted and cross-ply tires do not differ very much. This conclusion may not be justified, however, since the camber coefficient of cross-ply tires is usually higher than the value (of 0.015) specified in Figure 3. For instance, Nordeen and Cortese (1963) quoted a typical camber coefficient range of 0.20 to 0.30. With this range, the camber coefficient of bias-belted tires would be generally lower than that of cross-ply tires.

Tentative Conclusions

Radial-ply tires show markedly lower spring rates in all directions (vertical, lateral, longitudinal, torsional) than cross-ply tires. At speeds below 60 mph, radial-ply tires and, to a lesser degree, bias-belted tires develop distinctively lower rolling resistances than cross-ply tires. Differences in braking traction of all three construction types are insignificant. Cornering, camber, and aligning torque coefficients of bias-belted and radial-ply tires are significantly different (particularly in camber). The cornering coefficient of cross-ply tires is somewhat close to that of bias-belted tires; the camber coefficient of cross-ply tires seems generally to be higher than those of the two other tire types.

Effect of Tread Geometry

The effect of tread design on tire performance is most pronounced on wet roads. Here, tire grooves and sipes absorb and channel the water away from the road surface and thus facilitate the desired dry contact between tire and roadway. The draining effect is not only dependent upon

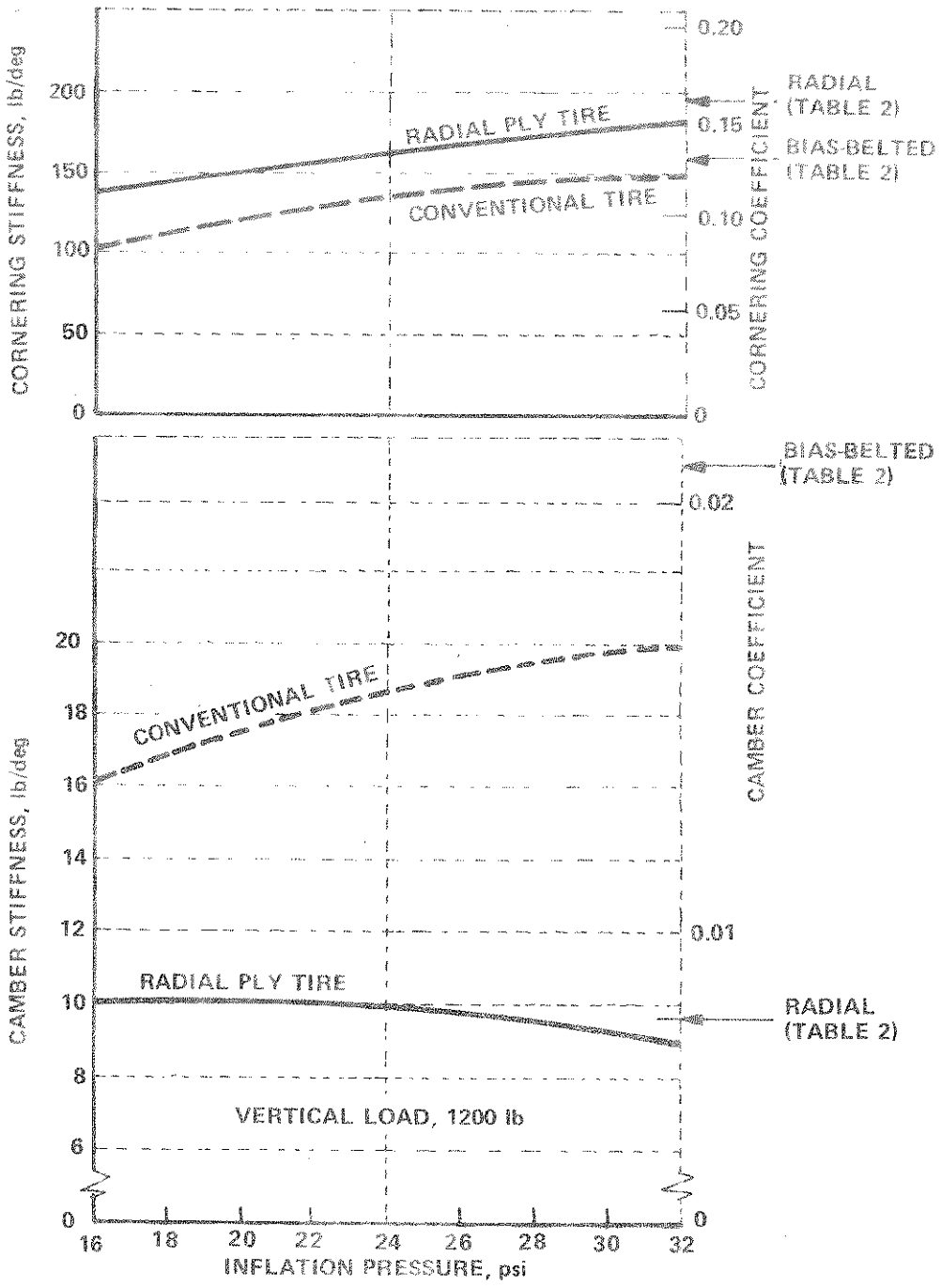

Figure 3 CORNERING AND CAMBER COEFFICIENT OF RADIAL-PLY AND CROSS-PLY ("CONVENTIONAL") TIRES
TIRE SIZE — 6.50 - 13 OR EQUIVALENT

From Bidwell (1965)

the tread pattern but also on the water depth and the road texture. On rough surfaces, the draining effect of the tread is less important than on smooth surfaces because the road asperities of a rough surface are likely to penetrate the water film and contact the tire surface directly; on smooth surfaces, all water must be removed through groove action. Figure 4 shows the tread effect on a smooth and a rough (wet) surface. On the smooth road surface, the patterned tire developed much higher friction forces than the smooth tire (especially at higher speeds); on the rough road surface, both tires develop almost identical forces.

Figure 5 depicts the maximum lateral coefficient of friction (F_{ymax}/F_z) of six commercial 5.60-15 tires with various tread patterns operated on a smooth wet surface. At low speed (20 mph), the coefficients vary within $\pm$ 13% of the mean, at high speed (75 mph), within + 60% -- a very large range indicating the large influence of the tread pattern on wet traction performance. The influence of tread pattern on tire performance is not only important for wet smooth surfaces but for dry surfaces as well. Table 3 lists performance characteristics of three tires of the same built with different tread patterns. All data were measured on a dry surface (flat-bed tester). It was found that the different tread patterns had very little influence on the vertical and lateral spring rates, K_z and K_y. Equally little affected was the cornering stiffness, C_α. The cambering stiffness, C_γ, and the longitudinal stiffness, C_s, however, were substantially influenced by the tread pattern. The open tread, and also the tread with six grooves, generated considerably less camber stiffness than the less compliant tread with only four grooves. Unfortunately, the influence of tread pattern on dry braking traction was not measured (the equipment was restricted to only 4% longitudinal slip).

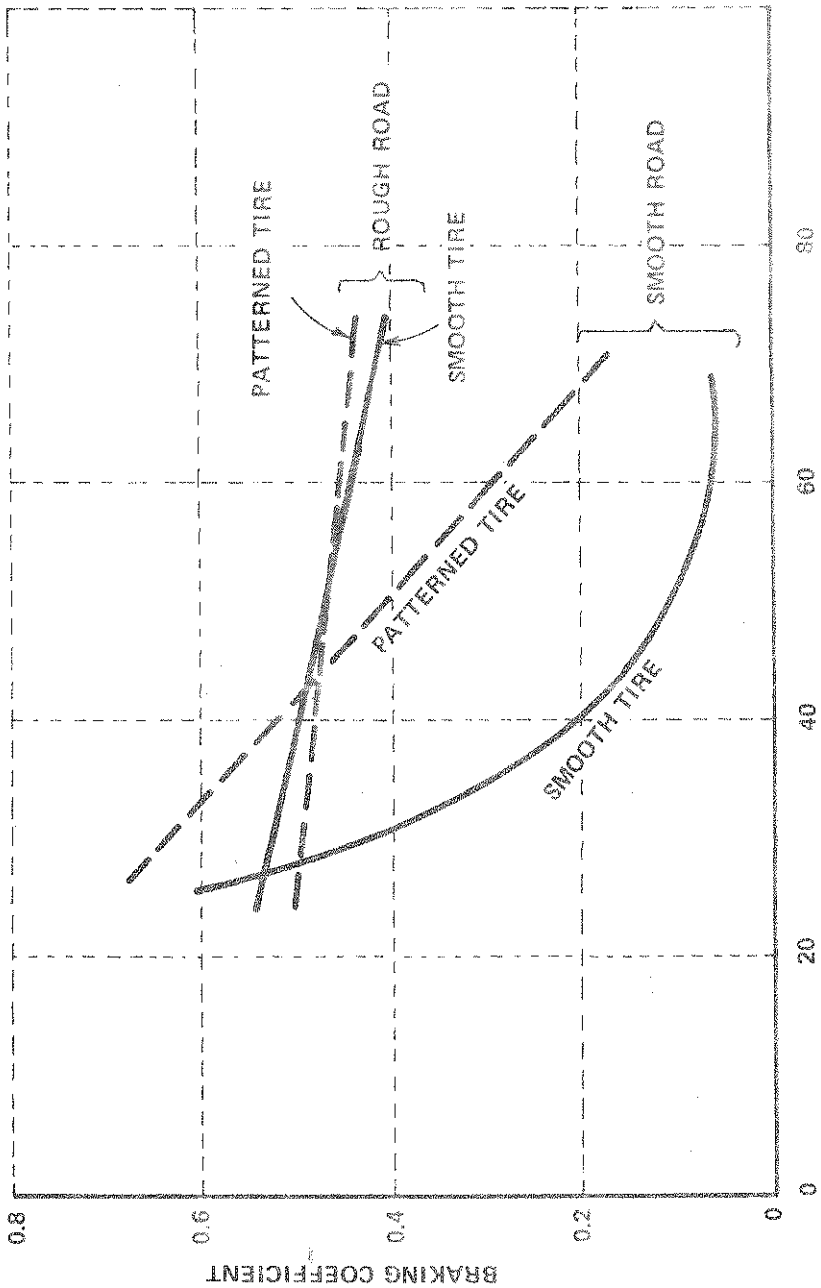

Figure 4 TREAD PATTERN EFFECT ON SMOOTH AND ROUGH SURFACES (WET)

From Sabey, Williams, and Lupton (1970)

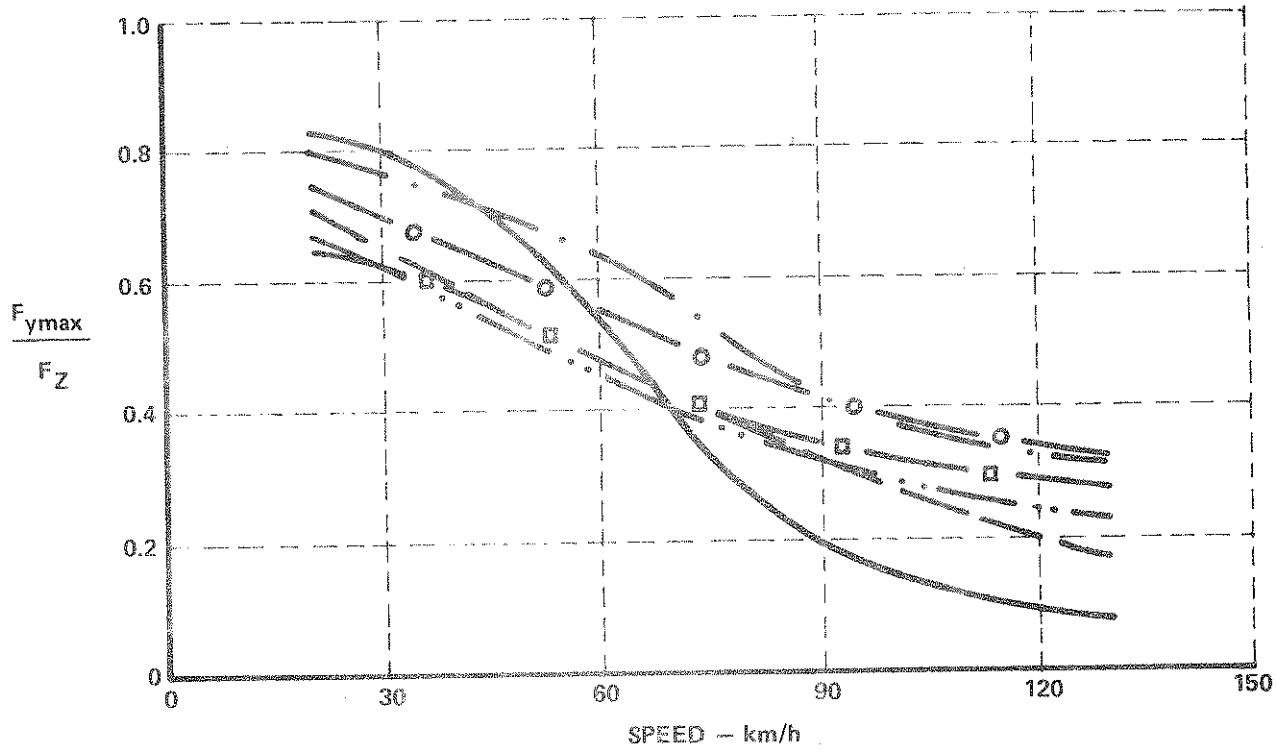

Figure 5 MAXIMUM LATERAL FRICTION COEFFICIENT (AS A FUNCTION OF SPEED) OF SIX COMMERCIAL 5.60 - 15 BIAS-PLY TIRES WITH VARIOUS TREAD PATTERNS

FULL TREAD DEPTH
VERTICAL LOAD — 660 lbs
PRESSURE — 22 psi
WATER DEPTH — 0.04 INCHES
SURFACE — SMOOTH, WET

From Gengenbach and Weber (1970)

		6 grooves	4 grooves	Open Tread (lugs)	
Circumferential Stiffness	$C_s = dF_x/ds \mid_{s=0}$	46000	42000	28000	lb/unit slip
Cornering Stiffness	$C_\alpha = dF_y/d\alpha \mid_{\alpha=0}$	508	523	516	lb/deg
Camber Stiffness	$C_\gamma = dF_y/d\gamma \mid_{\gamma=0}$	57	69	40	lb/deg
Lateral Spring Rate	Ky	1477	1618	1291	lb/in
Vertical Spring Rate	Kz	5032	4700	4500	lb/in

TABLE 3

Measured Performance Data of 10.00 -20F

Nylon Truck Tire in Three Tread Patterns

Surface - dry (Flat bed tests)

From Tielking, Fancher, and Wild (1973)

A general investigation of groove patterns and their influence on stopping and cornering traction was performed by Kelley (1968). He varied the amplitude (called point height) and wavelength (called pitch) of the zigzag grooves of a tire with four grooves and found that on a smooth roadway (μ = 0.1), the maximum deviations from the mean value due to variations of point height and pitch were $\pm$ 20% in stopping traction, and $\pm$ 2% in cornering traction. On a rough roadway (μ = 0.7), the variations in stopping distance did not exceed $\pm$ 3%.

In the same study, the influence of the tread radius on wet traction was investigated. Within the range of radii tested (from 8 to 12 inches), no difference in braking traction could be found. For cornering traction, the tire with 12 inch radius performed slightly better than the tires with smaller tread radius. The effect of tread width on stopping traction and cornering traction are small on a rough wet surface, according to Kelley. On a smooth wet surface, there appears to be an optimum tread or shoulder width (that is, if the same number of grooves is employed); a tire with a tread width between 5.00 and 5.40 inches exhibited a 15 to 30% better stopping traction than tires (of the same size, tread pattern, and number of grooves) with smaller or larger tread width. The respective differences in cornering traction were negligibly small, though.

Kelley also investigated the influence of radial slots applied at the tire shoulders. He found that on smooth wet surfaces, radial shoulder slots improved braking traction by 25% but added very little to wet cornering traction. On rough surfaces, shoulder radial slots produced no improvement of traction.

Allbert and Walker (1965-66) investigated the influence of the number of tread ribs on peak and slide braking coefficients and discovered

that seven ribs yielded more traction than six or five ribs, Figure 6. Maycock (1967) on the other hand, could not discern significant differences in braking performances on smooth wet surfaces although he changed the number of ribs systematically from five to thirteen, Figure 7. Kelley (1968), by contrast, reported that on a very smooth surface ($\mu = 0.1$), the braking performance of an eight-ribbed tire was more than 55% better than that of a four-ribbed tire. On a rough surface, however, he detected no significant influence of the rib number. Similarly, for cornering traction on a smooth wet surface, the effect of the number of ribs was negligible, too: a four-ribbed tire gave only 5% better cornering traction than an eight-ribbed tire.

The influence of groove width on tire traction has been established by many researchers. We quote here only the results published by Maycock (1967), Figure 8. On polished wet concrete, the peak brake coefficient increases rapidly at low groove widths, to stay almost constant at widths beyond 0.2 inches. Kelley points out, however, that on rough wet surfaces the effect of groove width on traction is much smaller, as expected.

The effect of groove depth on wet and dry traction has been carefully measured by Staughton (1970) and many other researchers. According to Staughton (Figure 9) the influence of groove depth is small on wet smooth concrete at lower speeds (up to approximately 50 mph) if less than 50% of tread depth are worn off; at higher speeds and with little groove depth left ($<$ 2mm), the loss of traction is considerable. On dry surfaces, tire stiffness (C_α , C_γ , C_s) usually goes up with decreasing groove depth. Table 4 shows that up to the half-worn state, the investigated tire increases in circumferential stiffness by 24%, in cornering stiffness by 32%, and in camber stiffness by 51%. These high

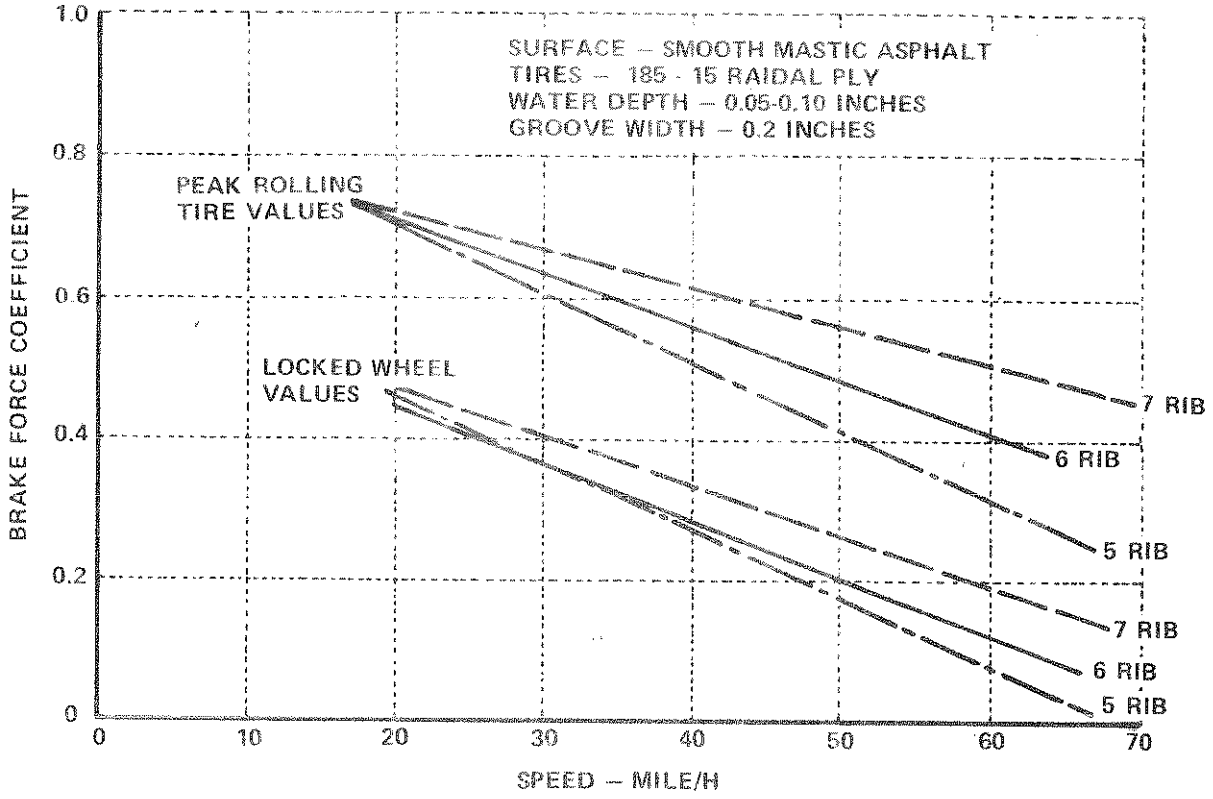

Figure 6 RESULTS OF BRAKING TESTS ON TIRES WITH FOUR, FIVE AND SIX EQUAL WIDTH CIRCUMFERENTIAL GROOVES

From Allbert and Walker (1965-66)

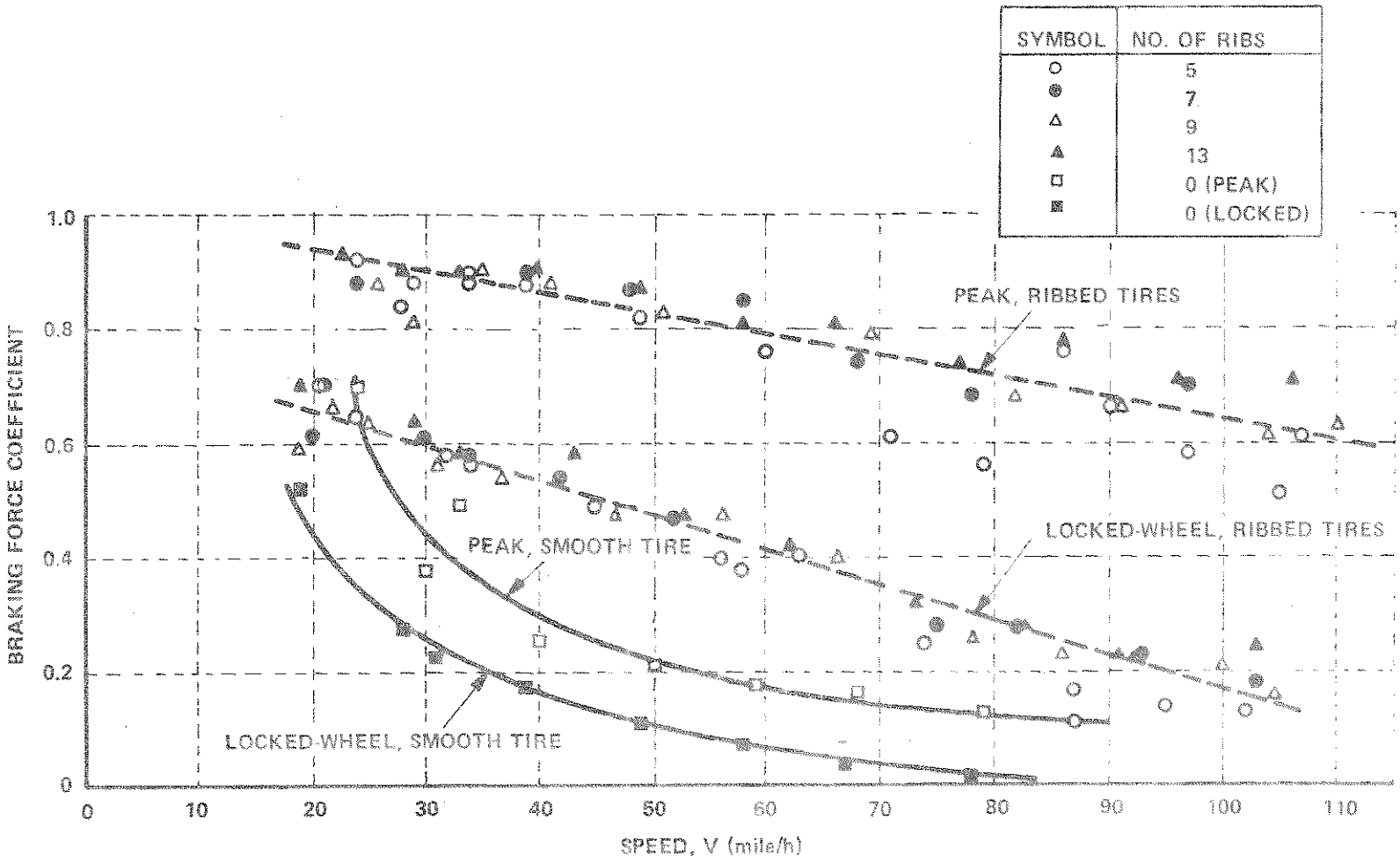

Figure 7 PEAK AND LOCKED-WHEEL BRAKING FORCE COEFFICIENT (AS FUNCTION OF SPEED) OF 185--15 RADIAL PLY TIRES WITH STRAIGHT RIBS: SURFACE -- POLISHED CONCRETE, WET

From Maycock (1967)

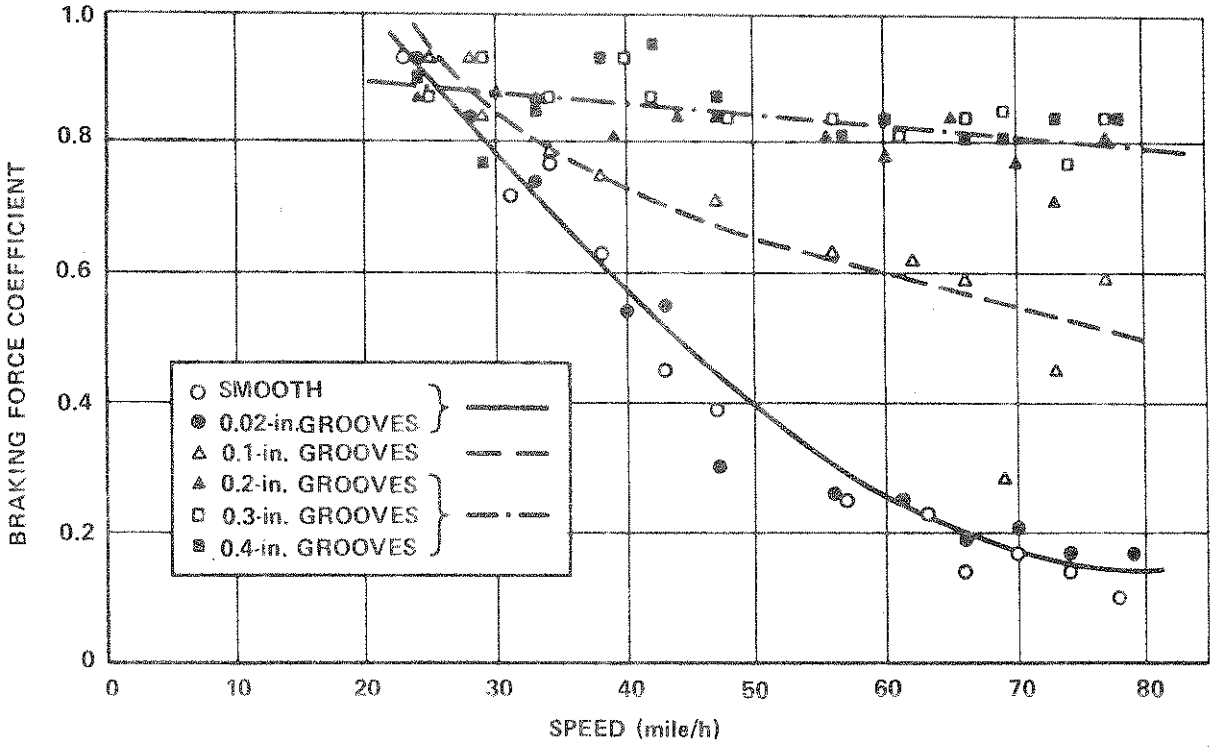

Figure 8 PEAK BRAKING FORCE COEFFICIENT (AS FUNCTION OF SPEED) OF 185–15 RADIAL PLY TIRES WITH FIVE STRAIGHT GROOVES OF VARIOUS WIDTHS
SURFACE – POLISHED CONCRETE, WET
RIB WIDTH – 0.5 INCHES

From Maycock (1967)

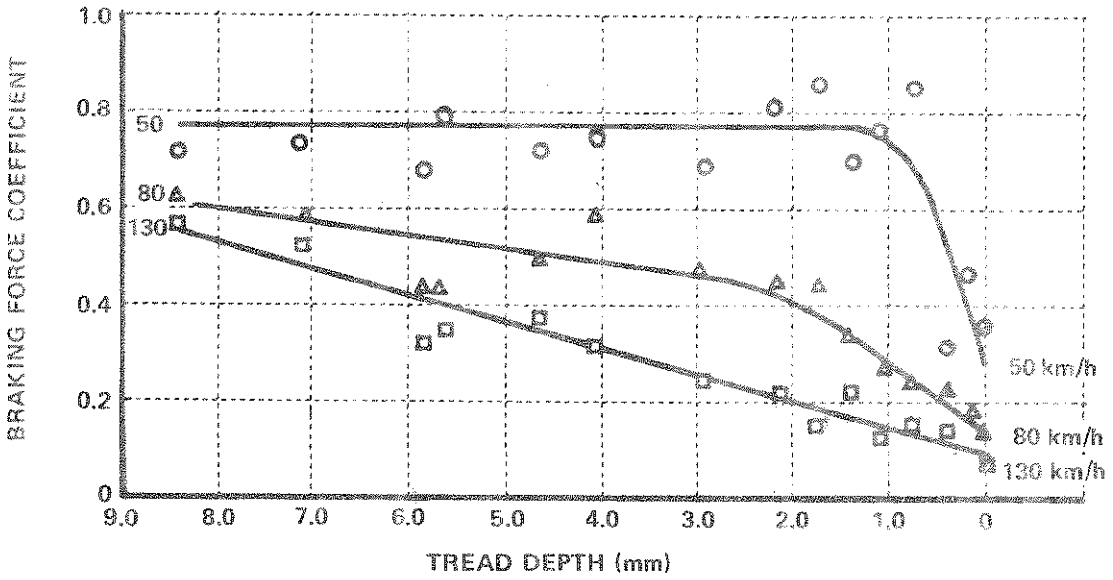

Figure 9 PEAK BRAKING COEFFICIENT AS FUNCTION OF TREAD DEPTH (AT VARIOUS SPEEDS)
SURFACE — SMOOTH CONCRETE, WET
TIRE — 5.60—13 CROSS PLY

From Staughton (1970)

	New	Half Worn	Fully Worn	
C_s	42000	52000 (+24%)	60000	lb/unit slip
C_α	523	690 (+32%)	771	lb/deg
C_γ	69	104 (+51%)	148	lb/deg
K_y	1618	1784 (+10%)	1886	lb/in
K_z	4700	3939 (- 16%)	4600	lb/in

TABLE 4

Measured Performance Data of 10.00 -20 1F Nylon Truck Tire in Three States of Wear. (For Explanation of C_s, C_α, etc., see Table 3.)

Surface - dry (Flat bed tests)

From Tielking, Fancher, and Wild (1973)

percentages indicate that even small reductions in tread depth may alter tire characteristics significantly.

Recently, investigations into the influence of tread depth were published by Dijks (1973, 1974), who measured braking and side force coefficients of various tires operated on wet surfaces at various speeds. Figure 10 summarizes his findings; they show that tread depth has an important influence on braking and cornering performance on smooth surfaces and at high speeds. At low speeds (smaller than 30 mph), the influence of tread depth is small. Note that on a rough surface, the worn tire yields better cornering performance than the new tire, even at higher speeds.

The influence of sipes (narrow slots, knive cuts, traction blades) on tire traction on wet surfaces is not firmly established. In a careful investigation, Neill (1971) found no improvement in traction due to sipes. On the other hand, Kelley (1968) showed an improvement of more than 200% in stopping distance of siped versus not-siped tires, Figure 11. This high figure applies to a wet surface with very low friction ($\mu = 0.1$); for a surface with $\mu = 0.7$, no improvement was discernible. Hence, sipes are perhaps important only on very slippery surfaces.

Conclusions

Generally, the effect of the tread pattern (number and shape of grooves, number of sipes, etc.) on tire performance is most pronounced on wet smooth roads at speeds larger than about 30 mph. At high speeds (> 70 mph), variations of maximum lateral force due to different commercial tread pattern may be very large. The influence of the number of tread ribs beyond four or five may be insignificant for medium and high friction surfaces although on very smooth wet surfaces more ribs (say eight instead of four) seem to improve braking traction significantly. The same observation seems to apply to the groove width. Beyond a width of 0.2 inches, no significant traction improvement could be established.

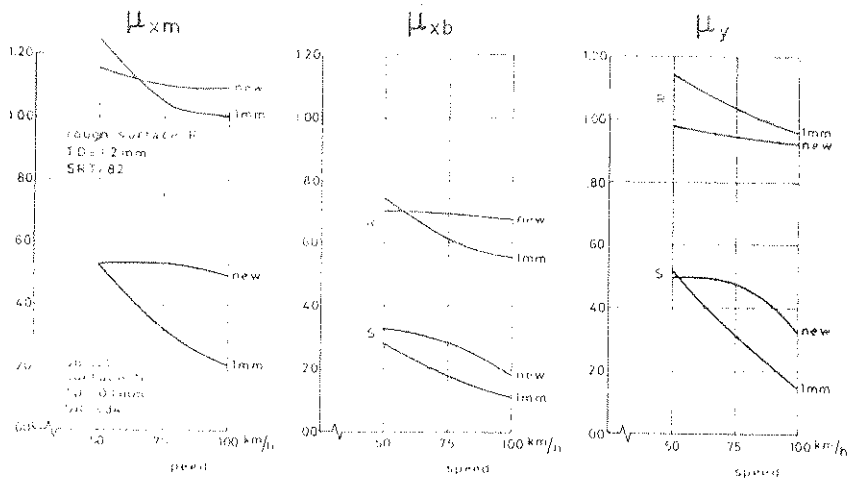

Figure 10 Influence of Tread Depth on Braking and Cornering Performance at Various Speeds

μ_{xm}	peak braking coefficient
μ_{xb}	locked-wheel braking coefficient
μ_y	cornering coefficient averaged over interval from 8 deg to 15 deg
TD	average texture depth of roadway
SRT	microroughness as measured with British Skid Resistance Tester

Water depth 7 ... 15 mil

Tire 165 SR 13

From Dijks (1974)

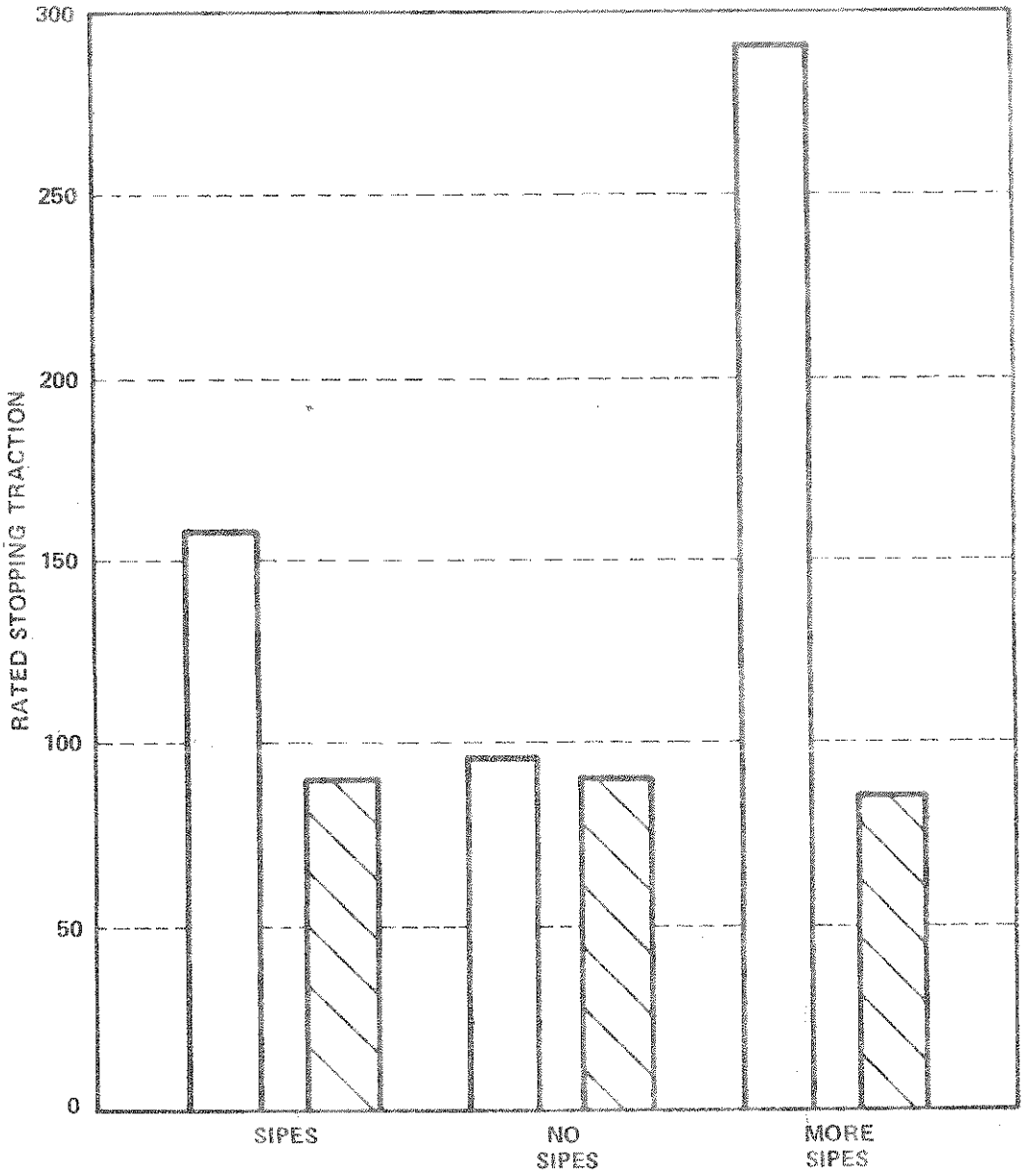

Figure 11 THE INFLUENCE OF SIPES ON STOPPING TRACTION
SMOOTH WET SURFACE, μ = 0.1
ROUGH WET SURFACE, μ = 0.7

From Kelley (1968)

Sipes appear to add significantly to wet traction on very smooth surfaces. On rough surfaces, their influence is small.

The effect of groove depth on wet traction is small if less than 50% are worn off. However, on dry surfaces, circumferential, cornering, and camber stiffness appears to increase significantly with wear. Also, on dry surface, the tread pattern (for instance, the number of ribs) influences the tire stiffness, notably the cambering and longitudinal stiffness. The cornering stiffness seems to be less affected.

The influence of tread radius on wet traction appears to be negligibly small, and so does the influence of tread width if the surface is rough. On very smooth surfaces, however, tread width affects braking traction notably.

Effect of Tread Compound

The two most common tread rubbers are natural rubber (NR) and styrene-butadiene rubber (SBR). Passenger car tires are usually made from SBR, often blended with butadiene rubber (BR) and nearly always extended with a heavy oil. However, new synthetic rubbers such as butyl and polybutadiene (PBD) are gaining importance, too. A survey of available literature indicates a traction variation of $\approx \pm$ 12% due to different tread compounds. Figure 12 shows, for a wetted public highway, the peak and slide braking coefficients of an NR treaded and an SBR treaded tire (as a function of speed). Except for the tread compound, both tires were identical. The peak braking coefficient deviated by approximately $\pm$ 12% from the average value; the sliding coefficient, by approximately $\pm$ 8%. These ranges give an indication of the maximum influence of tread compound on traction performance to be expected of most commercially available tires.

Most passenger car tires are treaded with synthetic rubber. Here, the range of traction performance is indicated in Table 5 which

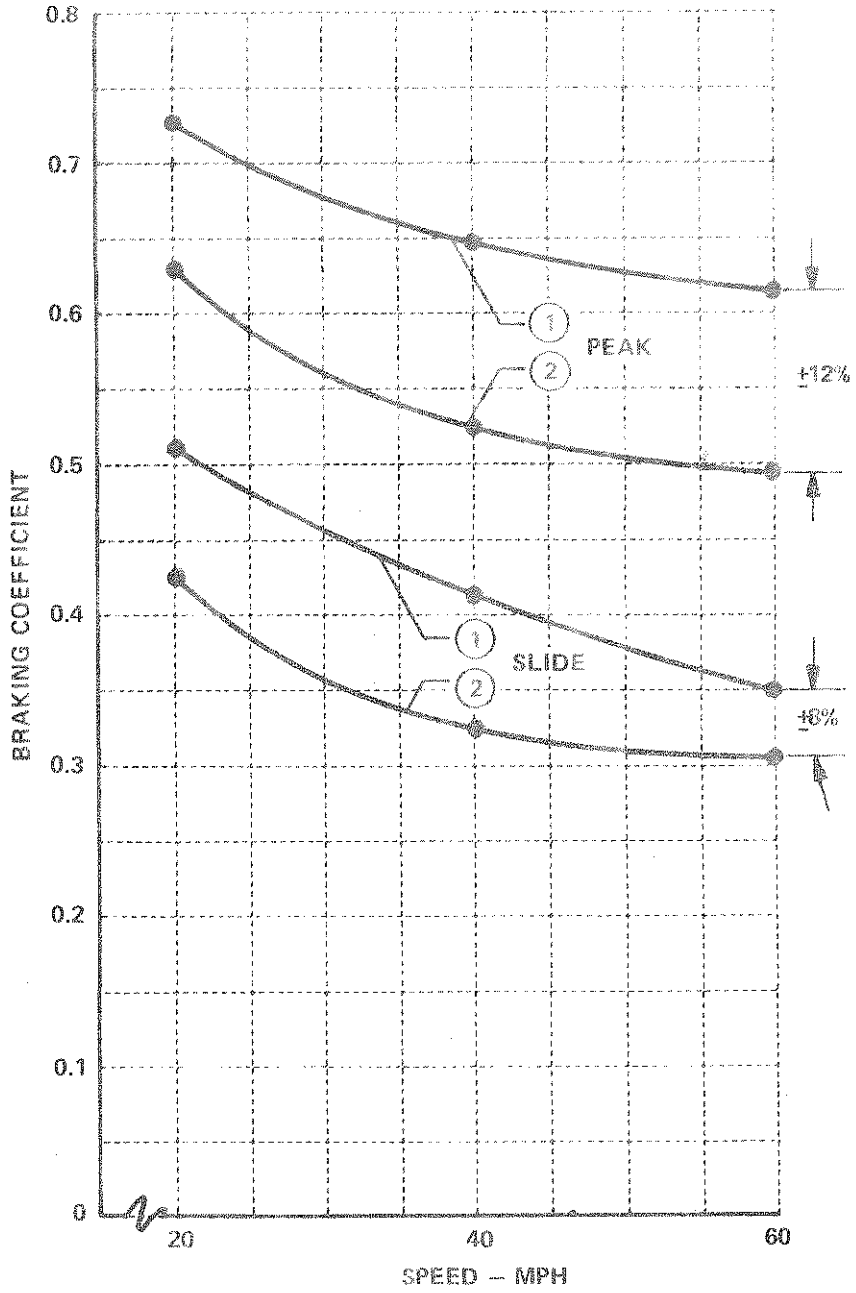

Figure 12 PEAK AND SLIDE BRAKING COEFFICIENTS OF IDENTICAL (SIPED) TIRES WITH

(1) SBR TREAD

(2) NR TREAD

ON PUBLIC HIGHWAY, WET

From Smithon and Herzegh (1971)

Tread Compound	Maximum Cornering Speed (mph)		Safe Panic Braking Speed Limit After 100 Ft. Penetration of Curve (mph)	
	Dry	Wet	Dry	Wet
Butyl	87	68	51	46
SBR	77	63	45	40

TABLE 5

Cornering Performance Tests

(With Unidentified Tires)

Test Conditions: Chevrolet (loaded wt. 4180 lb.).
Moderately coarse asphalt (μ = 0.7),
18 ft. roadway with 229 ft. outside radius.

From Umland, Bannister, and Tomlinson (1963)

presents cornering performance data of various tires treaded with butyl rubber and SBR rubber. On a dry road (typical highway), the maximum cornering speeds (before loss of traction) differed by approximately ± 6% from the average speed (all data pooled); on a wet road, by 4% to 7%. Since the cornering force increases with the square of speed, the corresponding percentages for cornering forces are ± 12% for the dry road, and between ± 8% to 14% for the wet road. However, the actual ranges may be smaller, for part of the measured differences must be assigned to variations in tire tread, tire construction, temperature, etc., all not specified in the paper.

The Highway Safety Research Institute (HSRI) of the University of Michigan and B. F. Goodrich performed a correlation program on cornering wet traction (Veith, 1972) using G78-15 tires provided with experimental tread compounds (characterized as low, medium, and high traction compounds). Figure 13 shows the lateral force coefficient for a slip angle of 12 degrees and for two surfaces, a low friction terrazo ground and a medium friction asphalt surface. The differences in cornering traction between the low and the high traction compounds are substantial - ± 23% for the smooth surface, ± 32% for the medium rough surface. These are rather extreme values; regular commercial tread compounds show much less variation in traction. The data indicate, however, that on wet rough surfaces a wider spread of traction data is to be expected than on wet smooth surfaces.

The results of a carefully planned traction test for various synthetic tread compounds is presented in Figure 14. Bias tires having the same construction, the same tread pattern, and the same geometric dimensions were traction tested on a wet rough surface (μ = 0.7) and a wet smooth surface (μ = 0.1). The maximum variation of the rated traction (stopping distance of test tire versus stopping distance of control tire) was about ± 1% for butyl and SBR-PBD blend on a smooth wet road, and ± 7% for the same compounds on a rough road.

We may conclude, then, that the variation in traction due to variation in synthetic tread compounds is the order of ± 12% or less.

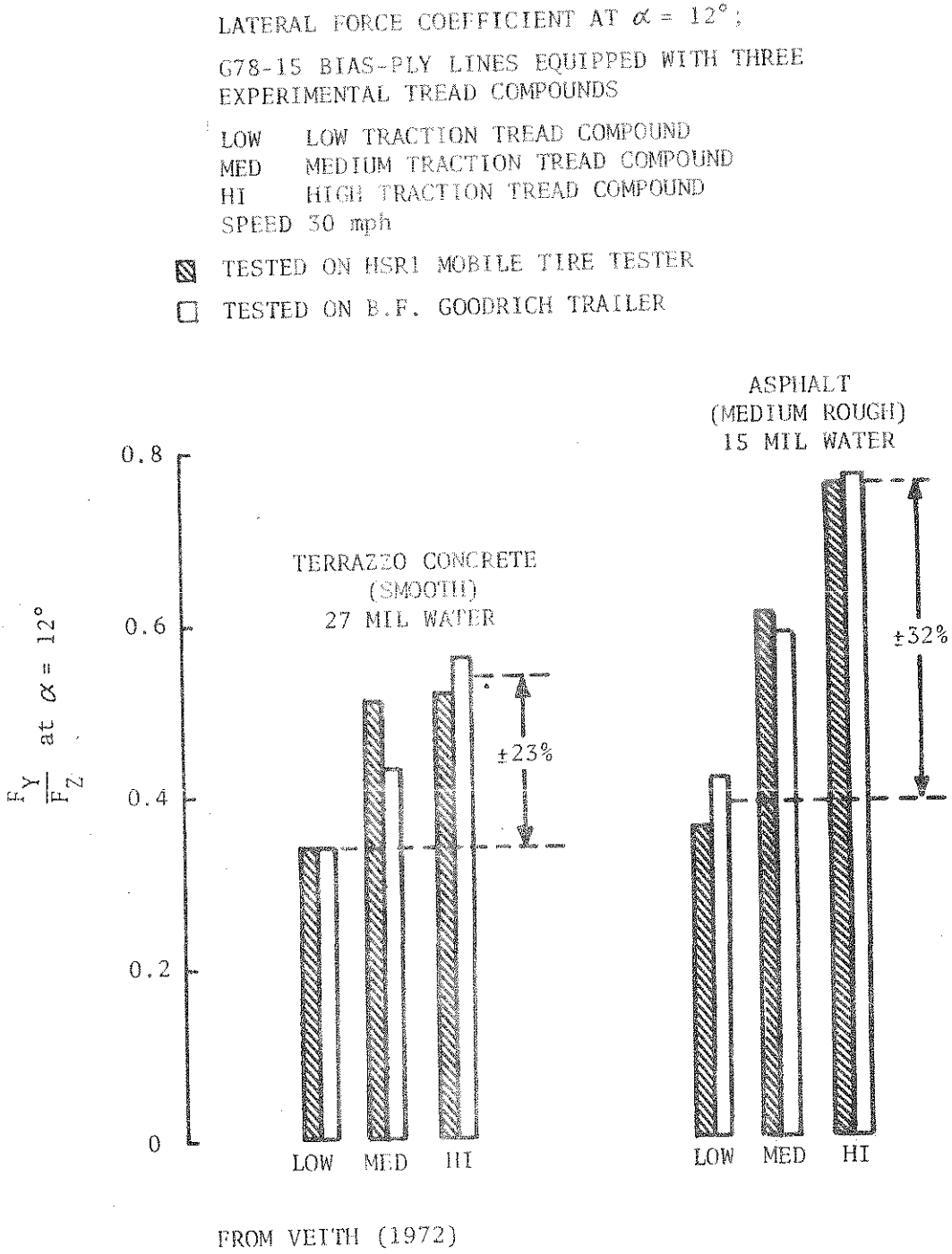

Figure 13 VARIATION OF LATERAL FORCE COEFFICIENT WITH TREAD RUBBER COMPOUND

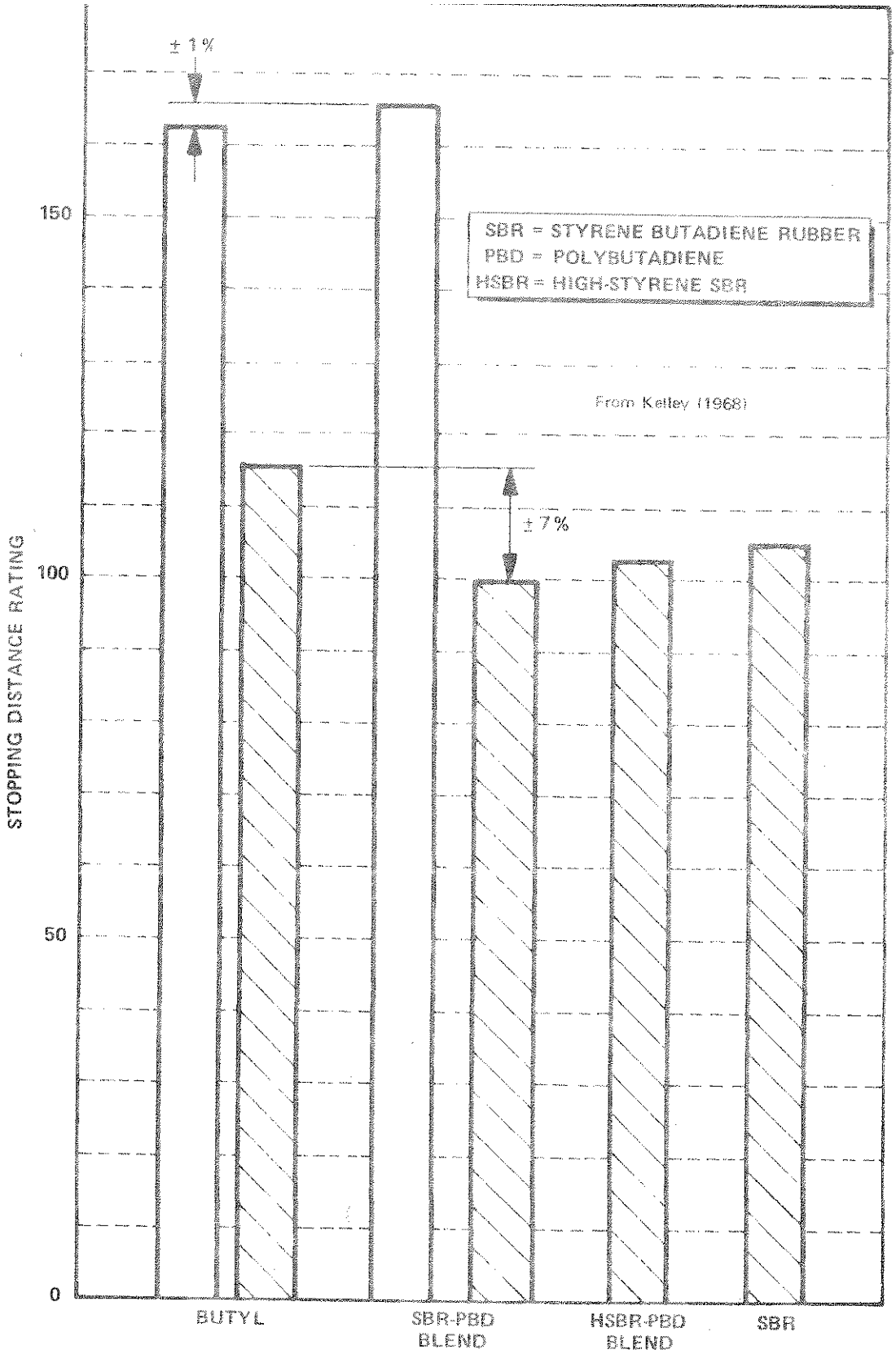

Figure 14 INFLUENCE OF TREAD COMPOUND VARIATION ON RATED STOPPING TRACTION-SAME BIAS TIRE WITH SAME TREAD PATTERN FOR ALL TESTS
LIGHT BAR = SMOOTH ROAD (μ = 0.1), WET
DARK BAR = ROUGH ROAD (μ = 0.7), WET

Effect of Road Wheel Dimensions

The reviewed literature did not reveal conclusive information on differences in tire performance due to differences in road wheel dimensions. Wild (1973) measured the tractive capabilities of 86 tires on three different wet road surfaces and found a general increase of traction with wheel diameter. He reported an increase of 1 to 18% of the peak brake coefficient, of 5 to 27% of the slide brake coefficient, and of -2 to 13% of the peak lateral coefficient, all for an increase of wheel size from 14 inches to 15 inches. These trends are not confirmed by tests performed by other researchers. Neill and Boyd (1973) performed a carefully planned series of braking tests with vehicles equipped with 13, 14, and 15 inch road wheels and tires of the same brand and model. Radial, bias, and bias-belted tires were tested. The authors could not discern significant differences in diagonal locked-wheel braking tests (from 40 mph) for 14 and 15 inch wheels, and perhaps a small difference between the 13-inch wheel and the two others. Similarly, break-away tests on J-curves failed to show any significant differences between the 14 and 15 inch road wheels. The 13-inch wheel performed somewhat better, but the difference was ascribed to the use of a different vehicle rather than to the 13-inch wheels.

These recent findings are corroborated by tests performed earlier by Joy and Hartley (1953-54) on a tire tester. Again, rim diameters of 15 and 16 inches failed to show significant differences in lateral tire force and self-aligning torque. The same observation applied to the influence of rim width, varied between 4 1/2 and 5 1/2 inches, on cornering force.

Recently, Schuring (1974) performed an analysis on the effect of rim width on the cornering performance of tires. His findings are summarized in Table 6. Phillips (1973) advanced an interesting idea about the influence of rim width on aligning torque. He observed that the lateral displacement of the center of pressure is not only a function of lateral force and tire construction but also of rim width: for a given lateral force and a given tire, the lateral displacement increases with rim width.

	Bias ply tires	Bias belted tires	Radial tires
Max slip-angle force	+	+	+
Cornering stiffness	+	0	-
Camber force	?	0	(-)
Camber stiffness	?	0	+
Max aligning torque with respect to slip angle	?	0	+
Aligning stiffness with respect to slip angle	?	0	(-)
Aligning torque with respect to camber angle		positive shift	(+)
Aligning stiffness with respect to camber angle	?	0	0

+	increasing with rim width
-	decreasing with rim width
( )	weak influence
0	no influence
?	influence unknown

TABLE 6

Effect of Rim Width on Cornering Performance
(tentative)

After Schuring (1974)

The lateral shift of the center of pressure, however, influences the aligning torque so that the aligning torque is a function of rim width. Phillips found this to be true particularly in the presence of larger driving or braking forces.

Rasmussen and Cortese (1968) investigated the influence of rim width on the vertical rolling spring rate and found that a 6 inch rim of a 8.25 - 14 tire raised the spring rate by about 5% as compared to a 5 inch rim - an increase equivalent to a pressure increase of about 1.5 psi.

We may conclude that the effects of rim diameter and rim width on tire performance are uncertain.

Effect of Aspect Ratio

Literature on the influence of the aspect ratio on tire performance is scarce. Curtiss (1973) points out the close relation between aspect ratio and cord angle.* "Almost all tires fall within the 30- to 40- degree range. Lower angles are required only where low aspect tires are desired for special applications. Higher angles are usually reinforced with belts to provide circumferential stiffness." Curtiss then lists almost twenty characteristics that are affected by the cord angle, among them section height and width, tread radius, rolling resistance, and lateral and cornering capabilities, Table 7. Since the data are given in qualitative form, their impact on the proposed tire test program cannot immediately be evaluated.

* bias-ply carcass

Parameter	Cord Angle	
	High	Low
Section height	higher	lower
Section width	narrow	wider
Tread radius	rounder	flatter
Rolling resistance	lower	higher
Shear stresses	lower	higher
Bead stresses	higher	lower
Cord tension	lower	higher
Deflection	higher	lower
Enveloping power	higher	lower
Road contact length	longer	shorter
Radial cracking in sidewall	more	less
Lateral stability	poorer	better
Tread wear	poorer	better
Tread cracking, circumferential	better	worse
Cornering power	poorer	better
Ride	softer	harder
Burst strength	higher	lower

TABLE 7

Effects of Cord Angle

From Curtiss (1973)

Allbert (1968) compared the limiting cornering coefficients of tires having the same overall diameter, the same groove and rib dimensions, and the same inflation pressure, but different aspect ratios of 0.50 and 0.80. On a wet, smooth surface, the tire with the low aspect ratio performed better at speeds below 20 mph, and worse at higher speeds, Figure 15. Presumably, the somewhat larger contact area of the low-aspect tire favored hydroplaning.

Recently, the HSRI completed an on-the-road traction program in which the influence of aspect ratio on traction performance (lateral and longitudinal) was investigated. Evaluation of these tests is not completed yet. Through personal communication, preliminary data in Table 8 were obtained. They indicate the influence of the aspect ratio not to surpass 20%, for the given set of tire and road parameters.

Effect of Cord Material

Very little data could be found in the open literature on the effect of cord material (carcass, belt) on tire performance. Holmes (1970) performed some braking tests on various wet surfaces with radial-ply tires -- a steel belted tire with rayon cords, a rayon belted tire with nylon cords, and a rayon belted tire with rayon cords. Unfortunately, the tread patterns of the three tires were quite different. Hence, no firm conclusion could be drawn as to the influence of cord material alone.

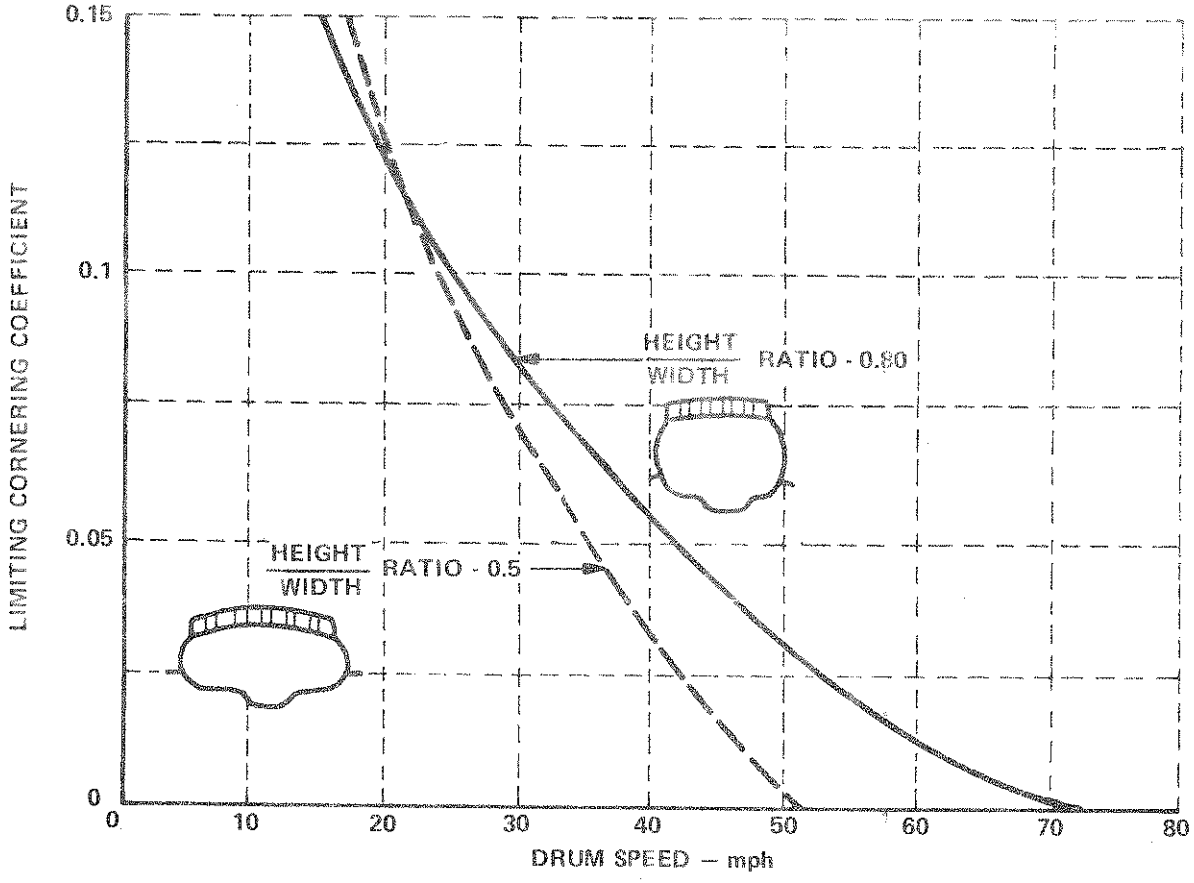

CORNERING FORCE MACHINE TEST
LOAD: 800 lb
INFLATION PRESSURE: 30 psi
AUTOMOBILE TIRES OF EQUIVALENT
OVERALL DIAMETER
SAME GROOVE & RIB DIMENSIONS FOR BOTH TIRES

Figure 15 COMPARISON OF TIRES HAVING DIFFERENT SECTIONAL SHAPE

From Albert (1968)

Tire (radial-ply)	Lateral Force, F_y - lbs. slip angle = 8°				Longitudinal Force, F_x - lbs. slip angle = 0°			
	free-roll		slide		peak		slide	
	concrete	asphalt	concrete	asphalt	concrete	asphalt	concrete	asphalt
F78-14	670	700	140	150	720	820	670	710
F70-14	750	740	140	150	820	900	720	700
F60-14	800	810	140	150	740	900	720	750

TABLE 8

Preliminary Data on the Influence of the Aspect Ratio on Tire Traction on Dry Surface, Speed 40 mph.

Radial-ply tires with polyester cords and fiberglas belt; same tread pattern, same load (800 lbs)

From Tielking (1973); personal communication

ANNOTATED BIBLIOGRAPHY

Alexander, Kenneth R., "Bias Angle Versus Radial Ply Versus Bias Belted Tires - Materials and Construction Comparisons", SAE Paper 680386, May, 1968, 5 pp.

The bias belted and radial tire concepts offer advancement in tire performance which cannot be met with the conventional bias tire. A review of the materials and construction of a conventional bias tire is included as a direct comparison to the materials and construction features of a radial and bias belted tires. A brief history of the evolution of tire materials is also given.

Tire construction type

Allbert, B. J., "Tires and Hydroplaning", SAE Paper 680140, Jan 1968, 11 pp

The paper discusses the phenomena which are primarily responsible for hydroplaning and includes results from studies of the effects due to individual tire parameter such as tread pattern design, tread material, and the construction and sectional shape of the casing.

It is shown that the most important of these tire factors is the geometric design of the tread pattern.

Tread geometry

Allbert, B. J., Walker, J. C., "Tyre to Wet Road Friction at High Speeds", Institution of Mech. Engineers Proceedings, Vol. 180, Part 2A, No. 4, pp 105-121, 1965-1966

The general problem of loss of tire grip on wet road surfaces is discussed.

Tread pattern and road surface design are shown to exert a considerable influence upon the rate of water displacement from the contact area and hence upon the relative sizes of the water-supported zones.

A section of the paper considers the wide scale effects of tread pattern, tread material and road surface characteristics and discusses the nature of the interactions between these three variables.

Some results of recent studies related to different types of tread pattern, specific pattern design features and the effect of tire casing construction are included.

Tire construction type

Tread geometry

Tread compound

Anon, "Oil-Extended Natural Rubber in Winter Tyre Treads", Natural Rubber Prod. Res. Assoc., Inc., England, Report No. TB-15/68 1968 22 p

This bulletin describes laboratory and road tests with passenger cars on icy surfaces, comparing the skid performance of winter tire treads made from oil-extended natural rubber with that of treads from oil-extended styrene/butadiene rubber. The tests involved skidding on icy road surfaces having temperatures ranging from 0°C (melting ice) down to -6°C (packed ice). Under all conditions, the oil-extended natural rubber treads had superior skidding resistance. Better traction in standard, winter, and studded winter tires and superior wear at cooler temperatures are cited as advantages of these tires. Rubber formulations are given.

Tread compound

Anon., "A Review of Current Constructions, Developments, Performance", Automobile Engineers, Vol 49, No 8, July 1969, pp 274 - 288

Recently, new types of radial-ply and the bias-belted tire have been developed. The basic characteristics of these three types of tire, current usage as original equipment, development of the latest tires, as well as future trends are considered in this article.

Tire construction Type

Bidwell, J. B., "Car-Tire Relationships", General Motors Publication GMR-502, presented at Akron Rubber Group Winter Meeting, Nov. 1965, 17 pp

This paper concerns itself with some of the more important tire parameters and, more specifically, with the differences in these characteristics between conventional bias angle tires and radial-ply tires and their influence on vehicle design.

Tire construction type

Bogan, R. F., Dobie, W. J., "Performance Comparison - 2-Ply Versus 4-Ply Passenger Car Tires", SAE Paper 660378, pp 557 - 562

This paper includes a comprehensive performance history comparing 2-ply versus 4-ply on millions of tires produced during this five year period. The results leave no doubt that the 2-ply tire has proven itself superior to the 4-ply on an overall basis.

Tire construction type

Briggs, G. J., Hutchison, E. J., Klingender, R. C., "Factors Affecting Skid Resistance of Polybutadiene", Rubber World, Vol. 150, No. 6, Sept. 1964, pp 41-53.

This article shows that satisfactory frictional properties on wet pavement may be obtained with treads containing cis-1,4 polybutadiene through compounding variations without sacrifice in other properties.

However, the authors conclude that the surface characteristics of the road determine the coefficient of friction that exists between the pavement and the tire tread under both dry and wet conditions to a much greater extent than any changes in the composition of the tire tread vulcanizate.

Tread compound

Buddenhagen, F. E., "Design and Construction Considerations of Radial Passenger Car Tires", SAE Paper 670470, May 1967, 5 pp

This paper reviews some of the more important construction and design considerations involved in radial passenger tire performance.

General

Carr, G. W., Holt, A. J., "A Comparison of the Rolling Resistance of Radial and Cross-Ply Tyres" MIRA Bulletin No. 5, 1970, Sept./Oct., pp 4-7

A discussion of the MIRA single-wheel rolling resistance trailer and measurements of rolling resistance for a radial and a cross-ply tire. Tests were performed at a variety of loads and pressures. The radial ply had less rolling resistance under all conditions.

Tire construction type

Chiesa, Arturo, Gough, V. E., Jones, F. B., Udall, W. S., "Take the Bias Out of Tires?", SAE Journal, May 1965, pp 32-39

The specific characteristics studied in this paper to determine the quantitative performance levels of radial-ply and cross-biased tires were:

1. Cornering power
2. Aligning torque.
3. Tire-road adhesion.
4. Tread wear
5. Ride quality
6. Spring rates and damping
7. Tire and vehicle oscillations
8. Noise generation and transmission
9. Rolling resistance

Tests were made on laboratory road-wheel machines, on proving grounds, and on public roads.

Tire construction type

Cox, J. H., "The Fleeting Tire Footprint", SAE Paper 970 D, Detroit, Jan. 1965

Examination of wet pavement traction test data, covering different designs and compounds on a wide range of road surfaces, disclose that the basic road surface is far more important than any variation in design or compound.

Tread geometry

Tread compound

Curtiss, W. W., "Principles of Tire Design", Tire Science and Technology, TSTCA, Vol 1, No 1, Feb. 1973, pp 77-98

Design procedures based on sound mechanical principles have become a necessity to meet the ever-increasing demands of performance placed upon the tire of today. This discussion gives an overview of the design process and calculations employed in developing the modern tire: performance and sizing, envelope shape as a function of construction, structural stress, design of the tire skin, and construction of the "green" tire.

Aspect ratio

Curtiss, W. W., "Low Power Loss Tires", SAE Paper 690108, Jan. 1969, 14 pp

The paper discusses the property of rolling resistance as applied to pneumatic tires. Basic relationships of rolling resistance are discussed as associated with structural and environmental factors in both low and high speed operation. The discussion covers only tire service over hard surfaces and is primarily concerned with passenger car tires.

Tire construction

Tread geometry

Road wheel dimensions

Aspect ratio

Davisson, J. A., "Design and Application of Commercial Type Tires", SAE Paper SP-344, Jan. 1969, 39 pp.

Basic tire design factors, performance properties, application requirements, and their interrelated effects are discussed to furnish general insight into commercial-vehicle tire engineering. The subject is covered comprehensively to illustrate the numerous considerations and decisions affecting the design and use of commercial-vehicle tires. The information is presented primarily from the perspective of the tire engineer with the objective of providing a fundamental background for the vehicle designer and operator.

General

DeVinney, W. E., "Factors Affecting Tire Traction" SAE Paper 670461, May, 1967, 8 pp.

Of the many variables involved in the problem of wet skidding, the most significant single factor is speed.

On wet surfaces, the effects of speed on the apparent coefficient of friction are reduced as the surface texture becomes more coarse. Other factors considered in this paper are: tread design and compound, tire construction, inflation pressure, road surface, tire load, and temperature.

Tread geometry

Tread compound

Dijks, A., "Tests to Determine the Minimum Permissible Tread-Depth for Passenger-Car Tyres", Automobiltechnische Zeitschrift, (In German), ATZ, Jan., 1973, Vol. 75, No. 1, pp 1-6

Experiments were conducted on three different types of standard radial tires and one type of cross-ply tire to determine the effect of tread-depth on tire adhesion to wet road-surfaces. For each tire-type, five tires of differing tread-depths (from above 4.0mm to below 0.4 mm) were tested.

Tests were carried out on a smooth, asphalt road-surface (low skid-resistance) at 50 and 80 km/h and on a cement-concrete surface (high skid-resistance) at 50 and 100 km/h, water being sprayed in front of the test-tire to a depth of 0.6 mm.

Results showed that the maximum value of the coefficient of longitudinal adhesion was found to be very dependent upon tread-depth; lateral adhesion was least affected by tread-depth. Coefficients of adhesions for tires with less than 2mm tread fell sharply, especially on the asphalt surface.

Tire construction type

Tread geometry

Dijks, A., "Wet Skid Resistance of Car and Truck Tires," Tire Science and Technology, TSTCA, Vol. 2, No. 2, May 1974, pp. 102-116.

Two test trailers for measuring tire characteristics are described. One of the trailers is specially built for testing car tires and can steer, camber, and brake the test tire. The determination of peak and locked wheel braking force coefficients is discussed. In addition, for car tires, a method for obtaining side force coefficients is given. Test results are given for both car and truck tires showing the influence of road surface texture, speed, and tread depth on skid resistance, and the results are compared.

Tread geometry

Elliott, D. R., Klamp, W. K., Kraemer, W. E., "Passenger Tire Power Consumption", SAE Paper 710575, June 1971, 14 pp

The body of this paper discusses the effect of operating conditions and tire design variations on the rolling resistance. Eighty tires were analyzed.

Tire construction type

Tread geometry

Cord material

Fancher, P.S., Jr., Dugoff, H., Ludema, K. C., Segel, L., "Experimental Studies of Tire Shear Force Mechanics -- A Summary Report", Highway Safety Research Institute, The University of Michigan, Ann Arbor, Mich., 48105, July 30, 1970, 16 pp

HSRI has gathered and analyzed data on the development of tire shear forces over a wide range of operating conditions. The data were obtained using a laboratory-installed flat bet tester and a vehicle-towed mobile tire tester (MTT).

This report provides findings on bias, bias-belted, and radial tires operated on dry and wet surfaces and makes specific recommendations for future research.

Tire construction type

Francher, P. S., Jr. and Segel, L., "Tire Traction Assessed by Shear Force and Vehicle Performance," Tire Science and Technology, TSTCA, Vol. 1, No. 4, Nov. 1973, pp. 363-381

Tire shear force data for ten different types of passenger tires tested on wet surfaces are studied to examine the influence of test surface, velocity, and load on the maximum lateral force, maximum braking force, maximum resultant force, and locked wheel braking force. Tire traction rankings based on these four measures are compared with each other and with rankings obtained from J-turn and diagonal braking tests on a vehicle equipped with the same types of tires using the rank difference correlation method. The findings show that rankings based on a small number of maximum lateral force tests correlate well with rankings based on J-turn tests.

Tire construction

Tread geometry

French, T. "Construction and Behaviour Characteristics of Tyres" IME Paper, Inst. Mech. Eng., 1960., 15 pp

In this paper the impact of new materials for making tires and constructional variations are discussed in relation to improved tire performance characteristics including comfort, road adhesion, ease of control, high speed running, tread pattern life, noise and power consumption.

General

Gardner, E. R., "Recent Trends in Tyre Compounding" Institution of Rubber Industry Transactions and Proceedings Vol 13, pp 248-260, Dec. 1966

In recent years there has been a considerable diversification in the compounds employed by the various companies in the different parts of the tire. Reasons for this are suggested. The main features of the compounds used in the tread, sidewalls, and casing of truck and car tires, both cross-ply and radial, are discussed.

Tread compound

Gengenbach, W., Weber, R., "Measurement of Tire Deflection of Bias-Ply and Radial Tires", (in German), Automobiltechnische Zeitschrift (ATZ), Vol. 71, No. 6, June 1969, pp 196-198

The paper demonstrates that the rolling radius increases with speed; both, bias-ply and radial tires show approximately the same increase.

Tire construction type

Gengenbach, W., Weber, R., "The Restoring Moment of Motor-Vehicle Tyres Under the Combined Influence of Circumferential and Lateral Forces" Auto. Industrie, August 1970, Vol. 15, No. 3, pp 85-96, MIRA Translation No. 2071.

The relationship between side-force, circumferential force, and slip angle on the one hand and the restoring moment on the other was investigated for cross-ply and radial-ply tires. Graphs are presented showing: (1) side-force and restoring moment as functions of circumferential force for various slip angles, tread depths, wheel loads, and tire pressures; (2) the restoring moment as a function of slip angle and side-force. Caster of cross-ply and radial-ply tires is shown in polar diagrams. Slip angle and circumferential force have a strong influence on magnitude and direction of caster.

Tire construction type

Gengenbach, W., Weber, R., "The Influence of Road Surface, Speed and Tyre-Tread Depth on the Adhesion Under Wet Conditions", Auto. Industrie, Nov. 1970, Vol. 15, No. 4, pp 69-73, MIRA Translation No. 34171.

The adhesion of cross-ply and radial tires was measured as a function of tread depth (from 0 to 8 mm.) and of vehicle speed (from 0 to 100 km/hr) on four road surfaces artificially wetted to a depth of 1.5 mm., viz., traffic-worn concrete, freshly-laid concrete, new asphalt and very coarse asphalt. Results are presented and discussed. At 80 km/hr on a wet road, the effect on tire side-force coefficient of road surface is as great as that of tread depth. The decrease in wet-road adhesion with rising vehicle-speed becomes more marked with increasing tire-wear.

Tire construction type

Tread geometry

Giles, C. G., Sabey, B. E., "Rubber Hysteresis and Skidding Resistance" Engineering Vol 186, pp 840-2, December 1958

In this article the authors tried to explain the mechanism of the dependence of skidding resistance on temperature and the differences in performance between natural and synthetic tires.

Tread compound

Goudie, John J. Jr., "Performance Requirements for Passenger Car Tires", SAE Paper 660375, June 1966, 3 pp.

The purpose of this paper is to describe the requirements, presently made upon the performance of passenger car tires, to show how the industry strives to meet these requirements, and keep pace with constantly changing and more demanding conditions.

General

Gough, V. E., Allbert, B. J., "Tyres and the Design of Vehicles and Road for Safety", Vehicle and Road Design for Safety, The Institution of Mechanical Engineers, July 1968, Paper 8, 10 pp.

The paper discusses the aspects of state of tires, road layouts and vehicle features which tend to cause departures from safety.

It is an attempt to draw attention to the need to consider the subject as an entity rather than a number of separate specialized studies.

General

Gough, V. E., Jones, F. B., Udall, W. S., "Radial Ply, Rigid Breaker Tires", SAE Paper 990A, Jan. 1965, pp 1-12

The paper discusses the advantages of radial-ply tires: Increased resistance to tread wear, improved road holding and safety, reduction of wander at ridges in road surfaces, lower spring rate, reduced transmission of road roar generated on rough textured road surfaces, and reduced fuel consumption.

Tire construction type

Gough, V. E., French, T., "Tyres and Skidding from a European Viewpoint" Proc. 1st Int'l Skid Prevention Conf. Virginia Council Highway Invest. and Research, Charlottesville, Virginia, Aug 1959, pp 189-209

In this paper, it is stated that on flat, smooth, polished-texture road surface under wet conditions with locked wheels it has been established that:

Worn-smooth tires (bald tires) give very low coefficients.

Tire tread patterns can improve the effective coefficient of friction by a factor of 2 to 2 1/2 at ordinary road speeds.

The use of cuts or sipes improves rib patterns by amounts up to 30%.

With natural rubber tread, compounding was relatively unimportant, tread pattern design dominated the situation.

With synthetic treads, compounding ingredients and hardness have more specific effects

Tread geometry
Tread compound

Grosch, K. A., Maycock, G., "Influence of Test Conditions on Wet Skid Resistance of Tire Tread Compounds", Rubber Chemistry and Technology Vol 41, pp 477-494, 1968

The paper studies the skid resistance of a number of tread compounds on four different road surfaces and investigates to what extent the measured skid resistance of a tread compound is influenced by test conditions. Statistical analysis is employed to determine the interrelation of vehicle speed, road surface texture, tread compound, and the actual conditions under which the friction is obtained (i.e., maximum or locked wheel braking).

Tread compound

Hales, F. D., Berter, N. F., "The Effect of Roll Stiffness and Tyre Type on Vehicle Steady State Response", The Motor Industry Research Assoc., Report No. 1968/1, Nov. 1967.

The report reviews briefly the background to the experiments on the effect of roll stiffness and tire type on the steady-state response of an automobile, and describes the test vehicle and its associated instrumentation system.

Vehicle conditions investigated involved a tire change from radial to cross-ply tires.

The results fall naturally into four groups, depending on the type of tire and whether a rear anti-roll bar if fitted or not; the largest changes are produced by fitting the rear anti-roll bar; the tire change produces relatively much smaller variations.

Tire construction type

Holmes, K. E., "Braking Force/Braking Slip: Measurements Over a Range of Conditions Between 0 and 100 Per Cent Slip", Road Research Laboratory Report LR 292, 1970, 31 pp

The relationship between braking force coefficient (BFC) and braking slip for various tires and wet road surfaces has been investigated. Variables investigated include tread pattern, tread material, road surface texture, speed, and tire construction. In both peak and locked wheel conditions, measurements confirmed previous findings relating to effectiveness of tread patterns in relation to smooth tires, effectiveness of lower resilience tread materials, and differences in tire construction.

Tire construction type

Tread geometry

Tread compound

Cord material

Homes, K. E., Stone, R. D., "Tyre Forces as Functions of Cornering and Braking Slip on Wet Road Surfaces" Published in HS-011 272, Handling of Vehicles under Emergency Conditions, 1969, pp 35-55

In this paper, the braking and cornering forces of a given tire on a given wet surface at a given speed are presented. The effects of such factors as speed, road surface texture, tread pattern, tread resilience, and tire construction are reported. The test vehicle, test procedure and the methods of measuring and evaluating the data are briefly described.

Tire construction type

Tread geometry

Tread compound

Hutchinson, J. F., "Development of the Low Profile Passenger Tire", SAE Paper 983C, Jan. 1965, 4 pp.

The development of the low profile passenger tire is described. This tire provides improved handling and stability, faster cornering, improved high speed performance, and longer tread life, with no loss in noise level or riding comfort. Tire characteristics described include improved tread design and tread rubber compounding, contour shoulder, and low profile carcass. The effect of cord angle on tire inflation shape and speed are also discussed.

Aspect ratio

Hutchinson, J. F., Becker, H. D., "Determination of Passenger Tire Performance Levels - Traction", SAE Paper 690510, May 1969, 7 pp

By comparing test tires with production tires with known traction qualities, tire manufacturers produce tires which perform satisfactorily for wet traction. However, owing to the many variables which affect tire traction, and owing to wide deviations in the test data, the conclusion is reached that the state-of-the-art today for measuring traction does not warrant the recognition of a tire traction performance level which can be defined in specific terms.

Tread geometry

Johnson, Wade C., "Factors in Tires that Influence Skid Resistance, Part III The Effect of Carcass Construction, Size, Cord Angle, and Number of Plies", Proceedings from First International Skid Prevention Conference, Part I, Va. Council of Highway Investigation and Research, Charlottesville, Va., Aug, 1959, pp 163-166

The paper states that little can be done with the carcass of a conventional tire to improve its stopping ability.

Tire construction type

Joy, T. J. P., Hartley, D.C., "Tyre Characteristics as Applicable to Vehicle Stability Problems", Proceedings of the Automobile Divison, The Institution of Mechanical Engineers, 1953-54, Number 6, pp 113-122

The authors define the characteristics of a pneumatic tire which affect the handling, or stability, of a car, and briefly describe a machine which was developed to measure these characteristics.

The results are given of various experiments showing the effect of several factors on the characteristics; among others, the effect of rim diameters, number of plies, and section width.

Road wheel dimensions

Keller, R. C., "Improvement of Tire Traction with Chlorobutyl Rubber", Tire Science and Technology, TSTCA, Vol 1, No 2, May 1973, pp 190-201

The skid resistance of tires can be improved with tread compounds which have high hysteresis losses. Chlorobutyl rubber is a chlorinated isobutylene-isoprene copolymer of interest in tread compounds because of its high damping (low resilience) characteristics. Tire traction performance is determined with an automated vehicle designed to measure both peak and sliding skid resistance. Overall, significant improvements in traction performance have been found for radial tires with Chlorobutyl-containing tire treads; the level of improvement is directly proportional to the Chlorobutyl content of the polymer blend.

Tread compound

Kelley, J. D., Jr., "Factors Affecting Passenger Tire Traction on the Wet Road", SAE Paper 680138, Jan 1968, 13 pp

The part that the tread design of a passenger tire plays in its wet tractive ability is the most important single variable as far as the tire is concerned.

The external variables that affect wet traction are also considered. These include speed, surface coefficient, load, temperature, and inflation pressure.

All of these variables are discussed, with special emphasis placed on the tread design.

Tire construction type

Tread geometry

Tread compound

Kern, W. F., "Coefficient of Wet Friction of Tire Treads", Rubber Chemistry and Technology, translated by G. Leuca from Kautschuk und Gummi-Kunststoffe 19, (2) 91 (1966)

Small rubber specimen were tested on a friction-roller apparatus and the effect on wet friction coefficient of composition of the rubber compound and compounding techniques measured.

Tread compound

Klamp, W. K., Milligan, W. J., "Performance Characteristics - Radial Ply Tires", SAE Paper 670471, May 1967, 12 pp

This paper examines certain of the mechanical properties and principles that make up the performance characteristics of the radial ply tire. Harshness, tread wear, skid, and traction are discussed as are stability puncture resistance, standing height, and power consumption. Also discussed is the necessity for viewing tire performance only in respect to a particular vehicle.

Tire construction type

Krebs, H. G., "Cornering Characteristics of Car Tyres" International Colloquium on the Interrelation of Skidding Resistance and Traffic Safety on Wet Roads, Wehner, B. and Schulze, K. H., Wilhelm Ernst & Sohn, Berlin, Chap. 9, pp 483 - 499.

Starting from the characteristics of the pneumatic tire, the properties of which are affected by its tread material and design as well as by the operating conditions such as the inflation pressure, loads in the direction of the three space coordinates, and the condition of the road surface, recent test results classified into the various types of loading and states of motion are discussed.

Tread geometry

Krempel, G., "Experimental Contribution to Investigations on Automobile Tires", (in German), Ph. D. Dissertation, Technische Hochschule Karlsruhe, Germany, Feb 1965, Published in Automobiltechnische Zeitschrift (ATZ), Vol 69, No 1, Jan 1967, pp 1-8, and No. 8, Aug 1967, pp 262-268

The dissertation contains, among many other things, an experimental study of the influence of groove depth on aligning torque, lateral force, and tractive force.

Tread geometry

Kummer, H. W., Meyer, W. E., "Tentative Skid-Resistance Requirements for Main Rural Highways", National Cooperative Highway Research Program Report 37, 1967, 80 pp

The principal problems and causes of pavement slipperiness, the mechanism of rubber and tire friction and the various methods of measuring friction are reviewed with the object of elucidating the problems connected with specifying minimum skid-resistance requirements. Steps which can be taken and research which is needed to reduce skidding accidents and to improve the skid resistance of pavements are suggested.

Tread geometry

Lane, J. H., McCall, C. A., Gunberg, P. F., "Predicting Tire Tread Performance from Composition. I", Rubber Chemistry and Technology, Vol 43, No. 5, Sept. 1970, pp 1070-1081

Three experimental tread formulations were skid-tested with bias-ply and bias-belted tires, on a smooth and a rough surface. The differences in skid resistance turned out to be rather small (appr. 5%).

Tire construction type

Tread compound

Leland, Trafford J. W., "An Evaluation of Some Unbraked Tire Cornering Force Characteristics", National Aeronautics & Space Admin., Langley Research Center TND-6964, Nov. 1972, 36 pp.

This paper presents the results of an investigation conducted at the Langley aircraft landing loads and traction facility to determine the effect of runway surface condition on the cornering forces developed by tires having different tread patterns operating free-rolling at fixed yaw angles. In this investigation 6.50 x 13 automobile tires were used. The tests were made at yaw angles of 3°, 4.5°, and 6° at forward speeds up to 80 knots on two concrete surfaces of different texture under dry, damp, and flooded conditions.

Under dry surface conditions, the roughened concrete surface generally produced higher cornering force coefficients than the smooth concrete surface, with the smooth tire developing higher coefficients on both surfaces than any of the tires having a tread pattern.

On either surface when damp, cornering forces displayed a sensitivity to tread pattern, with the four-groove slotted tire being somewhat better than the other tread patterns. On the flooded surfaces a minor effect of tread pattern was observed only below the hydroplaning velocity.

Tread geometry

Leyden, J. J., "Radial Tire Compounding" Rubber Age Vol 104, No. 4, pp 51-53, Apr. 1972

Although some bias-belted tire compounds find their way into radial tires, for the most part new compounds have to be developed. Various radial compounds and how they differ from compounds used on bias-belted tires are discussed.

Tread compound

Litzler, C. A., "Advances in Tire Cord Processes. Pt. 1: Reinforcing Materials", Rubber Age, Vol 105, No 2, p 27-32, Nov. 1972

The most important single factor of concern to the U.S. tire industry today is the rapid acceptance of wire-reinforced tires and textile-reinforced tires of radial design. The next most important factor is the increase in the use of fiberglass filament in either bias-belted or nearly true radial-belted construction. Developments in reinforcing materials including DuPont Fiber B, polyester cord fiber, rayon cord, spun steel wire, and polyvinyl alcohol are discussed.

Cord material

Marick, Louis, "Factors in Tires that Influence Skid Resistance, Part II The Effect of Tread Design", Proceedings from First International Skid Prevention Conference, Part I, Va. Council of Highway Investigation and Research, Charlottesville, Va., Aug, 1959, pp 155-162

The paper states that the tread design is one of the most effective features of the tire in influencing its resistance to skidding on most common road surfaces when they are wet.

The tire industry has made a very marked improvement in skid resistance on wet pavements in recent years by the use of highly slotted antiskid designs.

On dry pavement the most effective tire is the one having the largest net contact area with the road, i.e., the "bald" tire.

Tread geometry

Maycock, G., "Studies on the Skidding Resistance of Passenger-Car Tyres on Wet Surfaces", Proceedings of the Institution of Mechanical Engineers, Vol 180, No 4: pp 122 - 157, 1965-1966

This paper reports investigations into the effect of tread pattern, pattern modifications, tread material and tire casing construction, on the skidding resistance of passenger-car tires at speeds between 25 and 80 mph on a range of wet road surfaces.

Tire construction

Tread geometry

Tread compound

Maycock, G., "Experiments on Tyre Tread Patterns", Road Research Laboratory Report LR 122, 1967, 11 pp

This report describes two experiments carried out to investigate the influence of certain features of tread pattern design on the skid resistance of tires. Measurements were made of peak and locked wheel braking force coefficients, on several wet surfaces at speeds between 20 and 105 mph, using a front wheel braking technique.

In the first experiment four tires were used having respectively 5, 7, 9 and 13 straight cut ribs and having the same overall tread area. Differences between these tires were small.

In the second experiment, the rib width was held constant, and the groove width varied. The results showed that no appreciable increase in coefficient was obtained when the groove width exceeded a critical value.

Tread geometry

Meades, J. K., "Braking Force Coefficients Obtained with a Sample of Currently Available Radial Ply and Crossed Ply Car Tyres", Road Research Laboratory, 1967, 17 pp.

This note gives the braking force coefficients of five radial ply and five crossed ply tires on four wet road surfaces at speeds of between 30 mile/h and 130 mile/h.

Comparisons between the two types of construction show that the low speed coefficients were very similar, but that in general the radial ply tires had larger coefficients than the crossed ply tires at the higher speeds.

Tire construction type

Meades, J. K., "The Effect of Tyre Construction on Braking Force Coefficients", Road Research Laboratory Report LR 224, 1969, 14 pp

Radial and cross ply tires have been compared in terms of peak and slide braking force coefficients at car speeds between 50 and 130 km/h (30 and 80 mph) on a range of wet surfaces.

The radial ply tires gave higher peak braking force coefficients on all the surfaces than did the cross ply tire. However the radial ply tires gave lower slide braking force coefficients on the coarse-textured surfaces than did the cross ply tires.

Tire construction type

Neill, A. H., Jr., "Wet Traction of Tractionized Tires", Nat. Bur. Stand. (U.S.), Tech. Note 566, Feb. 1971, 14 pp

A series of dynamic vehicle tests was performed at NBS to evaluate the performance of tractionized or siped tires. Stopping distance and lateral breakaway data is presented from a two wheel diagonally braked automobile which clearly shows that siped tires do not represent any improvement in the lateral stability or stopping distance characteristics of a typical passenger automobile.

Tread geometry

Neill, A. H., Jr., Boyd, P. L., "Research on Wet Tire Traction", Tire Science and Technology, TSTCA, Vol. 1, No. 2, May 1973, pp 172-189

This paper describes experiments and methodology employed in an attempt to develop a system for the grading of wet tire traction. Data from instrumented vehicle experiments and the University of Michigan Highway Safety Research Institute mobile tire tester are used. The vehicle tests include J-curve cornering and diagonal, locked-wheel braking. The maneuvers are used to generate information on tire tractive properties and their dependence on tread depth, rim size, suspension, and surface conditions.

Tread geometry

Road wheel dimensions

Nordeen, D. L., Cortese, A. D., "Force and Moment Characteristics of Rolling Tires", SAE Paper 713A, June 1963, 13 pp

Typical results for a 7.60-15 tire are presented to illustrate the effects of slip angle, camber angle, vertical load, inflation pressure, and wheel torque on cornering force and aligning torque.

General

Odgers, B. J., "The Performance and Failure of Car Tyres" Melbourne University, Mech. Engin. Dept., June 1966, 50 pp.

This report reviews some published literature and some unpublished information on the performance and failure of car tires and their relevance to vehicle accidents. A comparison of different types of tire construction and their braking and skidding characteristics is presented. Radial-ply tires have a higher cornering power and lower rolling resistance than cross-biased tires, but give a harsher ride. On a dry surface, a smooth tire has slightly better skid resistance than a treaded tire. Tires made of high hysteresis rubber have improved skid resistance.

Tire construction type

Tread geometry

Tread compound

Peterson, K. G., Rasmussen, R. E., "Mechanical Properties of Radial Tires" SAE Paper 730500, May 1973, 7 pp

This discussion is devoted to radial tires in general, although the data are mostly derived from tests of steel belted radials. Also covered are dimension, handling, ride, traction, noise, and power loss performance of the same tire.

Tire construction type

Phillips, B., "The Static Steady State and Dynamic Characteristics of Pneumatic Tires," PhD Thesis, Lanchaster Polytechnic, Coventry, April 1973

A comprehensive theoretical and experimental study of steady state and dynamic tire behavior. Of interest here are test results obtained on a flat bed tester on five tire types.

Tire construction type

Road Wheel Dimensions

Rasmussen, R. E., Cortese, A. D., "Dynamic Spring Rate Performance of Rolling Tires", SAE Paper 680408, May 1968, 7 pp

Spring rate is one of several factors that affect the ride performance of passenger car tires. The spring rate properties of many different tire designs have been measured. The effect of wear and several tire construction variables on spring rate is presented.

Tire construction

Road wheel dimensions

Aspect ratio

Rasmussen, R. E., Cortese, A. D., "The Effect of Certain Tire-Road Interface Parameters on Force and Moment Performance", Engineering Staff/ General Motors Corp. Report A-2526, July 1969, 24 pp

On G.M.'s flat-bed force and moment tire test machine an array of road surfaces have been tested. In addition to road surface, tire tread condition has also been investigated. Several tire construction types have been tested in the new, half worn, and fully worn tread conditions.

Tread geometry

Reinhart, M.A., "Factors in Tires that Influence Skid Resistance, Part IV: The Effect of Tread Composition", Proceedings from First International Skid Prevention Conference, Part I, Va. Council of Highway Investigation and Research, Charlottesville, Va., Aug. 195[illegible], pp 167-[illegible]

> At the present time in the U.S., SBR synthetic rubber treads are used on practically all of the passenger car tires. In the area of performance, the data show that SBR treads have the highest coefficient of friction of present commercial tire rubbers, on dry surface; and is comparable to the average coefficient of these rubbers on wet, ice, and packed snow surfaces.
>
> Tread compound

Sabey, B. E., Williams, T., Lupton, G. N., "Factors Affecting Friction of Tires on Wet Roads", SAE Paper 700376, 1970

> Different aspects of tread pattern design and tread material are considered in relation to factors external to the tire, the major ones being the influence of water depth over a range representative of conditions on the road, the interaction of road surface texture, and the effect of speed. The method of approach includes full-scale experiments on the British Road Research Laboratory's track using braked and rolling wheels under carefully controlled conditions, laboratory investigations of the viscoelastic properties of rubber together with rubber friction tests and theoretical considerations linking the different aspects.
>
> Tire construction type
>
> Tread geometry
>
> Tread compound

Schallamach, A., "Skid Resistance and Directional Control - Chapter 6", Mechanics of Pneumatic Tires, Samuel K. Clark, Editor, National Bureau of Standards Monograph 122, No [illegible] 1971, pp 501-544

> This chapter offers, among other things, a concise discussion of the effect of tread pattern, carcass construction, and tread compound on tire friction.
>
> Tire construction type
>
> Tread geometry
>
> Tread compound

Schuring, D. "Notes on the Influence of Road Wheel Dimensions on Tire Performance," Internal Document of TIRF Center, Calspan Corp., May 1974

A preliminary survey of the tire literature and of recent information from TIRF revealed that available data on the influence of road wheel dimensions on tire forces and moments are inconclusive for lack of systematic investigations. In many instances, the influence of rim dimensions on performance data such as braking coefficient, cornering stiffness, maximum lateral force, dynamic spring rate, and rolling resistance appeared to be significant; in other instances, such influences were less evident.

Road wheel dimensions

Smithson, F. D., Herzegh, F. H., "Investigation of Tire-Road Traction Properties", SAE Paper 710091, Jan 1971, 16 pp

This paper presents a method for categorizing road surface traction properties by evaluating the traction performance of road surfaces when tested with a series of special tires.

Tread geometry

Tread compound

Southern, E., Walter, R. W., "The Performance of Natural and Synthetic Radial-Ply Winter Tyres on Ice and Hard Packed Snow", I.R.I.J., Dec 1972, Vol 6, No 6, pp 249-252

Tests with natural and synthetic radial-ply tires on polished lake ice were conducted on a two-wheeled trailer. The two tire-compounds were always tested alternately and the results expressed in the form of ratings.

Results showed that the natural rubber compound gave up to 40% better grip on ice than the synthetic control, the overall average improvement being 15%.

Tread compound

Spelman, R. H., Tarpinian, H. D., Johnson, D. E., Campbell, K. L., "SAE Study - Wet Pavement Braking Traction" SAE Paper 700462, May 1970 26 pp.

This four-part study is based upon tests planned and conducted by the SAE Tire Committee.

Three basic methods were used, based upon stopping distance, vehicle deceleration, and towed skid trailers.

Test data from various types and sizes of tires are presented which show the effect of tire wear, vehicle speed, and various test surfaces.

Tread geometry

Road wheel dimensions

Staughton, G. C., "The Effect of Tread Pattern Depth on Skidding Resistance" Road Research Laboratory Report LR 323, 1970, 9 pp.

The effect of tread pattern depth on skidding resistance in wet conditions was investigated on six road surfacings of differing textures with tires of current tread design in various stages of wear. Measurement of locked wheel and peak braking force coefficients were made over a speed range of 50 km/h to 130 km/h.

It was found that on the rougher surfaces where the surface texture already provides adequate drainage paths for the surface water to get away, the tread depth generally has only a small effect on the braking force coefficient, though in some instances large effects occur below 1 mm tread depth. On the smoother surfaces a more pronounced change occurs in braking force coefficient with tire wear which becomes very marked for tread depths less than 1 to 2 mm.

Tread geometry

Staughton, C., Williams, T., "Tyre Performance in Wet Surface Conditions", Road Research Lab., Crowthorne (England), 1970, 89 pp.

Results are given of tests to investigate the effect of water depth for a range of car tires, loads, inflation pressures, water depths and speeds both of the free rolling and locked wheel condition and to relate the results to the wet conditions likely to occur on roads.

Tire construction type

Tread geometry

Taft, P. H., "New Trends in Tires", Published in Interagency Motor Equipment Advisory Committees Management Conference Minutes, 1969, pp 12-17

The design and advantages of bias ply, radial ply, and belted bias ply tires, various tire materials, cords, and other factors are reviewed.

Tire construction type

Thieme, van Eldik, H.C.A., Pacejka, H.B., "The Tire as a Vehicle Component - Chapter 7", Mechanics of Pneumatic Tires, Samuel K. Clark, Editor, National Bureau of Standards Monograph 122, Nov. 1971, pp 545-839

The chapter contains a discussion of the performance differences of bias-ply and radial-ply tires, in terms of load-deflection relations, effective radius, rolling resistance, and carcass constriction.

Tire construction type

Tielking, J. T., "Construction and Profile Study, Part I; Tire Traction Data Measured by the HSRI Mobile Tire Tester", Highway Safety Research Institute, March, 1973, 186 pp

This is a compilation of traction data taken on various surfaces, wet and dry, with cross-ply, bias-belted, and radial-ply tires of various aspect ratios. A data evaluation is not included; it will be published in a separate report.

Tire construction type
Aspect ratio

Tielking, J. T., Fancher, P. S., Wild, R. E., "Mechanical Properties of Truck Tires", SAE Paper 730183, Jan 1973, 11 pp

Mechanical properties have been obtained from a recent series of truck tire tests using the Highway Safety Research Institute's (HSRI) flat bed tire testing machine.

Carpet plots of lateral force versus tire operating variables such as camber and slip angle are used to illustrate the effect of changes in ply rating, tread pattern, and wear. Corresponding variations in the mechanical properties are noted.

Tread geometry

Umland, C. W., Bannister, E., Tomlinson, C. B., "The Skid Resistant Properties of Butyl Tyres", Instn. Mech. Engrs., Symposium on Control of Vehicles, 1963, pp 91 - 97

The choice of rubber for use in the tire tread can have a large influence on skidding characteristics. Data on the effect of high-hysteresis elastomers on the safety characteristics of tires on various road surfaces have been accumulated with a variety of tires under conditions of both panic braking and high-speed cornering.

Tread compound

Wilson, M. A., "Tire Progress - Past, Present, and Future", SAE Paper 721A, August 1963, 7 pp.

In this paper the author refers to the most important advancements made in recent years with new and improved materials, rubbers and textiles, advancements in tire design and construction methods. Specific examples of recent important major trends in passenger car, truck, and earthmover types of tires are given.

General

Żeranski, P., "Factors Affecting Force Transmission at the Pneumatic Tyre", K.F.T., (In German), March, 1973, No. 3, p. 78-81

The paper shows that the radial tire can transmit a higher braking force at constant slip than the cross-ply type, the superiority being more pronounced at higher wheel-loads. Greater forces and coefficients of friction can be transmitted in the lateral direction by the radial than the cross-ply tire at constant slip-angle and for the same wheel-load.

Camber changes at constant slip-angle cause greater fluctuations in transmissible side force with a cross-ply than a textile-belted radial tire.

Tire construction type

Zoeppritz, H. P., "Requirements and Performance of Automobile Tires", (in German), Automobiltechnische Zeitschrift (ATZ), Vol. 66, No. 9, Sept. 1964, pp 250-256.

A general discussion of the relations between tire construction and performance data.

General

Veith, A. G., "Cooperative Correlation Program: University of Michigan HSRI Mobile Tire Tester vs. B. F. Goodrich Cornering Trailer." Company Document, B. F. Goodrich Company, 15 Aug 1972.

The objective was to determine the degree of correlation between the HSRI Mobile Tire Tester and the B. F. Goodrich Cornering Trailer by testing six sets of new tires with different tread patterns and a wide range of experimental tread compounds. The tests were conducted on two wet surfaces; a low-coefficient, low-macrotexture terrazzo ground; and an asphalt aggregate with intermediate coefficient and intermediate macrotexture roughness. Cornering tests were run at 12 deg slip angle at speeds between 30 and 60 mph. Discussion of results.

Tread geometry

Tread compound

Wild, R. F., "Wet Traction Test Program, Final Report," Mich., U. Ann Arbor, Highway Safety Research Insf., Rep No. HSRI PF 73-3, Aug 1973.

Eighty-six tires were measured for longitudinal and lateral traction capability on jennite, asphalt, and concrete wetted surfaces. The resulting data were subjected to a simple but thorough statistical analysis. Findings of general interest emerged showing the fallibility of the skid number for characterizing a tire pavement combination, the independent nature of lateral traction with respect to longitudinal traction, and indications of the effects on traction of tire diameter and load rating. Traction uniformity on concrete between identical tires was found to be excellent, while the traction differences on concrete between tires of the same size but of different manufacture were found to be statistically significant.

Tire construction type

Road wheel dimensions

B.1 Introduction

The tire model used for the simulated vehicle studies of this program was capable of generating lateral force, aligning torque, overturning moment and tractive force as functions of vertical load, slip angle, inclination angle and slip ratio. The lateral force model previously used in the NHTSA hybrid simulation computer program was used with a modification to provide a lateral friction coefficient which varied nonlinearly with vertical load.

New models were derived for aligning torque and overturning moment based on tire data measured in pilot test program. The braking force model previously used in the simulation was retained as was the tractive force/lateral force interaction modeling in which only the coefficients were changed based on tire data measured in this program.

The following sections of this appendix deal with the derivation of the aligning torque and overturning moment models and with procedures for obtaining tire model coefficients from measured tire data.

B.2 Derivation of Tire Aligning Torque Model

Tire Aligning Torque has previously been modeled in handling simulations with a very simple model, if it is modeled at all. The simple model generally consists of a constant "pneumatic trail" term which is multiplied by the tire lateral force to create a moment. It was determined that a more sophisticated representation of tire aligning torque was necessary for this program to allow individual tire differences to be more easily detected.

APPENDIX B

TIRE MODELING AND TIRE DATA REDUCTION TECHNIQUES

by

D. T. Kunkel

BELTED BIAS PLY

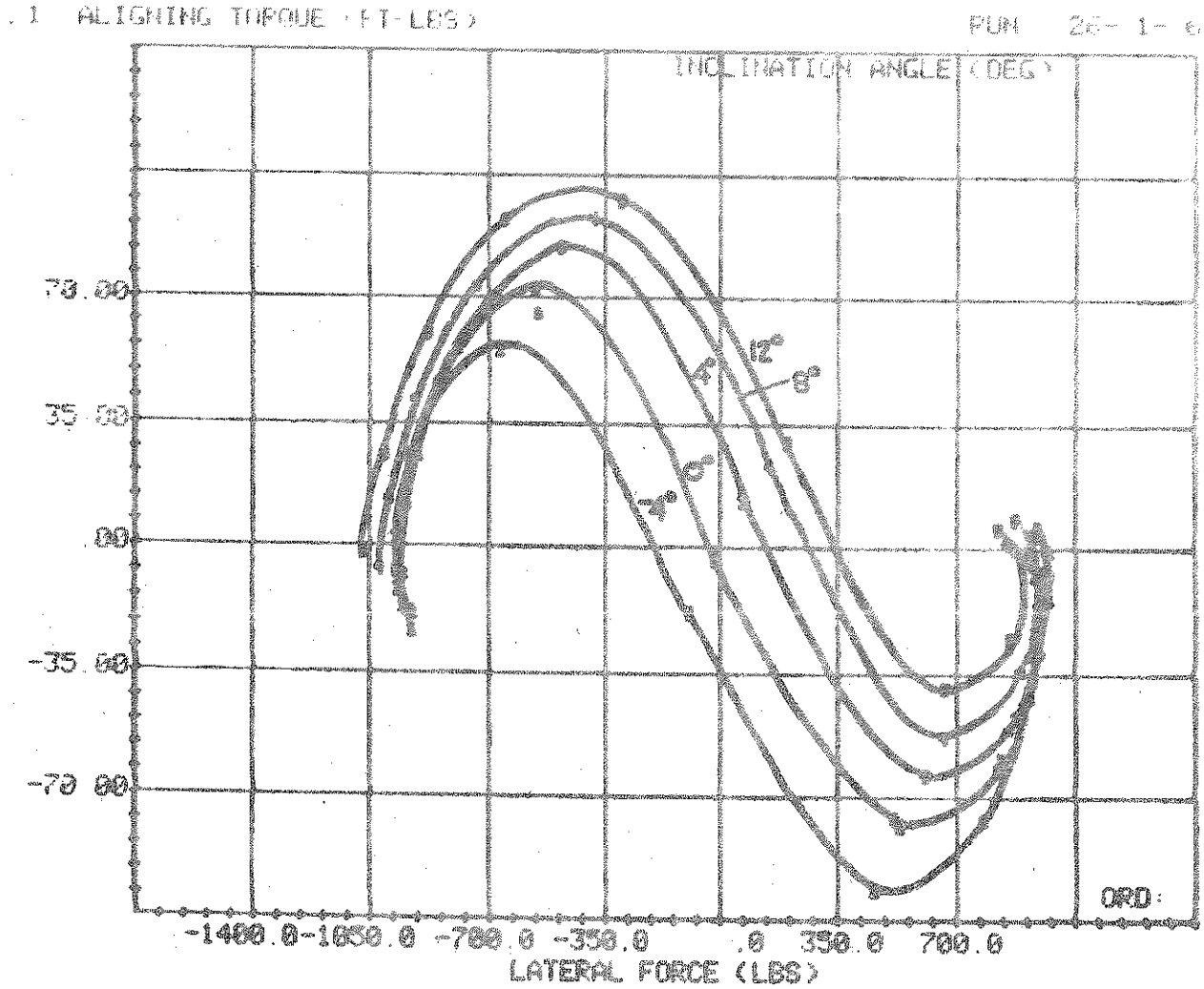

FIGURE B-1b

BIAS PLY

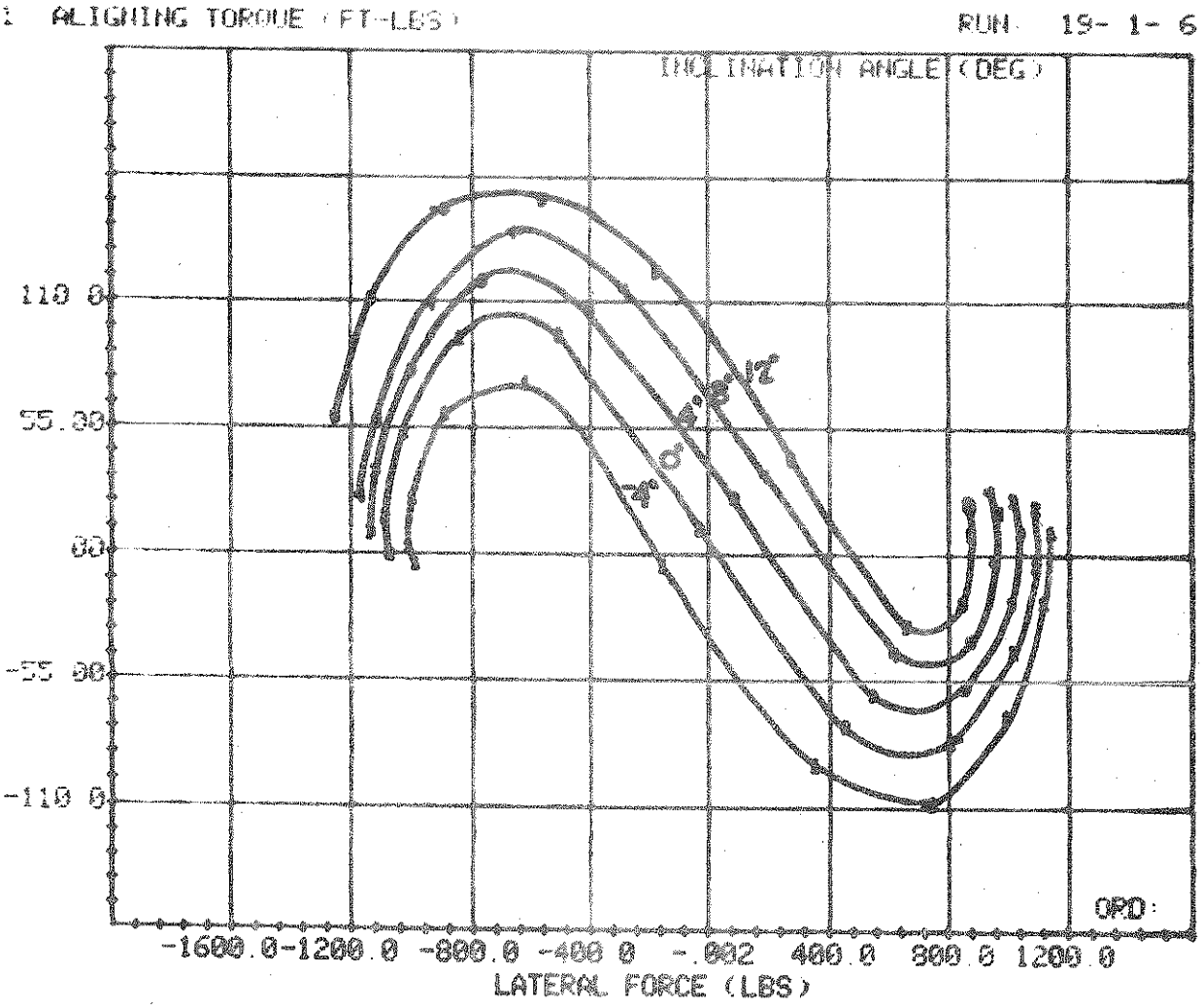

FIGURE B-1a

The first step in the determination of a new aligning torque (M_z) model was the determination of a suitable independent variable or variables. It was decided to use lateral force (F_y) as the primary independent variable for several reasons: lateral force would provide an automatic limit for aligning torque in a high slip angle situation, lateral force was a well-modeled function in its own right, and aligning torque was a well-behaved function of lateral force (see Figure B-1 for example).

Referring to the M_z - F_y plots of Figure B-1, it can be seen that the aligning torque is very nearly a parabolic function of the lateral force in the second and fourth quadrants. The curves also have a vertical shift due to inclination angle, which incorporates an inclination angle (γ) term in the expression. This gives us an expression of the form:

$$M_z = C_1 + C_2 F_y + C_3 F_y^2 + C_4 \gamma \qquad (1)$$

Neglecting the inclination angle effects for a moment and concentrating on the fourth quadrant, we plot lines of constant normal load on a lateral force - aligning torque plot (Figure B-2).

Upon close examination, it can be seen that this family of parabolas consists of parabolas of nearly identical shape, differing mainly in their vertical and horizontal shifts.

The general form of the expression for a parabola which is shifted down and to the right (but <u>not</u> rotated) is:

$$Y = -k_o + k_1 (x - k_2)^2 \qquad (2)$$

where all k_i are positive numbers and:

k_o is the vertical shift constant
k_1 is the shape constant
k_2 is the horizontal shift constant

RADIAL

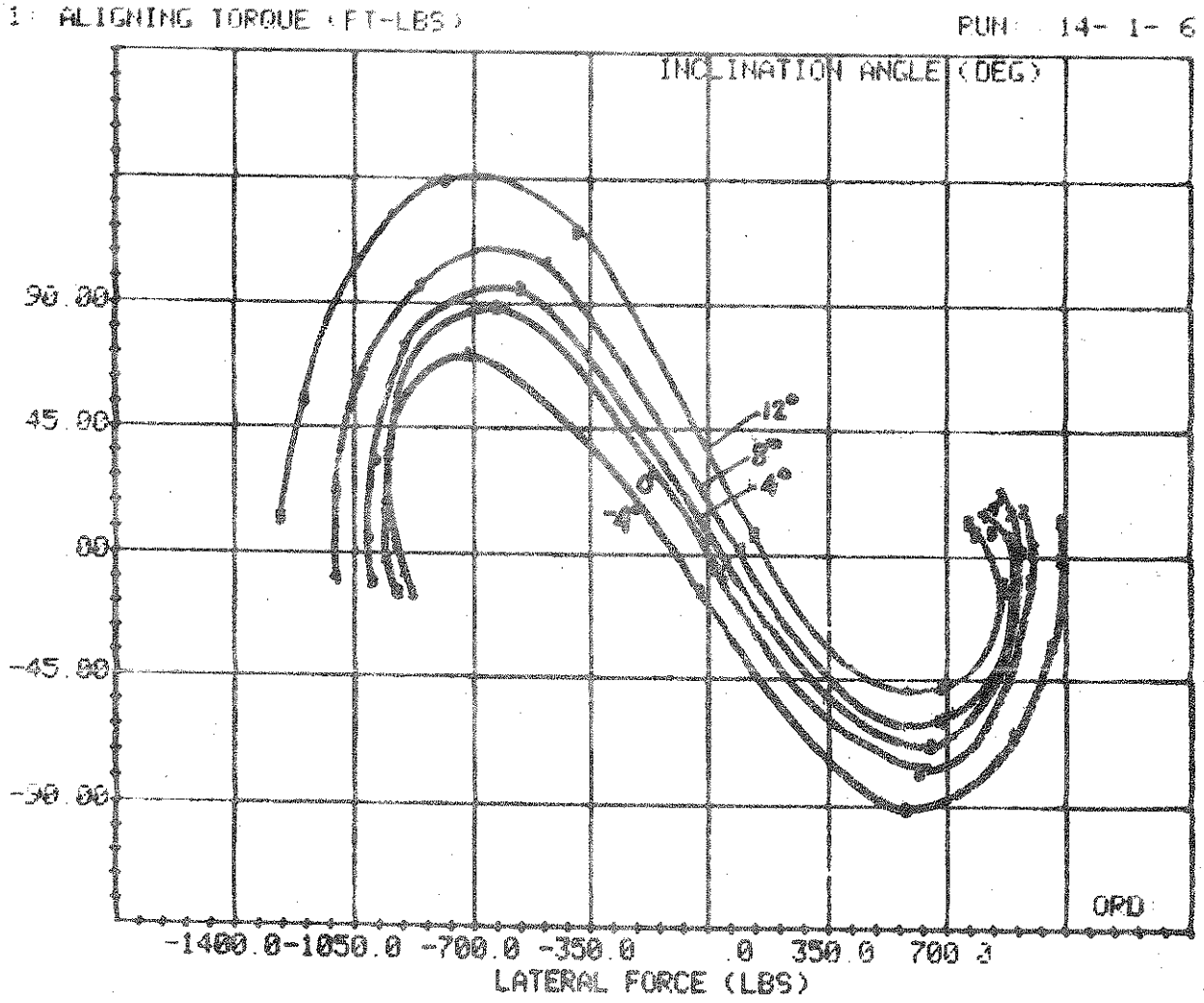

FIGURE B-1c

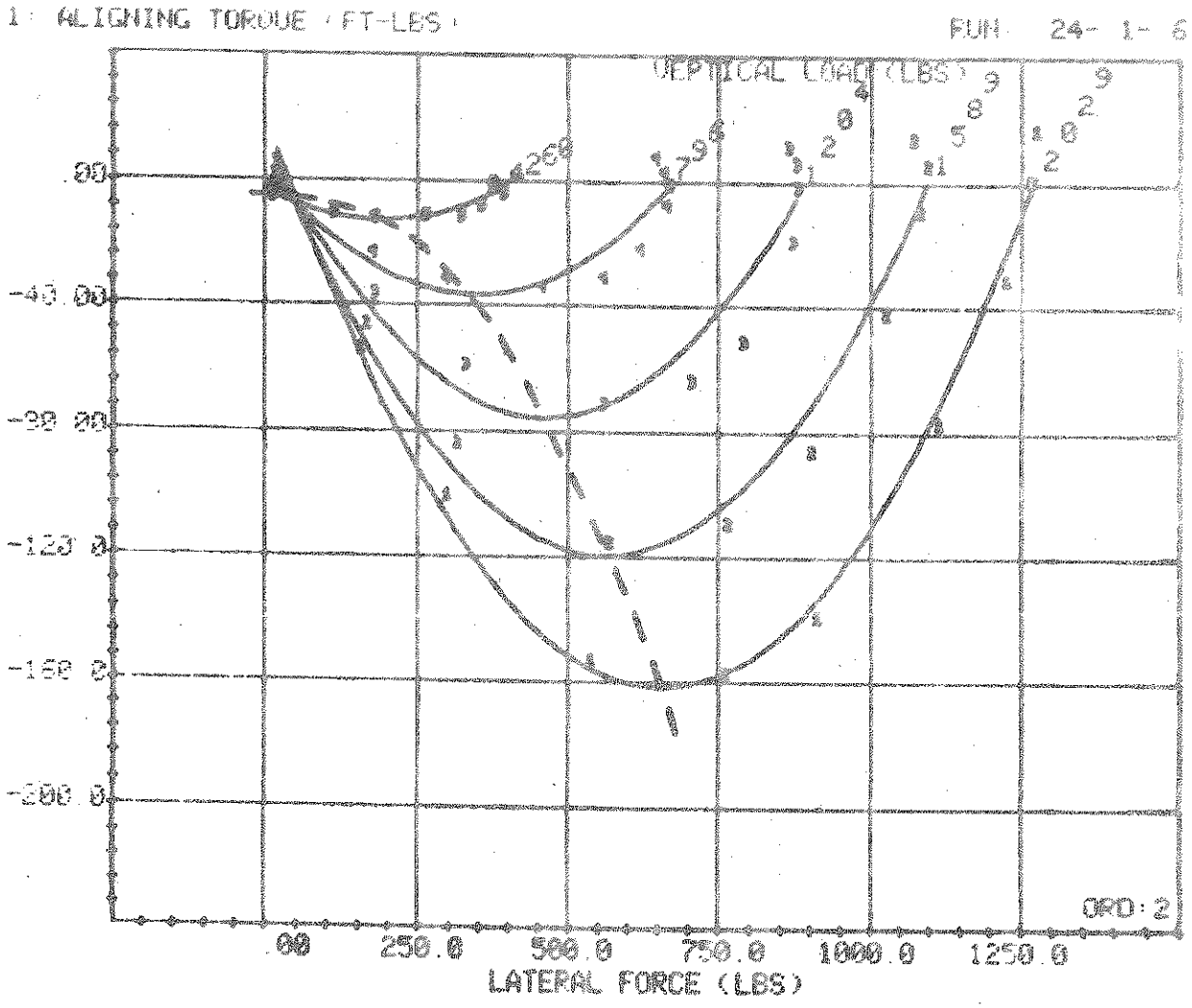
ALIGNING TORQUE (FT-LBS)
RUN 24- 1- 6
VERTICAL LOAD (LBS)
.00
-40.00
-80.00
-120.0
-160.0
-200.0
.00
250.0
500.0
750.0
1000.0
1250.0
LATERAL FORCE (LBS)
ORD: 2

FIGURE B-2

Since we are restricting X (lateral force) and Y (aligning torque) to both equal zero at the origin (i.e. - when $F_y = 0$, $M_z = 0$), the vertical shift and the horizontal shift are interrelated and we have:

$$k_o = k_1 k_2^2 \tag{3a}$$

or

$$k_2 = \sqrt{\frac{k_o}{k_1}} \tag{3b}$$

The vertical and horizontal shifts vary along a parabola with the same shape as the curves themselves (shown as the dashed line in Figure B-2).

Rewriting (2) we have:

$$M_z = -k_1 k_2^2 + k_1 (F_y - k_2)^2 \tag{4a}$$

or

$$M_z = -k_o + k_1 (F_y - \sqrt{\frac{k_o}{k_1}})^2 \tag{4b}$$

where:

k_1 is constant for <u>all</u> normal loads
k_o or k_2 = f (normal load)

Expanding:

$$M_z = -k_1 k_2^2 + k_1 F_y^2 - 2k_1 k_2 F_y + k_1 k_2^2 \tag{5a}$$

$$M_z = (-2k_1 k_2 + k_1 F_y) F_y \tag{6a}$$

or

$$M_z = -k_o + k_1 F_y^2 - 2k_1 \sqrt{\frac{k_o}{k_1}} F_y + k_o \tag{5b}$$

$$M_z = (-2 k_1 \sqrt{\frac{k_o}{k_1}} + k_1 F_y) F_y \tag{6b}$$

Now define two constants K_1 and K_2 such that:

$$K_1 = -2\sqrt{M C_2} \tag{14}$$

and

$$K_2 = C_2 \tag{15}$$

We then arrive at the simplified aligning torque expression (neglecting inclination angle effects):

$$M_2 = K_1 F_z F_y + K_2 F_y^2 \tag{16}$$

The inclination angle effect can be taken into account with a simple vertical shift of the parabola obtained from (16). The magnitude of the shift is dependent on both inclination angle and normal load; i.e.:

$$\text{Vert. Shift} = f(F_z, \gamma)$$

The shift appears to be a first order relation with F_z and a square root relation with γ, so substituting the shift into (16) we finally obtain the aligning torque as a function of F_y, F_z and γ.

$$M_z = K_1 F_z F_y + K_2 F_y^2 + K_3 F_z \gamma^{1/2} \tag{17}$$

The final form of the aligning torque expression, written in FORTRAN, is given below:

```
MZ = K1 * FZ * FY + K2 * SIGN (1, FY) * FY ** 2
+ K3 * SIGN (1, GAMMA) * FZ * SQRT
(ABS (GAMMA))
```

(18)

A polynomial expression obtained for a second order fit of aligning torque to lateral force will be of the form:

$$M_z = C_o + C_1 F_y + C_2 F_y^2 \tag{7}$$

in which C_o should be zero to satisfy the condition that $M_z = 0$ when $F_y = 0$; C_1 will always be a negative number; and C_2 will be either positive or negative, depending on the quadrant. The k_i's of Equation 2 can now be computed from the C_i's of Equation 7. In the fourth quadrant ($F_y > 0$, $M_z < 0$) we have:

$$k_o = \frac{C_1^2}{4C_2} \tag{8}$$

$$k_1 = C_2 \tag{9}$$

$$k_2 = -\frac{C_1}{2C_2} \tag{10}$$

Since k_o and k_2 are interdependent (from (3)), we choose the most convenient of the two to be a function of normal load (F_z). This appears to be k_o, which has a second order variation with normal load. We can write:

$$k_o = f(F_z) = M F_z^2 \tag{11}$$

Substituting (9) and (11) into (6b) we obtain:

$$M_z = \left(-2C_2 \sqrt{\frac{M F_z}{C_2}} + C_2 F_y\right) F_y \tag{12}$$

$$M_z = \left(-2 F_z \sqrt{M C_2} + C_2 F_y\right) F_y \tag{13}$$

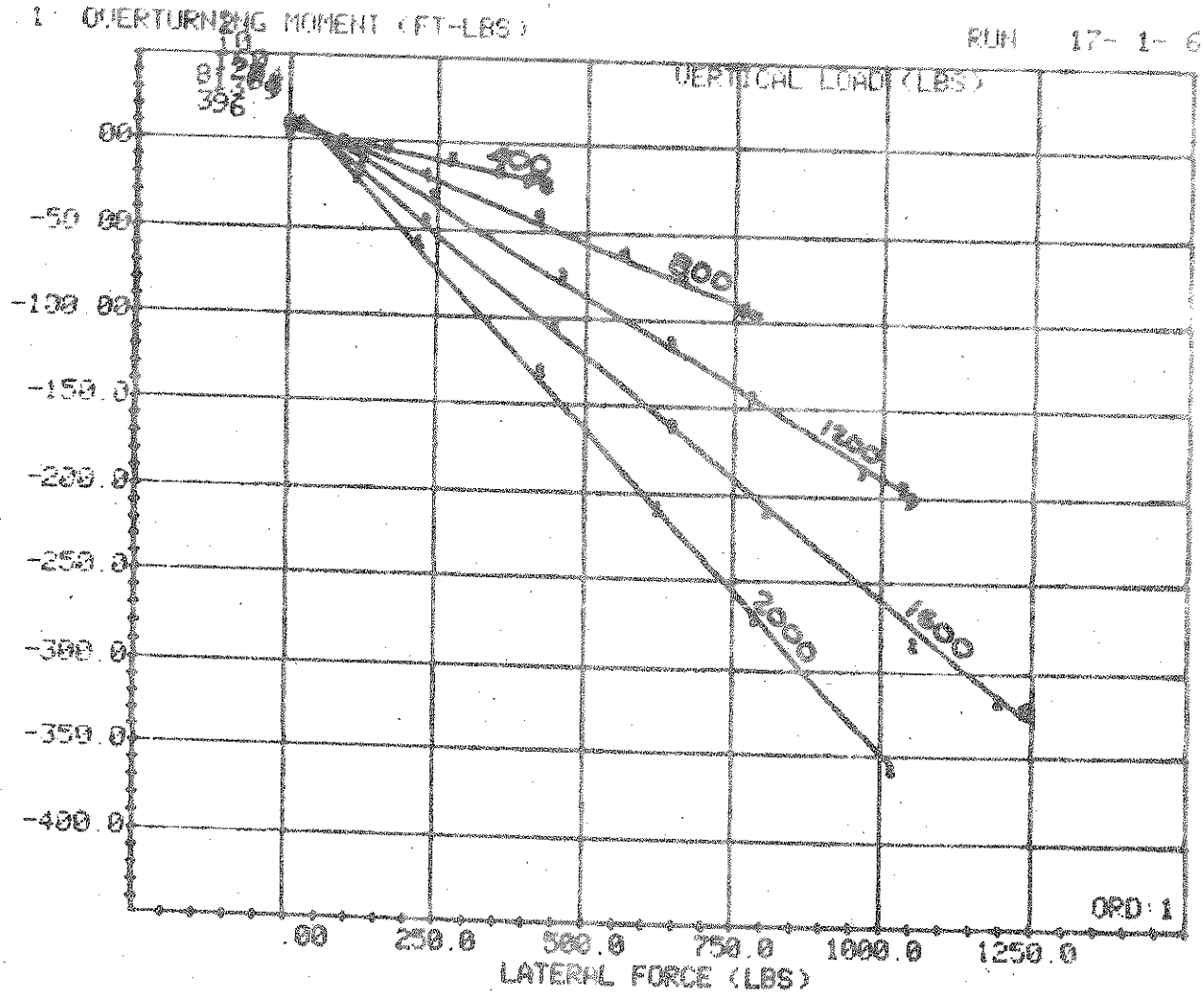
1 OVERTURNING MOMENT (FT-LBS)
RUN 17- 1- 6
VERTICAL LOAD (LBS)
396
400
800
1200
1600
2000
00
-50.00
-100.00
-150.0
-200.0
-250.0
-300.0
-350.0
-400.0
.00
250.0
500.0
750.0
1000.0
1250.0
LATERAL FORCE (LBS)
ORD: 1

FIGURE B-3

B.3 Derivation of Overturning Moment Model

The first step in modeling overturning moments, (M_x), as in modeling aligning torques, is the selection of a suitable independent variable or variables. It was decided to use lateral force as the primary independent variable for the same reasons as those used in its choice in the aligning torque model.

Referring to the overturning moment - lateral force plot in Figure B-3, it can be seen that overturning moment is a linear function of lateral force, with a slope dependent on normal load. The plot shows five normal loads: 2000, 1600, 1200, 800, and 400 pounds.

If inclination angles were always zero (as they were in the case of Figure B-3), overturning moment could simply be modeled as:

$$M_x = K_1 F_y \tag{19}$$

where

$$K_1 = f(F_z)$$

The coefficient K_1 is approximately linear with normal load, and goes to zero when the normal load goes to zero. Therefore we can write:

$$K_1 = C_1 F_z \tag{20}$$

and

$$M_x = C_1 F_z F_y \tag{21}$$

An inclination angle causes the slope of the lines in Figure B-3 to change, and also causes an overturning moment when the lateral force is zero.

RUN: 17- 1- 6

NORMAL LOAD	CORNERING STIFFNESS
2000	110
1600	120
1200	128
800	123
400	89

CORNERING FORCE COEFFICIENTS:

A0 = 3815.44
A1 = 6.71
A2 = 2613.78

RUN: 18- 1- 6

NORMAL LOAD	CAMBER STIFFNESS
2000	36
1600	33
1200	30
800	24
400	13
0	0

CAMBER FORCE COEFFICIENTS:

A3 = 2.09
A4 = 3934.38

RUN: 17- 1- 6

NORMAL LOAD	FRICTION COEFFICIENT
2000	.72
1600	.79
1200	.89
800	1.00
400	1.11

LATERAL FRICTION COEFFICIENTS:

A5 = 1.255
A6 = -.350E-03
A7 = .421E-07

FIGURE B-4 LATERAL FORCE COEFFICIENT PROGRAM OUTPUT

The change in slope due to inclination angle is approximately linear and can be accomodated by adding an additional term to (21):

$$M_z = (C_1 + C_2 \gamma) F_z F_y \tag{22}$$

The intercept shift can be modeled as a linear function of inclination angle and normal load:

$$\text{Intercept} = C_3 \gamma F_z \tag{23}$$

Combining (22) and (23) we obtain the overturning moment function

$$M_x = (C_1 + C_2 \gamma) F_z F_y + C_3 \gamma F_z \tag{24}$$

The final form of the overturning moment function, written in FORTRAN, is given below:

```
MX = FZ * (C1 * FY + C2 * FY * GAMMA
+ C3 * GAMMA)                                    (25)
```

B.4 Procedure for Obtaining Lateral Force Coefficients From Tire Test Data

The Lateral Force Tire Model has seven coefficients (excluding the velocity sensitive term of the lateral friction coefficient). These coefficients are obtained using a data reduction program written for the TIRF computer (see Section B.7). Figure B-4 is an example of the output from this program.

The camber stiffness coefficients, A_3 and A_4, are obtained in a similar manner to the cornering stiffness coefficients, using data from the γ -F_z run. Inclination angles outside the range $-5° \leq \gamma \leq 5°$ are eliminated and a third order function is fitted through the side force - inclination angle data to obtain the camber stiffness (C_γ, lb/deg) for each normal load. After conversion to lb/rad, the camber stiffnesses are fit to the normal loads to obtain:

$$C_\gamma = C_1 + C_2 F_z + C_3 F_z^2 \tag{30}$$

The coefficients A_3 and A_4 are:

$$A_3 = C_2 \tag{31}$$

$$A_4 = -C_2/C_3 \tag{32}$$

The lateral friction coefficients, A_5 - A_7, are obtained using data from the α -F_z run. The data is limited to slip angles greater than 5° or less than -5°, depending on the slip angles used in the run being fitted. A second order function is fitted through the normalized lateral force - slip angle data for each normal load. The maximum value of this function is solved for and printed out as the friction coefficient (μ_y). A second order fit was chosen to describe the data in this range since it is the highest order function to have a definite maximum. This maximum should coincide closely with the actual peak if one occurs, or extrapolate to determine the peak if none occurs within the measured range of slip angles (as in the case of high normal loads). The friction coefficients are fit to the normal loads to obtain the following equation:

$$\mu_y = B_3 + B_1 F_z + B_4 F_z^2 \tag{33}$$

which defines B_3, B_1, B_4. The lateral friction velocity sensitivity coefficient is B_2.

Two types of tire test runs are required to obtain the lateral force coefficients -

a run varying the slip angle (α) and normal load at zero inclination angle (α -F_z run), and

a run varying the inclination angle and normal load at zero slip angle (γ -F_z run).

The cornering stiffness coefficients, A_0, A_1, and A_2, are obtained using data from the α-F_z run. The slip angles outside the range $-5° \leq \alpha \leq +5°$ are eliminated, and a third order function is fitted through the lateral force - slip angle data for each normal load. The first derivative of this function at $\alpha = 0$ (multiplied by -1) is printed out as the cornering stiffness (C_{s0}, lb/deg). This cornering stiffness (multiplied by 57.3) is fitted to the normal load to obtain an equation of the form:

$$C_\alpha = C_1 + C_2 F_z + C_3 F_z^2 \tag{26}$$

The coefficients A_0 - A_2 are then:

$$A_0 = C_1 \tag{27}$$

$$A_1 = C_2 \tag{28}$$

$$A_2 = -C_2/C_3 \tag{29}$$

RUN: 17- 1- 6

NORMAL LOAD	PEAK ALIGNING TORQUE
2000	-195
1600	-148
1200	-100
800	-56
400	-24

ALIGNING TORQUE COEFFICIENTS:

K1 = -.314E-03
K2 = .365E-03

RUN: 19- 1- 6

CAMBER ANGLE	ALIGNING TORQUE
0	-2
4	46
8	81
12	104

ALIGNING TORQUE COEFFICIENTS:

K3 = .173E+00

RUN: 17- 1- 6

NORMAL LOAD	SLOPE
2000	-.34
1600	-.27
1200	-.20
800	-.13
400	-.06

OVERTURNING MOMENT COEFFICIENTS:

C1 = -.178E-03

RUN: 19- 1- 6

CAMBER ANGLE	INTERCEPT	SLOPE
0	1.1	-.19
4	-20.4	-.21
8	-35.6	-.24
12	-48.3	-.28

OVERTURNING MOMENT COEFFICIENTS:

C2 = -.352E-03
C3 = -.195E+00

FIGURE B-5 ALIGNING TORQUE AND OVERTURNING MOMENT COEFFICIENT PROGRAM OUTPUT

B.5 Procedure for Obtaining Aligning Torque Coefficients From Tire Test Data

The three Aligning Torque Coefficients (K_1-K_3) for the Tire Aligning Torque Model (see Section B.2), were obtained using a data reduction program written for the TIRF computer (see Section B.7). Figure B-5 is an example of the output from this program. Two different tire test runs are required to obtain the Aligning Torque Coefficients - a run varying slip angles and vertical loads at zero inclination angle, and a run varying slip angles and inclination angles at a constant vertical load.

Coefficients K_1 and K_2 are obtained from the slip angle - vertical load run by first examining the data and constraining the slip angles to be fitted to be all positive or all negative (depending on whether primarily positive or negative slip angles were used in the run being fitted). A second order function is then fit to the lateral force - aligning torque data to give:

$$M_z = C(1) + C(2)\, F_y + C(3)\, F_y^2 \tag{34}$$

for each normal load.

The peak value of the aligning torque for each normal load is then calculated:

$$M_{z\,max} = C(1) - \frac{C(2)^2}{4C(3)} \tag{35}$$

The load effect is accounted for by taking a load weighted average of the maximum aligning torques to obtain a "load factor"

$$\text{Load Factor} = \frac{\sum_{i=1}^{n} \frac{M_{z\,max\,i}}{F_{zi}}}{\sum_{i=1}^{n} F_{zi}} \tag{36}$$

Figure B-5 is an example of the output from this program. The same two run types are required to obtain the coefficients as were required for the Aligning Torque Coefficients - a run varying slip angles and vertical loads at zero inclination angle, and a run varying slip angles and inclination angles at a fixed vertical load.

Coefficient C_1 is obtained from the slip angle - vertical load run. The procedure is similar to that followed for the aligning torque coefficients - the slip angles are first constrained to be all positive or all negative, and then a function is fit to the lateral force-overturning moment data. In the case of the overturning moments, this is a first order fit to give:

$$M_x = C(1) + C(2)\, F_y \tag{41}$$

In this fit, C(1) is assumed to be zero and coefficient C_1 is simply a load weighted average of the C(2)'s:

$$C_1 = \frac{\sum_{i=1}^{n} C(2)_i}{\sum_{i=1}^{n} F_{z_i}} \tag{42}$$

Coefficients C_2 and C_3 are obtained from the slip angle - inclination angle run. For each inclination angle, a first order function is fit to the lateral force-normalized overturning moment data to give an equation of the same form as (41):

$$\frac{M_x}{F_z} = C(1) + C(2)\, F_y \tag{43}$$

The slopes (C(2)) and intercepts (C(1) of these functions are then fit to the inclination angles at which they were obtained to give two equations, the coefficients of which are the overturning moment coefficients C_1 and C_2:

$$C(2) = C_2\, \gamma \tag{44}$$

$$C(1) = C_3\, \gamma \tag{45}$$

The shape coefficient, K_2, is the average value of the second order coefficients of (34).

$$K_2 = \frac{\sum_{i=1}^{n} C(3)}{n} \qquad (37)$$

The load shift coefficient, K_1, is calculated next:

$$K_1 = -2\sqrt{K_2 \cdot \text{Load Factor}} \qquad (38)$$

The inclination angle effect coefficient is calculated using data obtained from the run varying slip angle and inclination angle. The Aligning Torques are first normalized by dividing by the normal load. Next, a second order curve is fit to the lateral force - normalized aligning torque data for each inclination angle to give an equation of the same form as (34):

$$\frac{M_z}{F_z} = C(1) + C(2)\, F_y + C(3)\, F_y^2 \qquad (39)$$

The zero lateral force intercept of the second order curve is given by C(1), which then gives a set of C(1) for different inclination angles. K_3 is then the first order coefficient of a fit to this data:

$$C(1) = K_3\, \gamma \qquad (40)$$

B.6 Procedure for Obtaining Overturning Moment Coefficients From Tire Test Data

The three Overturning Moment Coefficients (C_1-C_3) for the Overturning Moment Model (see Section B.3) were obtained using the same program as that used for the Aligning Torque Coefficients.

```
RUN NO. 13982   DATE  06/06/74    TIME  1448           LISTING OF MODULE KUTASK2F

DESCRIPTION          TIRE LF MODEL COEFFICIENTS

MASTER FILE          PROGMDEV
ADDED TO MASTER      06/06/74
LAST DATE COPIED       NONE
LAST UPDATE          06/06/74  1446

PASSWORD             WVVG
PROGRAMMER           D.KUNKEL
PROC PARAMETER       $NOJCL
```

```
C TASK 2F
C *************************************************************************
C
C       LATERAL FORCE MODEL COEFFICIENT GENERATING SUBTASK OF TASK 21
C
C *************************************************************************
C
C SEE THE DISPLAY PROGRAM FOR AN IDENTIFICATION OF THE VARIABLES
C IN COMMON
      COMMON NCHAR,LPTR,ERROR,LINE,LUN08,LUN09,C
      COMMON JMODE,JTYPE,NVARS,LVARS,NAUTO,LAUTO,JAUTO
      COMMON NXVAR,NXNUM,IXVAR,XMIN,XMAX,XLOW,XORG,XFACT
      COMMON NYVAR,NYNUM,IYVAR,YMIN,YMAX,YLOW,YORG,YFACT
      COMMON NRUN,NOVER,IOVER,DATA
      COMMON NPARM,NPNUM,IPARM,PMIN,PMAX,PLOW,PORG,PFACT
      COMMON NTEM1,TEMP1,NTEM2,TEMP2,NTEM3,TEMP3,NTEM4,TEMP4
      COMMON NCNST,ICVAR,ICNUM,CNST,PREC,NREPS,IREPS
      DIMENSION LINE(72),C(4)
      DIMENSION IXVAR(6),XMIN(3),XMAX(3),XLOW(3),XORG(3),XFACT(3)
      DIMENSION IYVAR(6),YMIN(3),YMAX(3),YLOW(3),YORG(3),YFACT(3)
      DIMENSION IOVER(6,6),DATA(31)
      DIMENSION IPARM(6),PMIN(3),PMAX(3),PLOW(3),PORG(3),PFACT(3)
      DIMENSION TEMP1(20),TEMP2(20),TEMP3(20),TEMP4(20)
      DIMENSION ICVAR(20),ICNUM(20),CNST(20),PREC(31),IREPS(6,6)
      DIMENSION IN(1)
C COPY COMMON FROM FILE 62
      REWIND 3
*      B    Z3
* Z1   DATA MAINCO
*      DATA COMMON
* Z2   DATA 0
*      DATA 0
*      DATA X'C4C2'
* Z3   LA   3,FF-FFF
*      SA   3,COMMON
*      ST   3,Z2
*      MLA  1,Z2
*      LA   3,Z1
```

B.1 Data Reduction Computer Program Listings

```
      20    WRITE(1,21)(IOVER(I,1),I=1,3)                                    00000920
      21    FORMAT(10X,'RUN: ',I3,'-',I2,'-',I2)                            00000930
            WRITE(1,22)                                                      00000940
      22    FORMAT(//,8X,'NORMAL      CORNERING',                            00000950
           1//,9X,'LOAD       STIFFNESS',//)                                00000960
            NSPAC=0                                                          00000970
            SIGN=-1.                                                         00000980
            GO TO 40                                                         00000990
      C CHECK IF CAMBER RUN WAS SUPPLIED                                     00001000
      30    WRITE(1,21)(IREP5(I,I),I=1,3)                                    00001010
      31    FORMAT(46X,'RUN: ',I3,'-',I2,'-',I2)                            00001020
            WRITE(1,32)                                                      00001030
      32    FORMAT(//,44X,'NORMAL       CAMBER',                           00001040
           1//,45X,'LOAD       STIFFNESS',//)                                00001050
            NSPAC=36                                                         00001060
            SIGN=1.                                                          00001070
      C REPEAT FOR EACH NORMAL LOAD                                          00001080
      40    DO 50 NFIT=1,NFITS                                               00001090
            GO TO(44,47),NXNOW                                               00001100
      44    IF(TEMP4(NFIT)-100.)45,45,47                                     00001110
      45    IF(NFIT-1)99,46,50                                               00001120
      46    CALL FIT(0.,0.,1,2,1)                                            00001130
            GO TO 50                                                         00001140
      C GET STIFFNESS                                                        00001150
      47    CALL FIT(C.,0.,NFIT,3,3)                                         00001160
      C CHANGE SIGN IF CORNERING STIFFNESS                                   00001170
            C(2)=SIGN*C(2)                                                   00001180
            CALL SPACE(NSPAC)                                                00001190
      C PRINT OUT THE VALUES                                                 00001200
            DUMMY=(TEMP4(NFIT)+45.)/100.                                     00001210
            IDUMM=DUMMY                                                      00001220
            DUMMY=IDUMM                                                      00001230
            VL=DUMMY*100.                                                    00001240
            IVAL1=VL                                                         00001250
            IVAL2=C(2)                                                       00001260
            WRITE(1,41)IVAL1,IVAL2                                           00001270
      41    FORMAT(6X,I5,8X,I4)                                              00001280
            IF(NFIT-1)99,42,43                                               00001290
      C SET UP FOR FITTING CORNERING FORCE AND CAMBER FORCE FUNCTIONS        00001300
      42    CALL FIT(C.,0.,1,2,1)                                            00001310
      C ACCUMULATE WEIGHTED SUMS                                             00001320
      43    C(2)=C(2)*57.3                                                   00001330
            CALL FIT(VL,C(2),1,2,2)                                          00001340
      50    CONTINUE                                                         00001350
      C GET COEFFICIENTS FOR CORNERING FORCE AND CAMBER FORCE FUNCTIONS      00001360
            CALL FIT(0.,0.,1,2,3)                                            00001370
            C(3)=-C(2)/C(3)                                                  00001380
            GO TO(60,70),NXNOW                                               00001390
      60    WRITE(1,61)                                                      00001400
      61    FORMAT(//,4X,'CORNERING FORCE COEFFICIENTS:')                    00001410
            WRITE(1,62)C(1),C(2),C(3)                                        00001420
      62    FORMAT(//,12X,'A0 =',F8.2,/,12X,'A1 = ',F7.2,/,12X,'A2 =',F8.2)  00001430
            GO TO 80                                                         00001440
```

```
*       SA    3,MAINLD                                                  00000390
*       SXBS  *127                                                      00000400
C DEFINE VARIABLES FOR THE LATERAL FORCE FUNCTIONS                      00000410
      NRUN=1                                                            00000420
      NXVAR=2                                                           00000430
C STEER ANGLE                                                           00000440
      IXVAR(1)=3                                                        00000450
C CAMBER ANGLE                                                          00000460
      IXVAR(2)=4                                                        00000470
      NYVAR=1                                                           00000480
      NYNOW=1                                                           00000490
C LATERAL FORCE                                                         00000500
      IYVAR(1)=8                                                        00000510
      NPARM=1                                                           00000520
      NPNOW=1                                                           00000530
C NORMAL LOAD                                                           00000540
      IPARM(1)=5                                                        00000550
C DEFINE CONSTRAINTS ON ANGLES AND NORMAL LOAD                          00000560
      NCNST=5                                                           00000570
C 1. STEER ANGLE GE -5                                                  00000580
      ICVAR(1)=3                                                        00000590
      ICNUM(1)=4                                                        00000600
      CNST(1)=-5.                                                       00000610
C 2. STEER ANGLE LE 5                                                   00000620
      ICVAR(2)=3                                                        00000630
      ICNUM(2)=2                                                        00000640
      CNST(2)=5.                                                        00000650
C 3. CAMBER ANGLE GE -5                                                 00000660
      ICVAR(3)=4                                                        00000670
      ICNUM(3)=4                                                        00000680
      CNST(3)=-5.                                                       00000690
C 4. CAMBER ANGLE LE 5                                                  00000700
      ICVAR(4)=4                                                        00000710
      ICNUM(4)=2                                                        00000720
      CNST(4)=5.                                                        00000730
C 5. NORMAL LOAD GT 100                                                 00000740
      ICVAR(5)=5                                                        00000750
      ICNUM(5)=5                                                        00000760
      CNST(5)=100.                                                      00000770
C COPY REPEAT RUN DATA INTO OVERLAY MATRIX                              00000780
      DO 5 I=1,6                                                        00000790
5     IOVER(2,I)=IREPS(I,1)                                             00000800
C REPEAT FOR SLIP RUN AND CAMBER RUN                                    00000810
10    DO 80 NXNOW=1,2                                                   00000820
      GO TO(11,12),NXNOW                                                00000830
C CHECK IF A SLIP RUN WAS SUPPLIED                                      00000840
11    IF(NOVER)80,80,12                                                 00000850
C CHECK IF A CAMBER RUN WAS SUPPLIED                                    00000860
12    IF(NREPS)80,80,13                                                 00000870
C FIT LATERAL FORCE TO THE ANGLE AS A FUNCTION OF NORMAL LOAD           00000880
13    CALL FITYP(0,0,0,XSIGN,NFITS)                                     00000890
      CALL HOME                                                         00000900
      GO TO(20,30),NXNOW                                                00000910
```

```
      CALL FIT(0.,0.,NFIT,2,3)                                                  00001980
C USING THE COEFFICIENTS OF THE SECOND ORDER FIT, SOLVE FOR THE MAXIMUM         00001990
C (OR MINIMUM) VALUE OF NORMALIZED LATERAL FORCE AND CALL IT THE                00002000
C EFFECTIVE COEFFICIENT OF FRICTION FOR THAT LOAD.                              00002010
      EMU=C(1)-C(2)**2/(4.*C(3))                                                00002020
C CHECK THE SIGN OF THE FRICTION COEFFICIENT                                    00002030
      IF(EMU)111,111,112                                                        00002040
111   EMU=-EMU                                                                  00002050
112   DUMMY=(TEMP4(NFIT)+45.)/100.                                              00002060
      IDUMM=DUMMY                                                               00002070
      DUMMY=IDUMM                                                               00002080
      VL=DUMMY*100.                                                             00002090
      IVALI=VL                                                                  00002100
C PRINT OUT THE VALUES                                                          00002110
      WRITE(1,104)IVALI,EMU                                                     00002120
104   FORMAT(21X,I5,19X,F4.2)                                                   00002130
114   IF(NFIT-1)99,115,116                                                      00002140
C SET UP FOR FITTING LOAD VARYING FRICTION FUNCTION                             00002150
115   CALL FIT(0.,0.,1,2,1)                                                     00002160
116   IF(TEMP4(NFIT)-100.)100,100,117                                           00002170
C ACCUMULATE WEIGHTED SUMS                                                      00002180
117   CALL FIT(VL,EMU,1,2,2)                                                    00002190
100   CONTINUE                                                                  00002200
C GET COEFFICIENTS FOR LOAD VARYING FRICTION FUNCTION                           00002210
      CALL FIT(0.,0.,1,2,3)                                                     00002220
      WRITE(1,105)                                                              00002230
105   FORMAT(//,22X,'LATERAL FRICTION COEFFICIENTS:',//)                        00002240
      WRITE(1,106)C(1),C(2),C(3)                                                00002250
106   FORMAT(29X,'A5 = ',F7.3,/,29X,'A6 = ',E10.3,/,29X,'A7 = ',E10.3)          00002260
90    CALL HOLD(IN)                                                             00002270
      CALL CHOUT(27)                                                            00002280
      CALL CHOUT(12)                                                            00002290
      WAIT(80)                                                                  00002300
*      LA    3,X'0821'                                                        00002310
*      SXBS *127                                                              00002320
99    STOP                                                                      00002330
      END                                                                       00002340
```

```
70      WRITE(1,71)                                                     00001450
71      FORMAT(//,41X,'CAMBER FORCE COEFFICIENTS:')                     00001460
        WRITE(1,72)C(2),C(3)                                            00001470
72      FORMAT(//,48X,'A3 = ',F7.2,/,48X,'A4 =',F8.2)                   00001480
80      NRUN=NRUN+1                                                     00001490
        CALL HOLD(IN)                                                   00001500
        CALL CHOUT(27)                                                  00001510
        CALL CHOUT(12)                                                  00001520
        WAIT(80)                                                        00001530
C RETURN TO SLIP RUN TO COMPUTE LOAD VARYING FRICTION COEF. FUNCTION    00001540
        NRUN=1                                                          00001550
C REDEFINE VARIABLES FOR LOAD VARYING FRICTION COEFFICIENT FUNCTION     00001560
C STEER ANGLE                                                           00001570
        NXNOW=1                                                         00001580
C NORMALIZED LATERAL FORCE                                              00001590
        NYVAR=1                                                         00001600
        NYNOW=1                                                         00001610
        IYVAR(1)=27                                                     00001620
C EXAMINE RANGE OF DATA                                                 00001630
        NCNST=0                                                         00001640
        CALL XTRMS(XSGN,PSIGN)                                          00001650
C REDEFINE CONSTRAINTS                                                  00001660
        NCNST=2                                                         00001670
        IF(XMAX(1)-ABS(XMIN(1)))120,110,110                             00001680
C RESTRICT STEER ANGLE TO VALUES GREATER THAN 5.0 DEGREES OR LESS THAN  00001690
C -5.0 DEGREES, DEPENDING ON WHETHER POSITIVE OR NEGATIVE STEER ANGLES  00001700
C WERE USED IN THE RUN BEING FITTED.  THE ELIMINATION OF STEER ANGLES   00001710
C IN THE RANGE OF -5.0 < SA < 5.0 IS DONE TO IMPROVE THE QUALITY OF     00001720
C THE SECOND ORDER FIT IN THE RANGE OF STEER ANGLES OF INTEREST.        00001730
C 1. STEER ANGLE GE 5.0                                                 00001740
110     ICVAR(1)=3                                                      00001750
        ICNUM(1)=4                                                      00001760
        CNST(1)=5.0                                                     00001770
        GO TO 130                                                       00001780
C 1. STEER ANGLE LE -5.0                                                00001790
120     ICVAR(1)=3                                                      00001800
        ICNUM(1)=2                                                      00001810
        CNST(1)=-5.0                                                    00001820
C 2. VERTICAL LOAD GT 100                                               00001830
130     ICVAR(2)=5                                                      00001840
        ICNUM(2)=5                                                      00001850
        CNST(2)=100.                                                    00001860
C FIT NORMALIZED LATERAL FORCE TO THE SLIP ANGLE                        00001870
C AS A FUNCTION OF VERTICAL LOAD                                        00001880
        CALL FITYP(0,0,0,XSIGN,NFITS)                                   00001890
        WRITE(1,102)((ICVER(I,J),I=1,3)                                 00001900
102     FORMAT(29X,'RUN: ',I3,'-',I2,'-',I2)                            00001910
        WRITE(1,103)                                                    00001920
103     FORMAT(//,21X,'NORMAL',17X,'FRICTION',/                         00001930
     *,22X,'LOAD',16X,'COEFFICIENT',//)                                 00001940
C REPEAT FOR EACH NORMAL LOAD                                           00001950
        DO 160 NFIT=1,NFITS                                             00001960
        IF(TEMP4(NFIT)-100.)114,114,118                                 00001970
```

```
C ASK FOR SLIP ANGLE - LOAD RUN                                          00000390
11    CALL MEMO4(19)                                                     00000400
      CALL SPACE(13)                                                     00000410
      NOVER=0                                                            00000420
      CALL RUNS(1,IOVER,NOVER)                                           00000430
      IF(ERROR)12,12,11                                                  00000440
111   CALL MEMO4(17)                                                     00000450
      GO TO 11                                                           00000460
C ASK FOR SLIP ANGLE - CAMBER ANGLE RUN                                  00000470
12    WRITE(1,2)                                                         00000480
2     FORMAT(*+ SLIP - CAMBER RUN?*)                                     00000490
      CALL SPACE(22)                                                     00000500
      NREPS=0                                                            00000510
      CALL RUNS(1,IREPS,NREPS)                                           00000520
      IF(ERROR)13,13,121                                                 00000530
121   CALL MEMO4(17)                                                     00000540
      GO TO 12                                                           00000550
C PROCEED??                                                              00000560
13    CALL MAYBE(ABORT)                                                  00000570
      IF(ABORT)14,14,10                                                  00000580
14    CALL ERASE                                                         00000590
C COPY SLIP ANGLE - CAMBER ANGLE RUN DATA INTO OVERLAY MATRIX            00000600
      DO 15 J=1,6                                                        00000610
15    IOVER(2,J)=IREPS(1,J)                                              00000620
C DEFINE VARIABLES FOR ALIGNING TORQUE FUNCTION                          00000630
C AND OVERTURNING MOMENT FUNCTION                                        00000640
      NKON=1                                                             00000650
      NXVAR=1                                                            00000660
      NYVAR=2                                                            00000670
      NPARM=2                                                            00000680
      NXNOW=1                                                            00000690
      NYNOW=1                                                            00000700
      NPNOW=1                                                            00000710
C LATERAL FORCE (X VARIABLE)                                             00000720
      IXVAR(1)=8                                                         00000730
C ALIGNING TORQUE (Y VARIABLE)                                           00000740
      IYVAR(1)=12                                                        00000750
C OVERTURNING MOMENT (Y VARIABLE)                                        00000760
      IYVAR(2)=10                                                        00000770
C VERTICAL LOAD (PARAMETER)                                              00000780
      IPARM(1)=5                                                         00000790
C CAMBER ANGLE (PARAMETER)                                               00000800
      IPARM(2)=4                                                         00000810
C EXAMINE RANGE OF STEER ANGLES AND VERTICAL LOADS OR CAMBER ANGLES      00000820
      VLMAX=0.0                                                          00000830
      CAMAX=0.0                                                          00000840
      CAMIN=0.0                                                          00000850
16    SAMAX(NRUN)=0.0                                                    00000860
      SAMIN(NRUN)=0.0                                                    00000870
C GET NUMBER OF SLEWS IN THE RUN                                         00000880
      NSLEW=IOVER(NRUN,6)                                                00000890
C POSITION TO FIRST DATA RECORD                                          00000900
      CALL POSITE(LUN09,IOVER(NRUN,5))                                   00000910
```

RUN NO. 13953 DATE 06/06/74 TIME 1127 LISTING OF MODULE KUTASK77

DESCRIPTION AT AND OM MODEL COEFFICIENTS

MASTER FILE PROGMDEV
ADDED TO MASTER 06/06/74
LAST DATE COPIED NONE
LAST UPDATE NONE

PASSWORD MJKS
PROGRAMMER D.KUNKEL
PROC PARAMETER $NOJCL

```
C  TASK 77                                                                    00000010
C  ************************************************************************00000020
C                                                                            00000030
C   ALIGNING TORQUE AND OVERTURNING MOMENT COEFFICIENT GENERATING TASK       00000040
C                                                                            00000050
C  ************************************************************************00000060
C                                                                            00000070
      COMMON NCHAR,LPTR,ERROR,LINE,LUNO8,LUNO9,C                             00000080
      COMMON JMODE,JTYPE,NVARS,LVARS,NAUTO,LAUTO,JAUTO                       00000090
      COMMON NXVAR,NXNOW,IXVAR,XMIN,XMAX,XLOW,XORG,XFACT                     00000100
      COMMON NYVAR,NYNOW,IYVAR,YMIN,YMAX,YLOW,YORG,YFACT                     00000110
      COMMON NRUN,NOVER,IOVER,DATA                                           00000120
      COMMON NPARM,NPNOW,IPARM,PMIN,PMAX,PLOW,PORG,PFACT                     00000130
      COMMON NTEM1,TEMP1,NTEM2,TEMP2,NTEM3,TEMP3,NTEM4,TEMP4                 00000140
      COMMON NCNST,ICVAR,ICNUM,CNST,PREC,NREPS,IREPS                         00000150
      DIMENSION LINE(72),C(4)                                                00000160
      DIMENSION IXVAR(6),XMIN(3),XMAX(3),XLOW(3),XORG(3),XFACT(3)            00000170
      DIMENSION IYVAR(6),YMIN(3),YMAX(3),YLOW(3),YORG(3),YFACT(3)            00000180
      DIMENSION IPARM(6),PMIN(3),PMAX(3),PLOW(3),PORG(3),PFACT(3)            00000190
      DIMENSION IOVER(6,6),DATA(31)                                          00000200
      DIMENSION TEMP1(20),TEMP2(20),TEMP3(20),TEMP4(20)                      00000210
      DIMENSION ICVAR(20),ICNUM(20),CNST(20),PREC(31),IREPS(6,6)             00000220
      DIMENSION ITYPE(6,2),MODE(3,2),ICONS(6),LDUM(20),LDT(9)                00000230
      DIMENSION SAMAX(2),SAMIN(2),IANG(2),CASUM(20),FZSUM(20),FITN(20)       00000240
      LUNO9=184                                                              00000250
      JMODE=1                                                                00000260
      MODE(1,1)=219                                                          00000270
      MODE(1,2)=668                                                          00000280
      ICONS(1)=256                                                           00000290
      ICONS(2)=221                                                           00000300
      ICONS(3)=219                                                           00000310
      ICONS(4)=211                                                           00000320
      ICONS(5)=220                                                           00000330
      ICONS(6)=225                                                           00000340
      CALL ERASE                                                             00000350
      WAIT(80)                                                               00000360
10    WRITE(1,1)                                                             00000370
1     FORMAT(/,'ALIGNING TORQUE AND OVERTURNING MOMENT FUNCTIONS',//)         00000380
```

```
      FLSUM=0.0                                                          00001450
      FSSUM=0.0                                                          00001460
      FLNL=0.0                                                           00001470
      FSNL=0.0                                                           00001480
C REPEAT FOR EACH VERTICAL LOAD                                          00001490
      DO 100 NFIT=1,NFITS                                                00001500
      IF(TEMP4(NFIT)-100.)100,100,30                                     00001510
C CONVERT VERTICAL LOAD TO NOMINAL VERTICAL LOAD                         00001520
30    DUMMY=(TEMP4(NFIT)+40.)/100.                                       00001530
      IDUMM=DUMMY                                                        00001540
      DUMMY=IDUMM                                                        00001550
      VL=DUMMY*100.                                                      00001560
      GO TO(31,36),NYNOW                                                 00001570
C FIT THE CURVE                                                          00001580
31    CALL FIT(0.,0.,NFIT,2,3)                                           00001590
      ATMAX=C(1)-C(2)**2/(4.0*C(3))                                      00001600
C PRINT OUT THE VALUES                                                   00001610
      IVAL1=VL                                                           00001620
      IVAL2=ATMAX                                                        00001630
      WRITE(1,5)IVAL1,IVAL2                                              00001640
5     FORMAT(4X,I5,6X,I4)                                                00001650
C ACCUMULATE LOAD WEIGHTED SUMS FOR LOAD FACTOR CALCULATION              00001660
      FACTL=ATMAX/VL                                                     00001670
      FLSUM=FLSUM+FACTL                                                  00001680
      FLNL=FLNL+VL                                                       00001690
C ACCUMULATE SUMS FOR SHAPE FACTOR CALCULATION                           00001700
C ELIMINATE FROM THE CALCULATION ALL COEFFICIENTS OBTAINED FOR VERTICAL  00001710
C LOADS LESS THAN 22% OF THE MAXIMUM TEST VERTICAL LOAD                  00001720
      IF(VL-(0.22*VLMAX))100,100,32                                      00001730
32    FSSUM=FSSUM+C(3)                                                   00001740
      FSNL=FSNL+1.                                                       00001750
      GO TO 100                                                          00001760
C FIT THE CURVE                                                          00001770
36    CALL FIT(0.,0.,NFIT,1,3)                                           00001780
C PRINT OUT THE VALUES                                                   00001790
      IVAL1=VL                                                           00001800
      WRITE(1,511)IVAL1,C(2)                                             00001810
511   FORMAT(4X,I5,2X,F4.2)                                              00001820
C ACCUMULATE LOAD WEIGHTED SUMS FOR LOAD FACTOR CALCULATION              00001830
      FLSUM=FLSUM+C(2)                                                   00001840
      FLNL=FLNL+VL                                                       00001850
100   CONTINUE                                                           00001860
      GO TO(39,139),NYNOW                                                00001870
C SOLVE FOR THE FACTORS                                                  00001880
C LOAD FACTOR (LOAD WEIGHTED AVERAGE)                                    00001890
39    FACTL=FLSUM/FLNL                                                   00001900
C SHAPE FACTOR (TRUNCATED AVERAGE)                                       00001910
      FACTS=SGN*FSSUM/FSNL                                               00001920
C SOLVE FOR K1                                                           00001930
      XK1=-1.0*SQRT(-SGN*FACTL*FACTS)                                    00001940
C PRINT OUT THE VALUES                                                   00001950
      WRITE(1,6)                                                         00001960
6     FORMAT(//,4X,'ALIGNING TORQUE COEFFICIENTS:')                      00001970
```

```
C SCAN THROUGH ALL THE SLEWS                                          00000920
      DO 110 I=1,NSLEW                                                00000930
C READ A DATA RECORD                                                  00000940
      READ(5)DATA                                                     00000950
C CHECK FOR MINIMUM AND MAXIMUM SLIP ANGLE                            00000960
      SA=DATA(3)                                                      00000970
      IF(SA-SAMAX(NRUN))102,102,101                                   00000980
101   SAMAX(NRUN)=SA                                                  00000990
102   IF(SAMIN(NRUN)-SA)1030,1030,103                                 00001000
103   SAMIN(NRUN)=SA                                                  00001010
1030  GO TO(104,106),NRUN                                             00001020
C CHECK FOR MAXIMUM VERTICAL LOAD                                     00001030
104   VL=DATA(5)                                                      00001040
      IF(VL-VLMAX)110,110,105                                         00001050
105   VLMAX=VL                                                        00001060
      GO TO 110                                                       00001070
C CHECK FOR MINIMUM AND MAXIMUM CAMBER ANGLE                          00001080
106   CA=DATA(4)                                                      00001090
      IF(CA-CAMAX)108,108,107                                         00001100
107   CAMAX=CA                                                        00001110
108   IF(CAMIN-CA)110,110,109                                         00001120
109   CAMIN=CA                                                        00001130
110   CONTINUE                                                        00001140
      GO TO(20,40),NRUN                                               00001150
C DEFINE CONSTRAINTS                                                  00001160
20    NCNST=2                                                         00001170
      IF(SAMAX(1)-ABS(SAMIN(1)))22,21,21                              00001180
C 1. STEER ANGLE GE 0                                                 00001190
21    ICVAR(1)=3                                                      00001200
      ICNUM(1)=4                                                      00001210
      CNST(1)=-0.2                                                    00001220
      SGN=-1.0                                                        00001230
      GO TO 23                                                        00001240
C 1. STEER ANGLE LE 0                                                 00001250
22    ICVAR(1)=3                                                      00001260
      ICNUM(1)=2                                                      00001270
      CNST(1)=0.2                                                     00001280
      SGN=1.0                                                         00001290
C 2. VERTICAL LOAD GT 100                                             00001300
23    ICVAR(2)=5                                                      00001310
      ICNUM(2)=5                                                      00001320
      CNST(2)=100.                                                    00001330
      WRITE(1,3)(IOVER(1,I),I=1,3)                                    00001340
3     FORMAT(10X,'RUN: ',I3,'-',I2,'-',I2)                            00001350
      GO TO(24,25),NYNOW                                              00001360
24    WRITE(1,4)                                                      00001370
4     FORMAT(//,8X,'NORMAL   PEAK ALIGNING',                          00001380
     */,9X,'LOAD        TORQUE',//)                                  00001390
      GO TO 26                                                        00001400
25    WRITE(1,411)                                                    00001410
411   FORMAT(//,8X,'NORMAL',/,9X,'LOAD         SLOPE',//)             00001420
C FIT MOMENTS TO LATERAL FORCE AS A FUNCTION OF VERTICAL LOAD         00001430
26    CALL FITYP(0,0,0,XSIGN,NFITS)                                   00001440
```

```
      READ(9)(LINE(I),I=1,46)                                          00002510
C GET NUMBER OF DATA POINTS FOR RUN                                    00002520
      MSLEW=LINE(46)                                                   00002530
C GET NUMBER OF SET POINTS FOR SLIP ANGLE AND CAMBER ANGLE             00002540
      DO 60 I=1,2                                                      00002550
60    IANG(I)=LINE(20+(2*I))                                           00002560
C SEE WHETHER RUN IS CORRECT AND WHICH ANGLE IS INNER AND OUTER VARIABLE00002570
      IF(IANG(1)-4)63,61,66                                            00002580
61    MPTS=LINE(34)                                                    00002590
      IF(IANG(2)-3)66,62,66                                            00002600
62    NPTS=LINE(36)                                                    00002610
      NROP=1                                                           00002620
      GO TO 67                                                         00002630
63    IF(IANG(2)-4)66,64,66                                            00002640
64    MPTS=LINE(36)                                                    00002650
      IF(IANG(1)-3)66,65,66                                            00002660
65    NPTS=LINE(34)                                                    00002670
      NROP=NPTS                                                        00002680
      GO TO 67                                                         00002690
66    WRITE(1,9)                                                       00002700
9     FORMAT(//,44X,'THIS IS NOT A SLIP -',/,50X,'CAMBER RUN')         00002710
      GO TO 98                                                         00002720
C INITIALIZE FIT ROUTINE AND COUNTERS                                  00002730
67    DO 68 NFIT=1,MFITS                                               00002740
      CASUM(NFIT)=0.0                                                  00002750
      FZSUM(NFIT)=0.0                                                  00002760
      FITN(NFIT)=0.0                                                   00002770
68    CALL FIT(0.,0.,NFIT,2,1)                                         00002780
C POSITION TO FIRST DATA RECORD                                        00002790
      CALL POSIT(LUN09,IOVER(2,5))                                     00002800
C SET COUNTERS                                                         00002810
      NI=1                                                             00002820
      NFIT=1                                                           00002830
C REPEAT FOR EACH DATA RECORD                                          00002840
      DO 75 NREAL=1,MSLEW                                              00002850
      READ(9)DATA                                                      00002860
C CHECK CONSTRAINTS                                                    00002870
      CALL CHECK(OK)                                                   00002880
      IF(OK)72,72,69                                                   00002890
C GET VALUE OF LATERAL FORCE                                           00002900
69    XVAL=DATA(6)                                                     00002910
      GO TO(70,71),NYNOW                                               00002920
C GET VALUE OF NORMALIZED ALIGNING TORQUE                              00002930
70    YVAL=DATA(12)/DATA(9)                                            00002940
      GO TO 720                                                        00002950
C GET VALUE OF NORMALIZED OVERTURNING MOMENT                           00002960
71    YVAL=DATA(10)/DATA(9)                                            00002970
C SUM VALUES OF NORMAL FORCE FOR LATER AVERAGING                       00002980
720   FZSUM(NFIT)=FZSUM(NFIT)+DATA(9)                                  00002990
C GET VALUE OF CAMBER ANGLE                                            00003000
      PVAL=DATA(4)                                                     00003010
C ADD CAMBER ANGLE TO SUM AND INCREMENT COUNTER FOR LATER AVERAGING     00003020
      CASUM(NFIT)=CASUM(NFIT)+PVAL                                     00003030
```

```
      WRITE(1,7)XK1,FACTS                                                    00001980
7     FORMAT(//,10X,'K1 =',E10.3,/,10X,'K2 =',E10.3)                         00001990
      GO TO 140                                                              00002000
C SOLVE FOR C1                                                               00002010
139   FACTL=FLSUM/FLNL                                                       00002020
C PRINT OUT THE VALUE                                                        00002030
      WRITE(1,611)                                                           00002040
611   FORMAT(//,2X,'OVERTURNING MOMENT COEFFICIENTS:')                       00002050
      WRITE(1,711)FACTL                                                      00002060
711   FORMAT(//,10X,'C1 =',E10.3)                                            00002070
C GO TO SLIP ANGLE - CAMBER ANGLE RUN                                        00002080
140   CALL HOME                                                              00002090
      NRUN=2                                                                 00002100
      NPNOW=2                                                                00002110
      GO TO(16,40),NYNOW                                                     00002120
C DEFINE CONSTRAINTS ON ANGLES                                               00002130
40    NCNST=2                                                                00002140
      IF(ABS(SAMAX(2)+SAMIN(2))-0.5)41,41,43                                 00002150
41    IF(ABS(CAMAX+CAMIN)-0.5)50,50,42                                       00002160
42    IF(CAMAX+CAMIN)51,50,50                                                00002170
43    IF(SAMAX(2)+SAMIN(2))44,46,46                                          00002180
44    IF(ABS(CAMAX+CAMIN)-0.5)51,51,45                                       00002190
45    IF(CAMAX+CAMIN)51,51,48                                                00002200
46    IF(ABS(CAMAX+CAMIN)-0.5)50,50,47                                       00002210
47    IF(CAMAX+CAMIN)48,50,50                                                00002220
48    WRITE(1,8)                                                             00002230
8     FORMAT(//,44X,'COEFFICIENT K3 CANNOT',/,44X,'BE FITTED TO DATA')       00002240
      GO TO 98                                                               00002250
C MAKE SLIP ANGLE AND CAMBER ANGLE POSITIVE                                  00002260
C 1. SLIP ANGLE GE 0                                                         00002270
50    ICVAR(1)=3                                                             00002280
      ICNUM(1)=4                                                             00002290
      CNST(1)=-0.2                                                           00002300
C 2. CAMBER ANGLE GE 0                                                       00002310
      ICVAR(2)=4                                                             00002320
      ICNUM(2)=4                                                             00002330
      CNST(2)=-0.2                                                           00002340
      SIGN=-1.0                                                              00002350
      GO TO 52                                                               00002360
C MAKE SLIP ANGLE AND CAMBER ANGLE NEGATIVE                                  00002370
C 1. SLIP ANGLE LE 0                                                         00002380
51    ICVAR(1)=3                                                             00002390
      ICNUM(1)=2                                                             00002400
      CNST(1)=0.2                                                            00002410
C 2. CAMBER ANGLE LE 0                                                       00002420
      ICVAR(2)=4                                                             00002430
      ICNUM(2)=2                                                             00002440
      CNST(2)=0.2                                                            00002450
      SIGN=1.0                                                               00002460
      GO TO(52,67),NYNOW                                                     00002470
C POSITION TO HEADER OF SLIP ANGLE - CAMBER ANGLE RUN                        00002480
52    CALL POSIT(LUNC9,IOVER(2,4))                                           00002490
C READ THE HEADER INTO ARRAY "LINE"                                          00002500
```

```
      FGSUM=FGSUM+FACTG                                                 00003570
      GAMNO=GAMNO+1.0                                                   00003580
      GO TO 200                                                         00003590
 86   CALL FIT(0.,0.,NFIT,1,3)                                          00003600
C MULTIPLY THE INTERCEPT AND SLOPE BY THE NORMAL FORCE                  00003610
      OM=C(1)*FZ                                                        00003620
      SL=C(2)*FZ                                                        00003630
C WRITE OUT THE VALUES                                                  00003640
      IF(GAMMA)860,861,861                                              00003650
 860  DUMMY=GAMMA-0.4                                                   00003660
      GO TO 862                                                         00003670
 861  DUMMY=GAMMA+0.4                                                   00003680
 862  IVAL1=DUMMY                                                       00003690
      WRITE(1,1008)IVAL1,OM,SL                                          00003700
1008  FORMAT(42X,I3,6X,F6.1,6X,F5.2)                                    00003710
      C(1)=-C(1)                                                        00003720
      C(2)=-C(2)                                                        00003730
      GAMMA=GAMMA/57.3                                                  00003740
C ACCUMULATE PARTIAL SUMS FOR FITTING C2                                00003750
      CALL FIT(GAMMA,C(2),19,1,2)                                       00003760
C ACCUMULATE PARTIAL SUMS FOR FITTING C3                                00003770
      CALL FIT(GAMMA,C(1),20,1,2)                                       00003780
 200  CONTINUE                                                          00003790
      GO TO(90,91),NYNOW                                                00003800
C GET K3                                                                00003810
 90   FACTG=FGSUM/GAMNO                                                 00003820
C WRITE OUT THE VALUE                                                   00003830
      WRITE(1,1004)                                                     00003840
1004  FORMAT(//,40X,'ALIGNING TORQUE COEFFICIENTS:')                    00003850
      WRITE(1,1005)FACTG                                                00003860
1005  FORMAT(//,46X,'K3 =',E10.3)                                       00003870
      GO TO 98                                                          00003880
C GET C2                                                                00003890
 91   CALL FIT(0.,0.,19,1,3)                                            00003900
      GAMS=C(2)                                                         00003910
C GET C3                                                                00003920
      CALL FIT(0.,0.,20,1,3)                                            00003930
      GAMI=C(2)                                                         00003940
C WRITE OUT THE VALUES                                                  00003950
      WRITE(1,1009)                                                     00003960
1009  FORMAT(//,38X,'OVERTURNING MOMENT COEFFICIENTS:')                 00003970
      WRITE(1,1010)GAMS,GAMI                                            00003980
1010  FORMAT(//,46X,'C2 =',E10.3,/,46X,'C3 =',E10.3)                    00003990
 98   CALL HOLD(IN)                                                     00004000
      CALL CHOUT(27)                                                    00004010
      CALL CHOUT(12)                                                    00004020
      WAIT(80)                                                          00004030
      GO TO(99,999),NYNOW                                               00004040
C START ROUTINE TO CALCULATE OVERTURNING MOMENT COEFFICIENTS            00004050
C RETURN TO SLIP ANGLE - VERTICAL LOAD RUN                              00004060
 99   NRUN=1                                                            00004070
C SELECT OVERTURNING MOMENT AS Y VARIABLE                               00004080
      NYNOW=2                                                           00004090
```

```
      FITN(NFIT)=FITN(NFIT)+1.0                                          00003040
C ACCUMULATE PARTIAL SUMS                                                00003050
      CALL FIT(XVAL,YVAL,NFIT,2,2)                                       00003060
C INCREMENT COUNTERS                                                     00003070
72    N1=N1+1                                                            00003080
      IF(N1-NROP)75,75,73                                                00003090
73    N1=1                                                               00003100
      NFIT=NFIT+1                                                        00003110
      IF(NFIT-MFITS)75,75,74                                             00003120
74    NFIT=1                                                             00003130
75    CONTINUE                                                           00003140
      WRITE(1,1001)(IOVER(2,I),I=1,3)                                    00003150
1001  FORMAT(46X,'RUN: ',I3,'-',I2,'-',I2)                               00003160
      GO TO(70,77),NYNOW                                                 00003170
70    WRITE(1,1002)                                                      00003180
1002  FORMAT(//,44X,'CAMBER      ALIGNING',                              00003190
     */,45X,'ANGLE       TORQUE',//)                                     00003200
      GO TO 78                                                           00003210
77    WRITE(1,1007)                                                      00003220
1007  FORMAT(//,41X,'CAMBER',/,42X,'ANGLE    INTERCEPT     SLOPE',//)    00003230
78    FCSUM=0.0                                                          00003240
      CAMNO=0.0                                                          00003250
C REPEAT FOR EACH CAMBER ANGLE                                           00003260
      DO 200 NFIT=1,MFITS                                                00003270
C INITIALIZE SUBROUTINE FIT ON FIRST PASS                                00003280
      IF(NFIT-1)999,79,80                                                00003290
79    GO TO(80,790),NYNOW                                                00003300
790   CALL FIT(0.,0.,15,1,1)                                             00003310
      CALL FIT(0.,0.,20,1,1)                                             00003320
C SEE IF THIS IS A CAMBER ANGLE THAT WAS ELIMINATED                      00003330
80    IF(FITN(NFIT))999,200,81                                           00003340
C COMPUTE AVERAGE CAMBER ANGLE AND AVERAGE NORMAL FORCE                  00003350
81    GAMMA=CASUM(NFIT)/FITN(NFIT)                                       00003360
      FZ=FZSUM(NFIT)/FITN(NFIT)                                          00003370
      GO TO(82,86),NYNOW                                                 00003380
C FIT THE CURVE                                                          00003390
82    CALL FIT(0.,0.,NFIT,2,3)                                           00003400
C MULTIPLY THE INTERCEPT BY THE NORMAL FORCE TO FIND THE ALIGNING         00003410
C TORQUE AT ZERO LATERAL FORCE                                           00003420
      AT=C(1)*FZ                                                         00003430
C WRITE OUT THE VALUES                                                   00003440
      IF(GAMMA)83,84,84                                                  00003450
83    DUMMY=GAMMA-0.4                                                    00003460
      GO TO 840                                                          00003470
84    DUMMY=GAMMA+0.4                                                    00003480
840   IVAL1=DUMMY                                                        00003490
      IVAL2=AT                                                           00003500
      WRITE(1,1003)IVAL1,IVAL2                                           00003510
1003  FORMAT(45X,I3,9X,I4)                                               00003520
      IF(IVAL1)85,200,85                                                 00003530
C ACCUMULATE SUMS FOR FITTING K3                                         00003540
85    GAMMA=GAMMA/57.3                                                   00003550
      FACTG=SIGN*C(1)/SQRT(ABS(GAMMA))                                   00003560
```

```
C SELECT VERTICAL LOAD AS PARAMETER                                    00004100
      NPNOW=1                                                          00004110
C DEFINE CONSTRAINTS                                                   00004120
      GO TO 20                                                         00004130
999   STOP                                                             00004140
      END                                                              00004150
```

APPENDIX C

VEHICLE TEST PROCEDURES AND DATA REDUCTION METHODS

by

D. E. Massing

The NHTSA Vehicle Handling Test Procedures (VHTP) formed the basis on which the full scale vehicle test program was executed. The six standard VHTP's in Reference 1 were designated for use in dry pavement testing. Test procedures 2, 5 and 4 were redesignated as procedures 7, 8 and 9 respectively for performance as wet pavement tests. VHTP 7 differed from VHTP 2 with regard to vehicle initial velocity; V_o was reduced to 30 mph. The reduction was required to lower the vehicle lateral acceleration to a level that provided stable tire adhesion on the wet test surface. As a result, the same steer angle employed in the dry test (VHTP 2), equivalent to 0.3g at 40 mph, was used in the wet test at 30 mph resulting in an initial lateral acceleration of 0.17 g.

In addition to the testing requirements of the VHTP, a formatting procedure was developed to augment the automated reduction and analysis of the test data. The procedure involved the recording of the run identification (I.D.) code and control command time synchronization pulse signals as shown in Figure 1. The serial pulse code is produced by an electronic device designed and fabricated at Calspan called an I.D. Serial Code Generator. The code consists of five pulses having amplitude format and serial locations representative of a schedule of numerical equivalents of vehicle, tire configuration, test procedure, and sequential run number information.

The vehicle control command time synchronization pulse was provided for the purpose of indicating in the data reduction process the useable portion of each vehicle response measurement. A summary of the location in time of each synchronizing pulse is as follows:

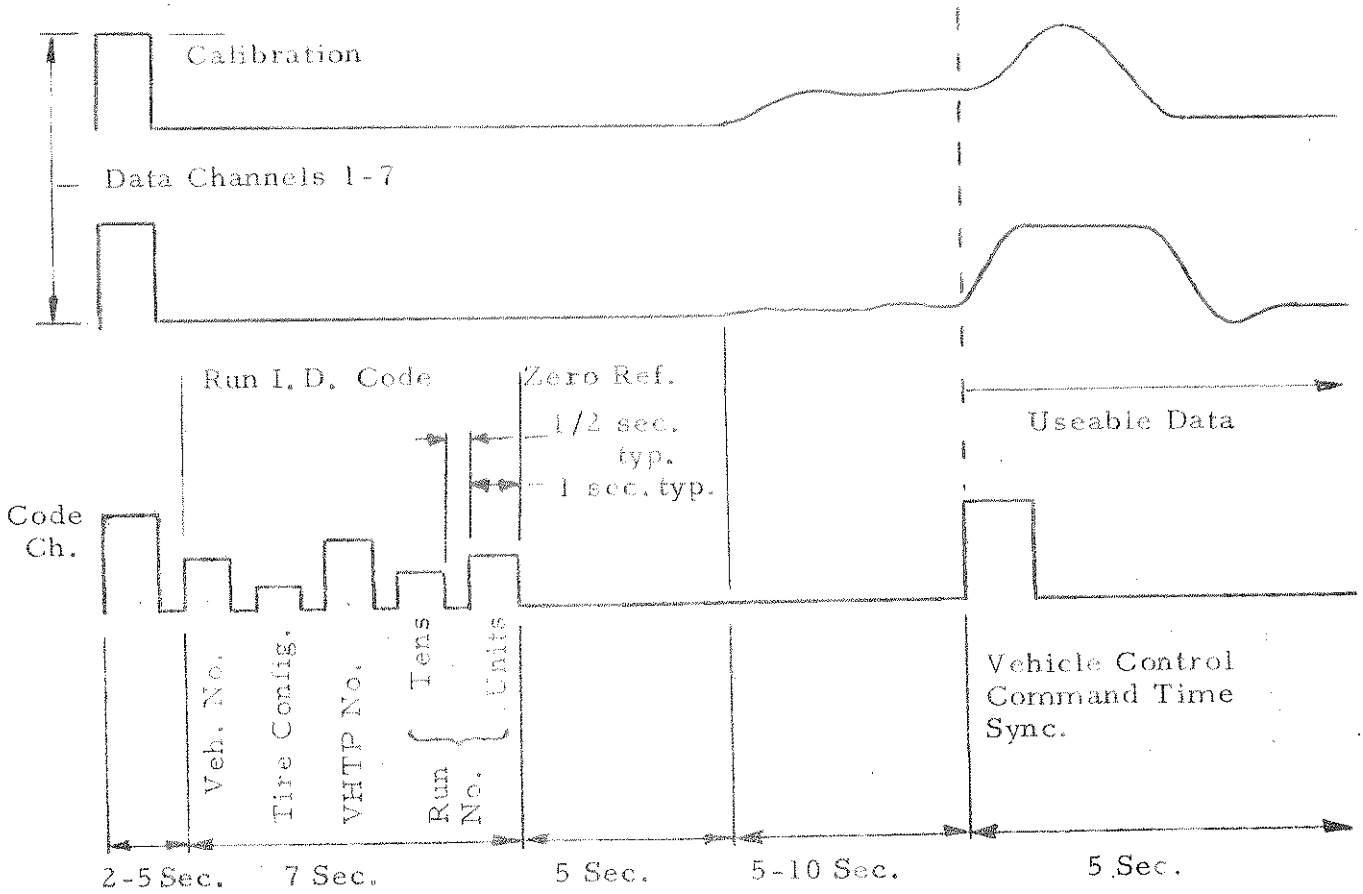

I.D. Code Translation

Vehicle No.
1. Dodge
2. Firebird
3. Brookwood
4. VW

Tire Config.
1. OE
2. Inferior Traction
3. Superior Traction
4. Inferior Cornering
5. Superior Cornering
6. Superior Wet Traction
7. Superior Wet Cornering
8. Inferior Load Sensitivity
9. Inferior Load Transfer Sensitivity

VHTP No.
1. Straight Line Braking-Dry
2. Braking in a Turn "
3. Rough Road Turning "
4. Trapezoidal Steer "
5. Sinusoidal Steer "
6. Drastic Steer & Brake "
7. Braking in a Turn Wet
8. Sinusoidal Steer "
9. Trapezoidal Steer "

Run No. 1 - 99

FIGURE 1 DATA RECORDING FORMAT

VHTP	TEST EVENT
1, 2, 7	Application of brakes
3	Entry of vehicle onto disturbance grid
4, 5, 8, 9	Initiation of steering command
6	Initiation of brake release command

The complement of instrumentation summarized in Table I provided measures of test conditions and vehicle responses in accordance with the requirements specified in the VHTP. Output signals from the various sensing devices were recorded on a FM tape transport mounted on-board the test vehicle in VHTP 4, 5, 6, 8, 9 or via FM telemetry link to a ground based recorder in VHTP 1, 2, 3, 7. The resulting data tapes were submitted by TTI to Calspan for reduction and analysis.

The reduction and analysis of vehicle test data recorded on FM tape was accomplished using Calspan's Analog/Hybrid computer facility. The facility is comprised of a Comcor CI 5000 analog computer and a Honeywell DDP-116 digital processor. A full complement of peripherals was available for processing a variety of I/O formats including an optional system linkup with Calspan's 370-168 digital computing facility via an IBM 2701 parallel data adapter. A block diagram representation of the operational elements contained in the system is shown in Figure 2. Input format was in the form of FM tape recordings containing analog signals representing measurements of the vehicle responses and certain additional identification and time synchronizing signals. Such input was contained on either 1/2 inch 7 track or 1 inch 14 track magnetic tape.

Input data signals were processed initially in the analog portion of the system with operations such as filtering, scaling, integration, and the like. The digital processor maintained supervisory control over the analog computer, thus enabling the detection of response transients, and, in addition, processing of certain intervals where data was converted and stored digitally for further analysis. This interaction provided a fast and

Variable	Symbol	Sensor Type and Mfg.	Calib. Range	Applicable VHTP
Longitudinal Acceleration	A_x	Stabilized Platform Accelerometer - Pot. Type Sensors Humphrey SA07-0301	1g	1, (A_x only) 2, 3, 7
Lateral Acceleration	A_y	Humphrey CF18-0107	1g	4, 5, 6, 8, 9
Roll Velocity	p	Rate Gyroscope - Pot Type Sensor Humphrey CF18-0107	30°/sec	6
Yaw Velocity	r	Rate Gyroscope - Pot Type Sensor Humphrey SA07-0301	100°/sec	2, 3, 7
		Humphrey CF18-0107		4, 5, 6, 8, 9
Longitudinal Velocity	V_5	Fifth Wheel Special Auto-Lift Device	70 mph	All
Wheel Rotation	W_{1-2}* W_{3-4}*	1 Pulse Per Revolution Discreet Signals - Devices Provided by TTI	N/A	1, 2, 7
Steer Angle	δ_{SW}	Pot Type Device - Part of Automatic Steering Controller	600°	4, 5, 6, 8, 9

* W_{1-2} Amplitude summation of two front axle wheel signals

W_{3-4} Same except rear axle

TABLE 1 FULL SCALE VEHICLE TEST INSTRUMENTATION SUMMARY

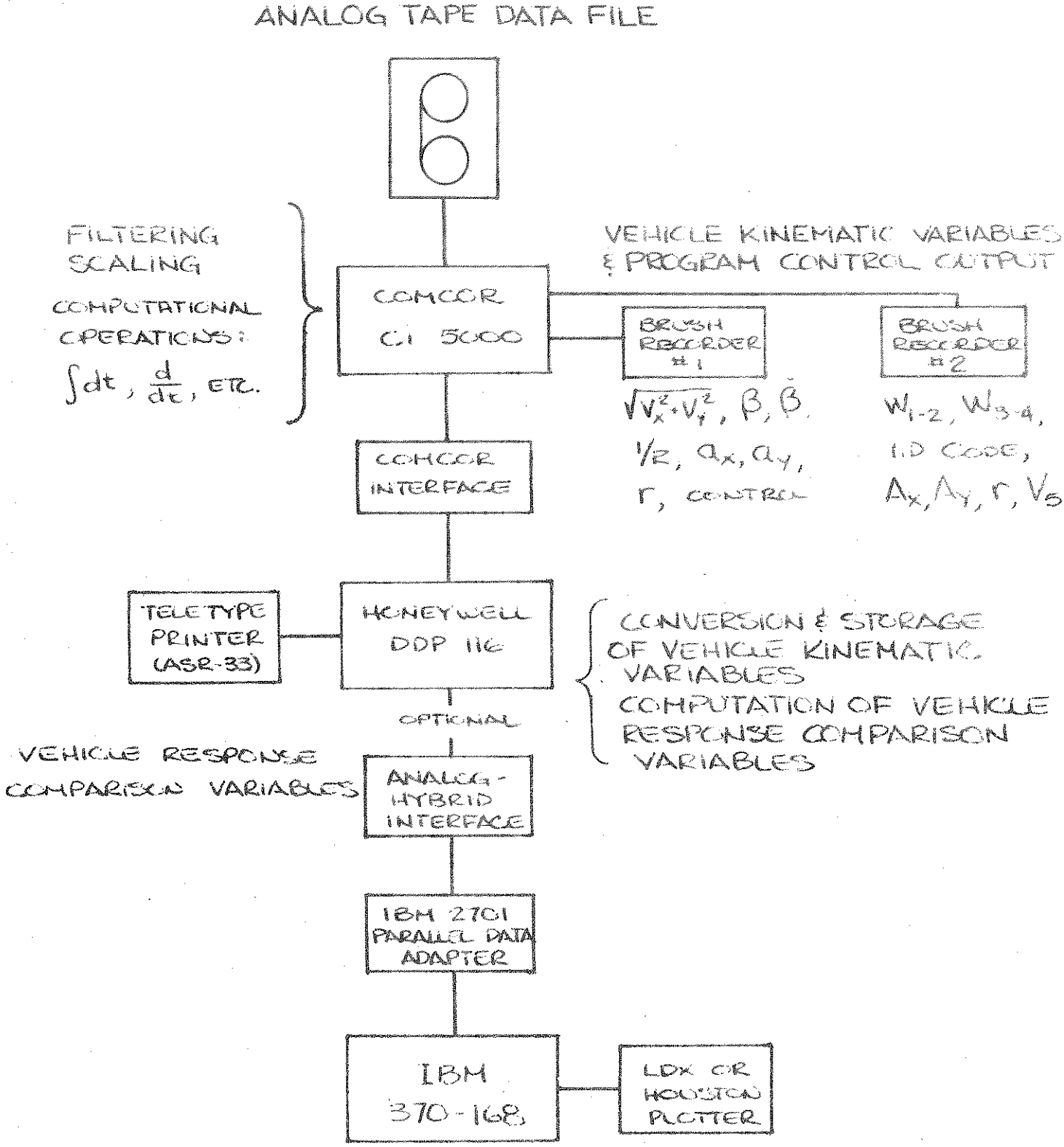
ANALOG TAPE DATA FILE
FILTERING
SCALING
COMPUTATIONAL
OPERATIONS:
$\int dt$, $\frac{d}{dt}$, ETC.
COMCOR
C/ 5000
VEHICLE KINEMATIC VARIABLES
& PROGRAM CONTROL OUTPUT
BRUSH
RECORDER
#1
BRUSH
RECORDER
#2
$\sqrt{V_x^2+V_y^2}$, β, $\dot{\beta}$,
$1/R$, a_x, a_y,
r, CONTROL
W_{1-2}, W_{3-4},
I.D CODE,
A_x, A_y, r, V_s
COMCOR
INTERFACE
TELETYPE
PRINTER
(ASR-33)
HONEYWELL
DDP 116
CONVERSION & STORAGE
OF VEHICLE KINEMATIC
VARIABLES
COMPUTATION OF VEHICLE
RESPONSE COMPARISON
VARIABLES
OPTIONAL
VEHICLE RESPONSE
COMPARISON VARIABLES
ANALOG-
HYBRID
INTERFACE
IBM 2701
PARALLEL DATA
ADAPTER
IBM
370-168
LDX OR
HOUSTON
PLOTTER

FIGURE 2

efficient mechanization whereby peak value detection, time averaging, and other digitally programmed processing schemes were carried out.

An intermediate data output medium was provided in the form of analog strip chart recordings of selected vehicle response time histories. Up to 16 channels of Brush recorder hard copy output provided time histories of scaled vehicle response measurements, computed vehicle response time histories based on such measurements, and other appropriate recordings of program control and diagnostic signatures needed to verify the results of a given test run. The results of further data analysis performed by the digital portion of the facility were printed out in tabular format on a teletype printer. Examples of analog and digital process output are contained in Figures 3 and 4 respectively. The code channel signal containing the run I.D. information was decoded by the Analog/Hybrid computer and utilized to automatically control the data reduction process. Each data reduction program prescribed for a specific VHTP (Comparison Variable Calculation, Reference 2 Appendix B) was called and executed in accordance with the decoded run identification. A summary of the vehicle response comparison variables specific to a given VHTP is presented in Table 2.

Initial test results dealing with VHTP 2, 7 were suspect with regard to a condition where the computed analog variable V_y failed to attain a zero level when the vehicle came to rest. It was subsequently determined that errors in the measurement of low levels of yaw velocity (r) were the cause of the post test non-zero V_y level. The yaw velocity gyroscope, a 100 deg/sec range instrument, indicated yaw velocities of 5-10 deg/sec during the steady state portion of the maneuver. As a result, the measurement uncertainty associated with the low range of the instrument could amount to 20 to 40 percent of reading even though the instrument was within the manufacturers specified error bounds; $\pm$ 2% F.S. at 100 deg/sec, $\pm$ 1 % F.S. at 0 deg/sec.

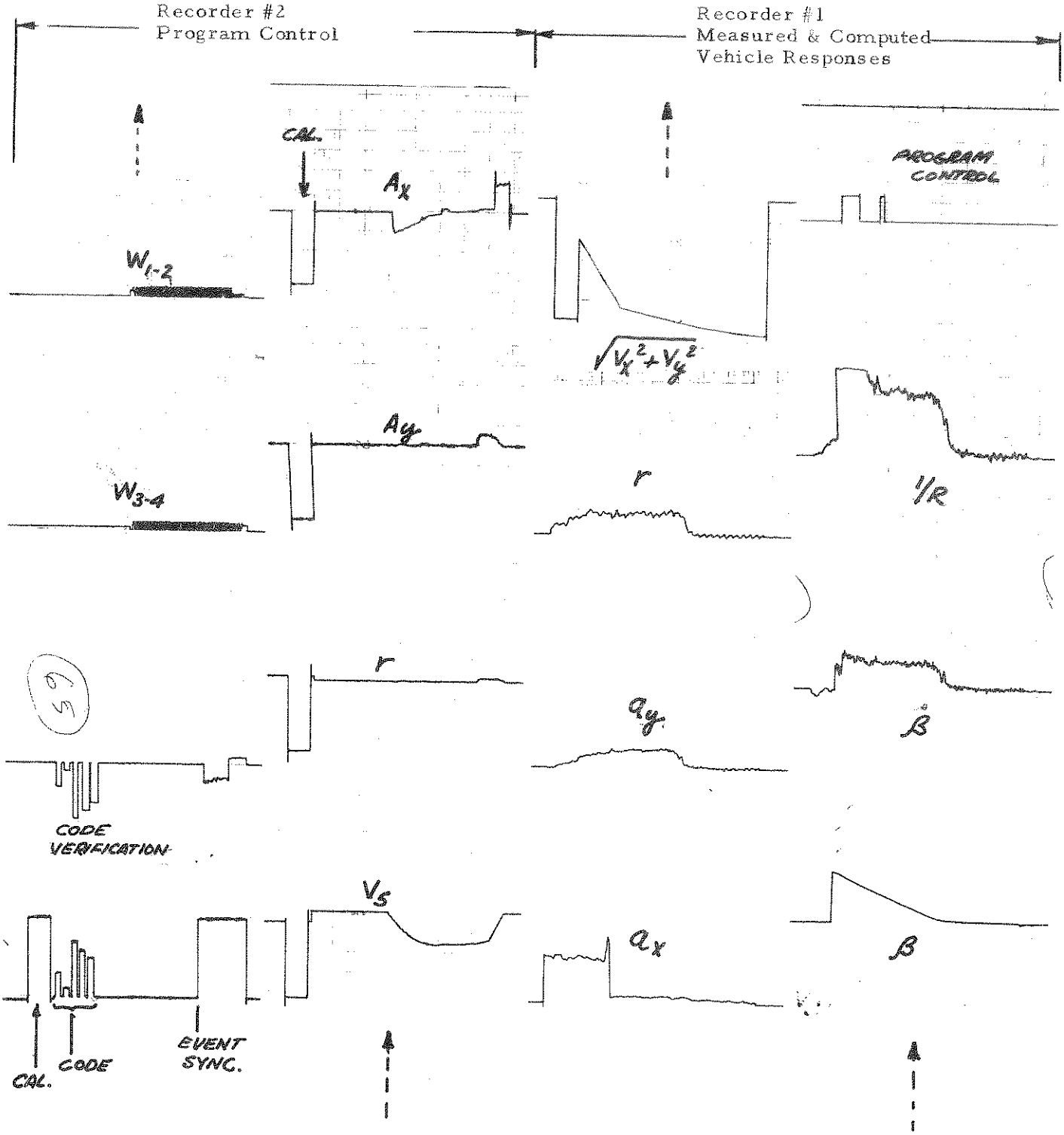

FIGURE 3 SAMPLE ANALOG OUTPUT -
ANALOG/HYBRID VEHICLE RESPONSE ANALYSIS

$Ax_{Ave.}$	$\dot{\beta}_p$	V_5	$(1/R)_{Ave.}$	$(1/R)_o$	$Ro(1/R)_{Ave.}$
Control	Veh. No.	Tire	VHTP No.	Run No. Tens	Run No. Units
+00055	+00003	+00001	+00007	+00007	+00000
-00516	+02058	+03436	+08670	+06869	+12621
+00056	+00003	+00001	+00007	+00007	+00001
-00494	+01948	+03511	+08224	+06314	+13025
+00057	+00003	+00001	+00007	+00007	+00002
-00486	+01780	+03561	+08004	+06633	+12066
+00058	+00003	+00001	+00007	+00007	+00003
-00503	+01327	+03476	-06537	-07816	+08362
+00059	+00003	+00001	+00007	+00007	+00004
-00496	+01891	+03555	-09600	-07551	+12713
+00060	+00003	+00001	+00007	+00007	+00005
-00494	+02200	+03452	-09750	-08223	+11857
+00061	+00003	+00001	+00007	+00007	+00006
-00537	+02024	+03391	+08831	+07017	+12584
+00062	+00003	+00001	+00007	+00007	+00007
-00597	+01987	+03457	+08607	+06756	+12740
+00063	+00003	+00001	+00007	+00007	+00008
-00472	+01404	+03535	-06011	-07598	+07910
+00064	+00003	+00001	+00007	+00007	+00009
-00443	+01493	+03494	-05583	-08320	+06710

FIGURE 4 SAMPLE DIGITAL OUTPUT - ANALOG/HYBRID VEHICLE RESPONSE ANALYSIS

TABLE 2 RESPONSE COMPARISON VARIABLE SUMMARY

VHTP	$(A_x)_{ave.}$	$R_o\left(\frac{1}{R}\right)_{ave.}$	$\dot{\beta}_p$	$R_s\left(\frac{1}{R}\right)_{ave.}$	β_p	A_{yp}	r_p	Δ	$\Delta\psi$	p_p	
1	•										Average Longitudinal Acceleration
2, 7	•	•	•								Average Path Curvature Ratio
3		•	•								Peak Body Sideslip Rate
4, 9			•	•	•	•	•				Normalized Path Curvature Ratio
5, 8					•	•	•	•	•		Peak Body Sideslip Angle
6										•	Peak Lateral Acceleration
											Peak Yaw Rate
											Lane Change Deviation
											Change in Heading Angle
											Peak Roll Rate

In addition, it was evident that yaw velocity measurement errors would be widely propagated throughout the computations of β, $\dot{\beta}$, and $1/R$ since each of these variables is a function of V_y or r.

As a result, the non-linear characteristics of the two rate gyroscopes (see Table 1) were mechanized in a table look-up subroutine contained with the digital software of the DDP-116. The data reduction program was arranged in a manner that permitted entry into the subroutine with equivalents (digital format) of indicated yaw velocity signals and subsequently obtain output in the form of corrected yaw velocity. This process was employed in reducing all yaw velocity data obtained for the duration of the vehicle test program.

A graphic indication of the degree of instrument error is contained in Figures 5 and 6. Note that the straight line of unity slope is the reference for an ideal error-free instrument. The two other curves are the actual error characteristics of the rate gyroscopes based on ten and one hundred percent of full scale calibration data.

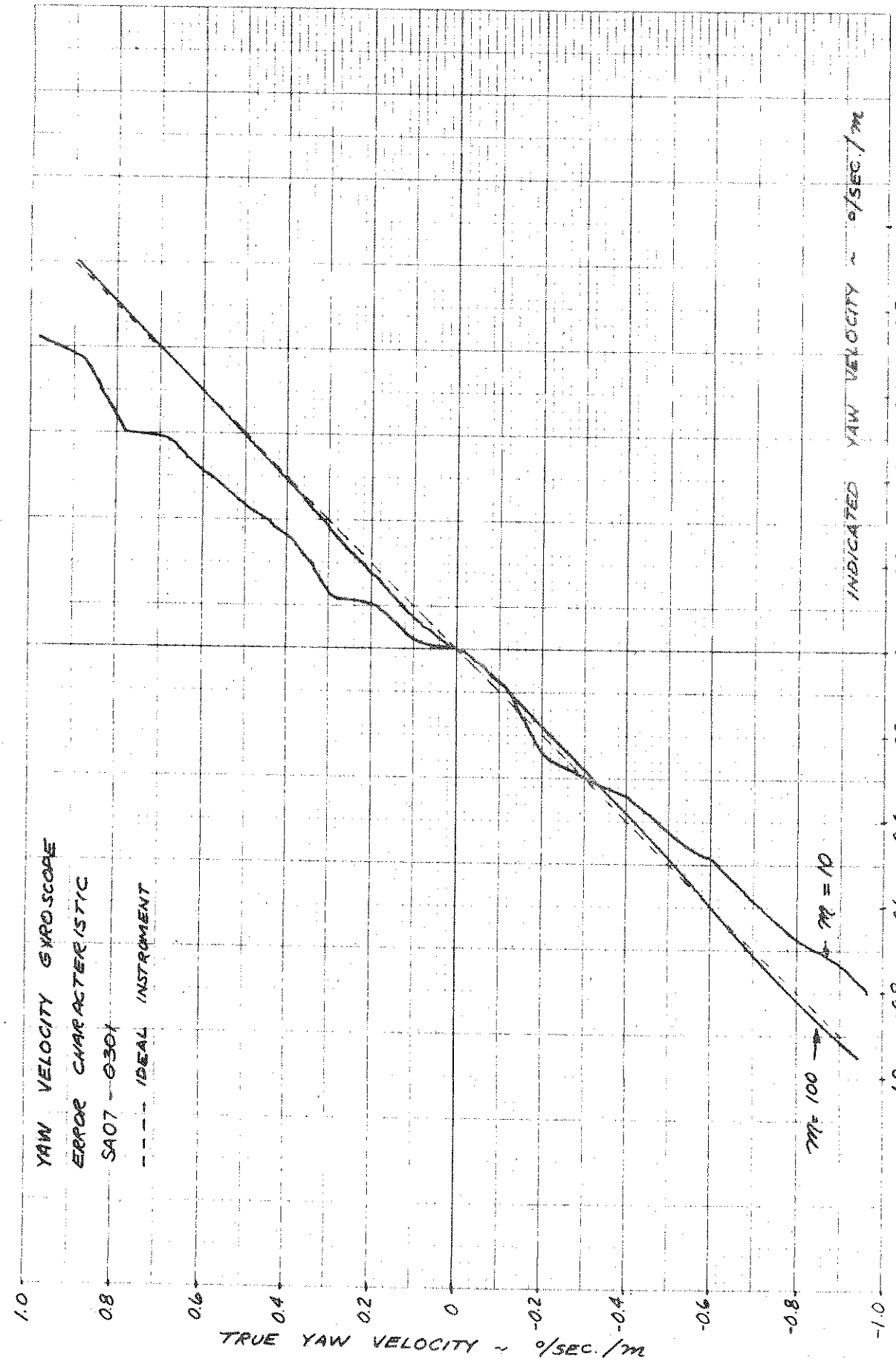
YAW VELOCITY GYRO SCOPE
ERROR CHARACTERISTIC
SA07 - 630A
- - - - IDEAL INSTRUMENT
INDICATED YAW VELOCITY ~ °/SEC./m
TRUE YAW VELOCITY ~ °/SEC./m
m = 10
m = 100
1.0
0.8
0.6
0.4
0.2
0
-0.2
-0.4
-0.6
-0.8
-1.0

Figure 5

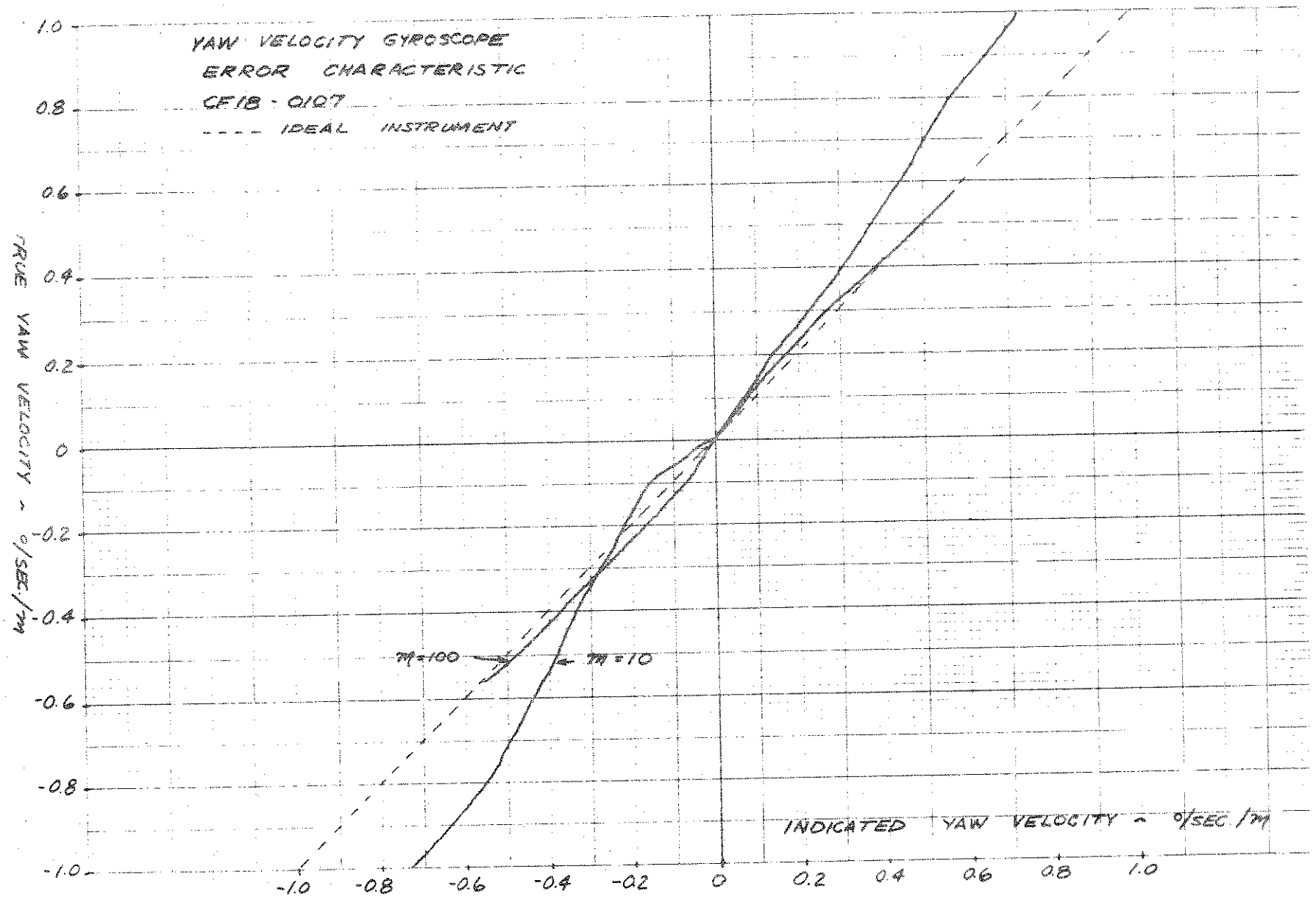
YAW VELOCITY GYROSCOPE
ERROR CHARACTERISTIC
CF18 - 0107
---- IDEAL INSTRUMENT
TRUE YAW VELOCITY - °/SEC / m
INDICATED YAW VELOCITY - °/SEC / m
m=100
m=10
1.0
0.8
0.6
0.4
0.2
0
-0.2
-0.4
-0.6
-0.8
-1.0
-1.0
-0.8
-0.6
-0.4
-0.2
0
0.2
0.4
0.6
0.8
1.0

Figure 6

REFERENCES

1. Ervin, R. D., Grote, P., et at, "Vehicle Handling Performance", Highway Safety Research Institute.

2. Bohn, P. F., "Modeling and Simulation in Vehicle Handling Research", The Johns Hopkins University, Applied Physics Laboratory, Report No. APL/JHU BCE-T-0421, April 1973.

APPENDIX D

MEASURED VEHICLE CHARACTERISTICS

compiled by

R. D. Roland

Parameter	Units	Chevrolet Brookwood	Dodge Coronet	Pontiac Trans. Am	Volkswagen Super Beetle	
a	in.	64.3	47.7	40.0	57.1	
		64.9	50.5	42.3	55.9	A.C.
		65.0	49.3	42.6	56.1	D.C.
b	in.	60.7	70.3	68.0	38.7	
		60.1	67.5	65.7	39.9	A.C.
		60.0	68.7	65.4	39.7	D.C.
T_F	in.	63.5	59.8	61.9	53.8	
T_R	in.	63.5	61.8	60.4	51.5	
T_S	in.	45.3	47.0	45.5	N.A.	
y_{SA}	in.	5.25[2]	4.59[2]	5.0[4]	3.75[2]	
z_F	in.	11.1	11.5	7.4	11.1	
		10.3	10.5	6.2	9.4	A.C.
		10.6	10.8	6.8	9.9	D.C.
z_R	in.	10.8	11.5	7.1	10.9	
		10.1	10.4	6.2	9.7	A.C.
		10.3	10.8	6.5	10.1	D.C.
a_p	in.	5.80	5.20	5.87	5.75	
a_L	in.	6.26	6.62	6.26	5.50	
Ω_{FC}*	in.	3.5	2.4	2.0	1.80	
Ω_{FT}*	in.	2.3	2.1	2.5	3.40	
Ω_{RC}*	in.	3.6	4.4	3.3	1.85	
Ω_{RT}*	in.	2.3	3.6	3.7	3.35	
h_R	in.	4.0	3.9	5.7	N.A.	
R_w	in.	14.4	13.2	12.8	12.6	

* bump stop locations are relative to static suspension displacement shown on pages A-5 and A-6 (no load vehicle configuration). Appropriate adjustments must be made for instrumented vehicle configurations, see table at bottom of page A-6.

NOTE: All data is for a no load vehicle configuration except where noted A.C. (automatic controller configuration) or D.C. (driver control configuration).

Parameter	Units	Chevrolet Brookwood	Dodge Coronet	Pontiac Trans. Am	Volkswagen Super Beetle	
I_{xs}	in. lb. sec.	5,920	3,120	2,760	1,300	
		6,800	3,830	3,720	2,060	A.C.
		6,120	3,760	3,520	1,940	D.C.
I_{ys}	in. lb. sec.	41,400	22,800	18,500	8,900	
		42,600	24,000	20,200	9,930	A.C.
		41,500	23,000	19,100	9,140	D.C.
I_{zs}	in. lb. sec.	41,700	22,600	18,900	7,900	
		43,500	24,300	21,300	9,390	A.C.
		42,400	23,300	20,100	8,530	D.C.
I_{xzs}	in. lb. sec.	1,790	530	230	0	
I_D	in. lb. sec	0.7[1]	0.7[1]	0.7[1]	0.3[1]	
I_{FW}	in. lb. sec.^{2}	10.0[3]	6.4[3]	8.0[3]	4.4[3]	
I_R	in. lb. sec.^{2}	750.	550.	530.	N.A.	
I_{WJ}	in. lb. sec.^{2}	14.8	9.4[1]	10.0[1]	7.35	
M_S	lb. sec./in.	10.3	7.57	8.00	4.23	
		11.6	8.82	9.27	5.50	A.C.
		11.2	8.43	8.82	5.09	D.C.
M_{uF}	lb. sec./in.	0.63	0.51	0.53	0.36	
M_{uR}	lb. sec./in.	1.03	0.82	0.86	0.57	
N_G	-----	16.2	14.2	15.5	17.0	
N_L	-----	1.08	1.27	1.07	0.957	
λ_{FC}	-----	2.0	1.8	2.0[4]	2.5	
λ_{FT}	-----	4.2	5.6	3.5	8.0	
λ_{RC}	-----	1.9	2.7	2.0[4]	1.6	
λ_{RT}	-----	5.1	7.2	5.0[4]	3.9	
$\overline{AR}$	-----	3.08	2.71	3.42	4.13	
K_F	lb./in.	141.	105.	99.	65.7	
K_R	lb/i	210.	120.	147.	115.	

Parameter	Units	Chevrolet Brookwood	Dodge Coronet	Pontiac Trans. Am	Volkswagen Super Beetle
K_{TF}	lb./in.	1,210.	1,450.	1,500.	760.
K_{TR}	lb./in.	1,680.	1,450.	1,500.	1,060.
R_F	in. lb./rad.	408,000.	40,400.	356,000.	93,000.
R_R	in. lb./rad.	-62,000.	-5,100.	630,000.	28,300.
K_{SC}	in. lb./rad.	8,000.[1]	8,000.[1]	8,000.[1]	7,000.[1]
K_{SL}	in. lb./rad.	91,700.	55,900.	87,000.	106,000.
K_{RS}	deg./deg.	0.033	0.020	-0.008	N.A.
k_{CF}	deg./K lb.	1.33	2.25	1.61	2.[illegible]
k_{CR}	deg./K lb.	2.13	1.90	1.98	1.38
k_{SR}	deg./100 ft lb.	0.16	0.12	0.18	0.15
C_{CR}	lb. sec./in.	11.0[2]	11.0[4]	11.0[4]	3.75[2]
C_{FCR}	lb. sec./in.	77.	54.	69.	57.
H_D	in. lb. sec./rad.	400.[2]	400.[2]	400.[2]	200.[2]
m_C	lb. sec.^{2}/in.	0.06[1]	0.06[1]	0.06[1]	0.05[1]
E_{sp}	deg.	12.0	16.0	14.0	18.0
E_p	deg.	0.40	0.45	0.67	0.0
ϕ_{si}	deg.	10.0	7.50	8.75	10.0
C'_F	lb.	43.	40.	35.	35.
C'_R	lb.	73.	38.	55.	40.
θ_{si}	deg.	-1.0	0.75	-1.0	2.0
E_i	deg.	0.37	0.27	0.42	0.16 front
		-----	-----	-----	0.0 rear
ϕ_i	deg.	0.50	0.38	0.75	1.0 front
		-----	-----	-----	-1.3 rear
$\overline{PT}$	in.	0.16	-0.66	-0.24	1.66

Parameter	Units	Chevrolet Brookwood	Dodge Coronet	Pontiac Trans. Am	Volkswagen Super Beetle	
CP_0	lb./lb.	-0.13[5]	-0.13[1]	-0.09	0.0[5]	front
		0.15[5]	0.15[1]	0.15	0.29[5]	rear
CP_1	lb./lb.	0.03[5]	-0.03[1]	-0.03[1]	0.03[5]	front
		0.015[5]	-0.015[1]	0.015[1]	0.03[5]	rear
CR_0	lb./lb.	0.022	0.089	0.064	0.089	front
		N.A.	N.A.	N.A.	0.130	rear
CR_1	lb./lb.	0.01[4]	0.01[4]	0.01[4]	0.01[4]	front
		N.A.	N.A.	N.A.	0.03[4]	rear

1 - estimated from similar measured data for other vehicles

2 - assumed from HSRI reported data (Contract DOT-HS-031-1-126)

3 - calculated from moment of inertia of wheel about spin axis

4 - assumed

5 - calculated from manufacturer's design data

VISCOUS DAMPING COEFFICIENTS FOR WHEEL RIDE MOTION

Vehicle	C_F*	C_R*
Brookwood	1.94 for $V > 0$	1.62 for $V > 0$
	12.1 for $0 > V > -10.2$	9.99 for $0 > V > -10.1$
	1.17 for $V < -10.2$	1.61 for $V \leq -10.1$
Coronet	4.33 for $V > 0$	1.50 for $V > 7.2$
	9.36 for $V < 0$	8.32 for $0 < V < 7.2$
		6.63 for $V < 0$
Trans Am	1.79 for $V > 21.9$	0.79 for $V > 15.8$
	7.78 for $10.2 < V < 21.9$	1.99 for $0 < V < 15.8$
	2.74 for $0 < V < 10.2$	4.58 for $0 > V > -11.3$
	21.0 for $0 > V > -7.46$	1.01 for $V < -11.3$
	3.10 for $V < -7.46$	
VW	1.81 for $V > 12.0$	1.89 for $V > 0$
	4.28 for $0 < V < 12.0$	8.06 for $0 > V > -19.1$
	5.73 for $0 > V > -12.6$	2.87 for $V < -19.1$
	11.4 for $-12.6 > V > -16.5$	
	4.44 for $V < -16.5$	

* damping coefficients and velocities effective at the wheels

STEER AND CAMBER AS FUNCTIONS OF WHEEL DISPLACEMENT FROM FULL REBOUND POSITIONS

	Displacement	Camber	Steer (+ toe in)
Brookwood (left front)	0	0	0
	1	0.85	-0.24
(static displacement* = 3.0)	2	1.68	-0.53
	3	2.18	-0.73
	4	2.43	-0.89
	5	2.47	-1.01
	6	2.29	-1.10
	7	1.96	-1.17
Coronet (left front)	0	0	0
(static displacement* = 3.0)	1	0.41	-0.37
	2	0.98	-0.59
	3	1.26	-0.85
	4	1.22	-1.05
	5	0.95	-1.21
	6	0.43	-1.36
Trans Am (left front)	0	0	0
(static displacement* = 4.0)	1	0.26	-0.03
	2	0.83	-0.18
	3	1.27	-0.31
	4	1.48	-0.39
	5	1.48	-0.40
	6	1.27	-0.40

VW (right rear)	0	0	0
(static displacement* = 3.0)	1	-0.72	0.06
	2	-1.44	0.08
	3	-2.16	0.07
	4	-2.90	0.02
	5	-3.60	0.05
VW (left front)	0	0	0
(static displacement* = 4.0)	1	-0.57	-0.17
	2	-1.25	-0.45
	3	-1.87	-0.73
	4	-2.46	-0.96
	5	-2.96	-1.14
	6	-3.42	-1.25
	7	-3.79	-1.30
	8	-4.08	-1.32

* static displacements are for no load vehicle configuration, the following adjustments must be made for instrumented vehicle configurations.

	Chevrolet Brookwood	Dodge Coronet	Pontiac Trans. Am.	Volkwagen Super Beetle	
C.G. shift (in.)	-0.7	-0.5	-0.6	-1.6	A.C.
	-0.6	-0.6	-0.8	-1.7	D.C.

DEFINITIONS OF PARAMETERS

A. DISTANCES

a	Longitudinal distance between sprung mass center of gravity and front wheels.
b	Longitudinal distance between sprung mass center of gravity and rear wheels.
T_F	Wheel tread width at front.
T_R	Wheel tread width at rear.
T_S	Distance between spring mountings on solid rear axle.
y_{SA}	Distance between wheel center and king pin axis; measured along wheel spin axis.
z_F	Static distance between the center of gravity of the sprung mass and the spin axis of the front wheels; measured along the z-axis.
z_R	Static distance between the center of gravity of the sprung mass and the roll center of the rear suspension; measured along the z-axis.
a_p	Length of Pitman arm.

a_L Length of steering linkage arm

Ω_{FC} Suspension deflection for initial front wheel contact with compression bump stop.

Ω_{FT} Suspension deflection for initial front wheel contact with tension bump stop.

Ω_{RC} Deflection for initial rear wheel contact with compression bump stop.

Ω_{RT} Suspension deflection for initial rear wheel contact with tension bump stop.

h_R Distance from center of rear axle to the roll center of the rear suspension.

R_w Undeflected tire radius.

B. MOMENTS OF INERTIA

I_{xs} Moment of inertia of sprung mass about the x-axis.

I_{ys} Moment of inertia of sprung mass about the y-axis.

I_{zs} Moment of inertia of sprung mass about the z-axis.

I_{xzs} Product of inertia of sprung mass about the x-z axes.

I_D Drive line moment of inertia about its spin axis.

I_{FW} Moment of inertia of one front wheel about the king pin axis.

I_R Moment of inertia of rear unsprung mass about an axis through its center of gravity and parallel to the x-axis.

I_{WJ} Moment of inertia of wheel about spin axis.

C. SPRUNG AND UNSPRUNG MASSES

M_S Sprung mass.

M_{uF} Total front unsprung mass.

M_{uR} Total rear unsprung mass.

D. DIMENSIONLESS PARAMETERS

N_G Gear ratio of steering gear box.

N_L Steering linkage gear ratio.

$\lambda_{FC}, \lambda_{FT}$ Spring rate proportionality factors for operation on front suspension deflection stops (compression and tension).

$\lambda_{RC}, \lambda_{RT}$ Spring rate proportionality factors for operation on rear suspension deflection stops (compression and tension).

$\overline{AR}$ Drive axle ratio.

E. SPRING RATES

K_F Suspension load-deflection rate for a single wheel in the quasi-linear range about the design position; effective at the front wheel.

K_R Suspension load-deflection rate for a single wheel in the quasi-linear range about the design position; effective at the rear spring.

K_{TF} Radial spring rate of a single front tire in the quasi-linear range.

K_{TR} Radial spring rate of a single rear tire in the quasi-linear range.

R_F Auxiliary roll stiffness of front suspension.

R_R Auxiliary roll stiffness of rear suspension.

F. ADDITIONAL STEERING AND SUSPENSION SYSTEM PARAMETERS

K_{SC}	Steering column-gear flexibility.
K_{SL}	Steering linkage flexibility between the output of the steering unit and the king pin.
K_{RS}	Roll steer gain of rear wheels relative to the vehicle coordinate system.
k_{CF}	front lateral force compliance camber coefficient
k_{CR}	rear lateral force compliance camber coefficient
k_{SR}	rear aligning torque compliance steer coefficient
C_{CR}	Viscous damping coefficient of steering system connecting rod.
C_{FCR}	Coulomb damping coefficient of steering system connecting rod.
H_D	Front wheel viscous damping derivative.
m_C	Mass of steering system connecting rod.
E_{sp}	Free play in the steering gear box.

E_p	Free play in steer of front wheel.
ϕ_{si}	King pin inclination angle; i = 1, 2 = right front, left front.
C'_F	Coulomb damping coefficient for a single wheel; effective at the wheel for the front suspension.
C'_R	Coulomb damping coefficient for a single wheel; effective at the wheel for the rear suspension.
Θ_{si}	Front wheel caster angle; i=1, 2 = right front, left front.
E_i	Front wheel toe-in angle (per wheel); i = 1, 2 = right front, left front
ϕ_i	Front wheel camber angle; i = 1, 2 = right front, left front.
$\overline{PT}$	Front wheel caster trail
C_F	Viscous damping function for a single wheel; effective at the wheel for the front suspension.
C_R	Viscous damping coefficient for a single wheel; effective at the wheel for the rear suspension.
CP_i	Anti-pitch coefficients
CR_I	Anti-roll coefficients

APPENDIX E

MEASUREMENT OF VEHICLE WHEEL FORCES

by

D. E. Massing

A preliminary test program was conducted at Calspan to evaluate the performance of a three component vehicle wheel force sensor. The sensor, a Lebow Model 6457-103, is shown in Figure 1. As evidenced in the photographs, the mounting interface is the standard rim bolt circle of the vehicle hub. A specially reworked rim, furnished by the sensor manufacturer was used to adapt the sensor to a specific tire-rim combination. The full scale range of the sensor's vertical longitudinal and lateral force axes is 3000 pounds - each axis. Additional specifications and performance criteria relevant to the sensor are contained at the end of this appendix.

The vertical (z) and longitudinal (x) force axes (strain gage balance) are sensitive to wheel rotational position. The signal output of these axes in proportion to applied load is a function of the wheel position. As a result, a magnetic pulse pickup (60 pulses/revolution) is included for the purpose of providing an angular reference signal (θ) for use in resolving the x and z force components. Reduction of the raw force signals (e_x, e_z) requires use of the following expressions:

$$F_x = K_1 e_z \cos \theta - K_2 e_x \sin \theta \quad \text{(lbs.)}$$

$$F_z = K_1 e_z \sin \theta + K_2 e_x \cos \theta \quad \text{(lbs.)}$$

K_1 and K_2 are scaling constants (lbs./volt)

The lateral force axis (y) is insensitive to wheel rotational position and the sensor's output signal (e_y) is therefore directly proportional to applied lateral force.

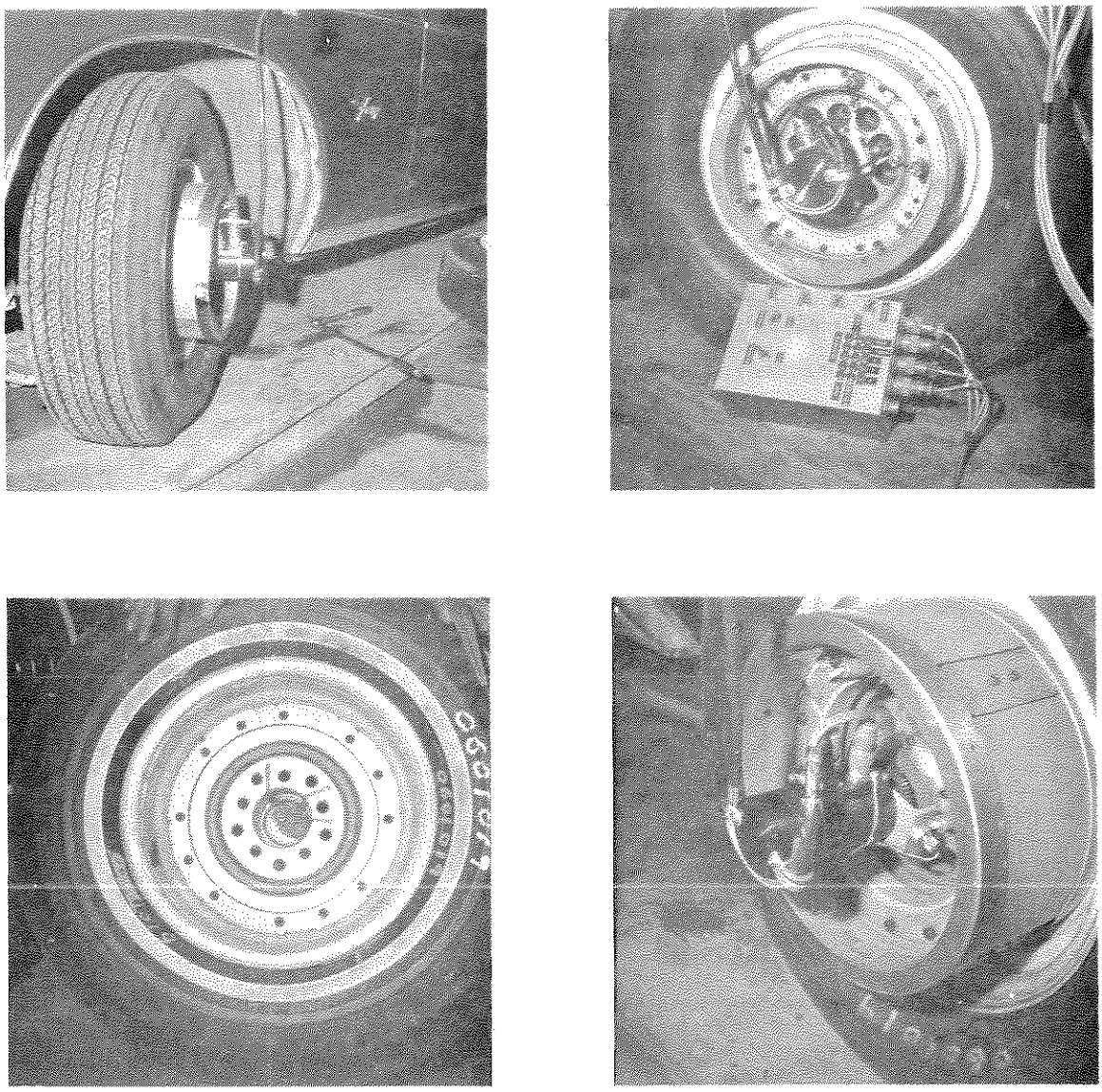

Figure 1 THREE COMPONENT WHEEL FORCE TRANSDUCER

The transducer is also equipped with an internal temperature sensor intended as a monitoring element to preclude overheating of the strain gages (200° F practical limit) particularly during extended periods of heavy braking of the vehicle.

A brief series of steady-state cornering and braking-in-a-turn tests were performed at lateral acceleration low levels (< 1/2g) in order to check out the transducer and it's associated signal conditioning. Figure 2 shows an analog time history of the signal output of each axis of the sensor as well as the rotation angle signal. The data was obtained from a steady-state cornering maneuver as evidenced by the steady level of lateral force and the symmetric sinusoidal nature of the vertical and longitudinal force components.

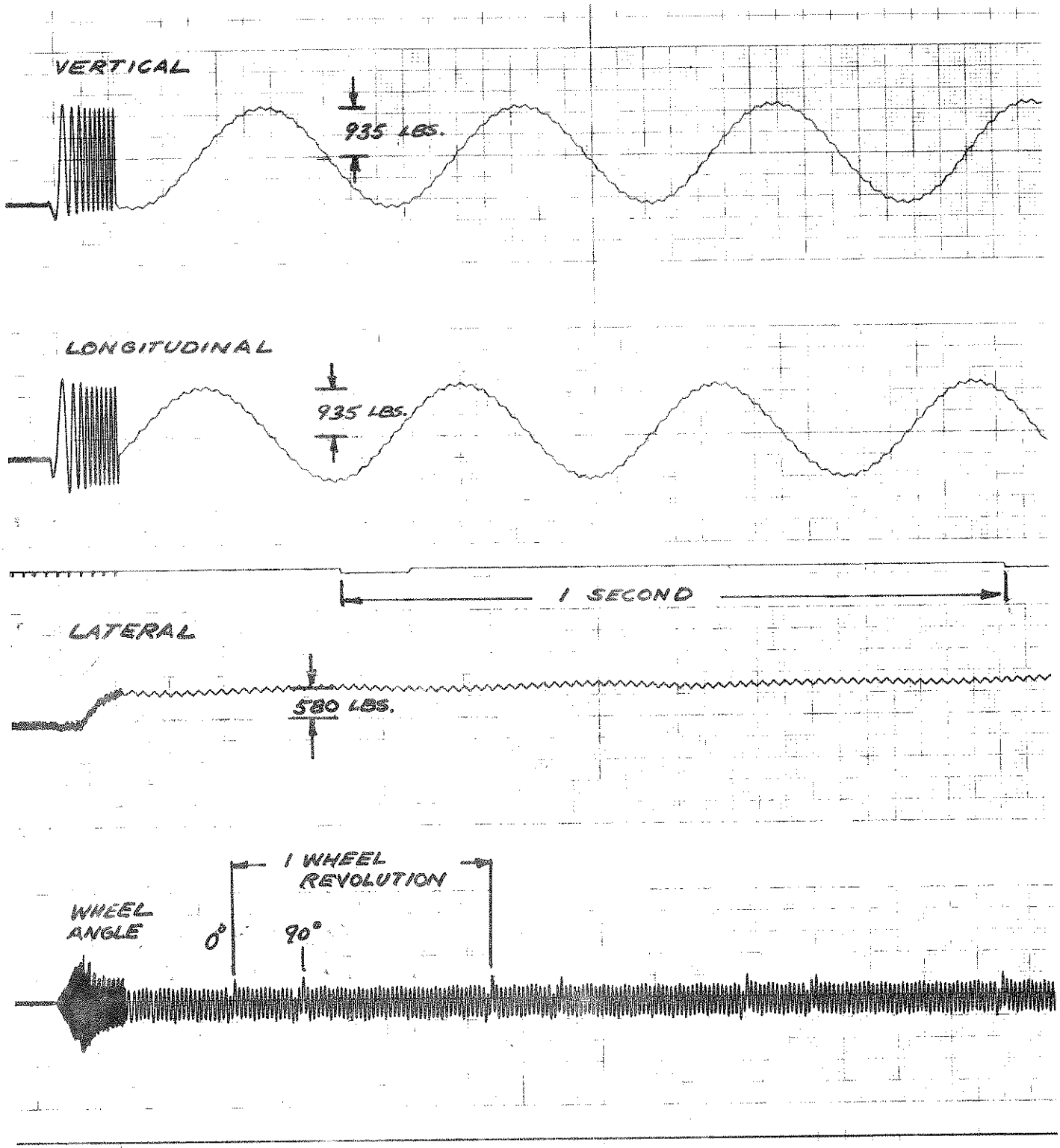

FIGURE 2 VEHICLE WHEEL FORCE SENSOR OUTPUT SIGNALS

Specifications for Three Component Vehicle
Wheel Force Transducer

1. DESCRIPTION

The Three Component Vehicle Wheel Force Transducer is a device intended for use in measuring three orthogonal force components that exist in the wheel of a vehicle undergoing braking cornering and acceleration maneuvers. The measurement of each force component is developed as an analog voltage proportional to the magnitude of each applied force component. A strain gage suspension is provided with sufficient stiffness so as not to alter the dynamic characteristics of the wheel/transducer assembly when compared to a conventional pressed steel automobile wheel. In addition, the geometry of the transducer installation is such that the tire footprint location is unchanged from that of a conventional wheel installation.

2. PERFORMANCE REQUIREMENTS

The following minimum performance requirements shall be verified by suitable calibration records furnished with the transducer:

2.1 Range and Orientation of Axes

a.

Axis	Orientation	Range
X	parallel to wheel plane longitudinal axis	± 3000 lbs.
Y	parallel to wheel rotation axis	± 3000 lbs.
Z	parallel to wheel plane vertical axis	± 3000 lbs.

b. Overrange: 150% of full range (each axis with no change in calibration).

2.2 Accuracy

a. Linearity: ± 1 1/2% of full range - each axis.

b. Hysteresis: ± 1% of full range - each axis.

c. Repeatability: ± 1/2% of full range - each axis.

d. Cross Coupling:
Between axes: ± 3% of full range - each axis.

Certification shall be provided showing the coupling component present on two unloaded axes with full range force applied to the third axis. The calibration shall be done on all three axes and data shall be furnished showing the six cross coupling components that exist on the three pairs of unloaded axes.

e. Common Mode Error: Application of full range force to one axis shall not cause a deviation outside the linearity band specified in 2.2a measured on either of the other two axes.

f. Zero balance: 0.00 ± 0.03 MV/V at 70°F.

2.3 Environmental Conditions

a. Operating temperature range: 70° - 250° F.

b. Thermal sensitivity shift: 0.0025% of reading (max.) per degree F over operating temperature range.

c. Thermal zero shift: 0.002% of full scale (max.) per degree F over operating temperature range.

3. DESIGN REQUIREMENTS

The following design requirements shall be met by the offerer in order to achieve compatability with specific electrical interface and mechanical mounting conditions. Offerer suggestions of design alternatives will be acceptable if accompanied with suitable documentation.

3.1 Electrical

a. Strain gage bridge impedance (each axis)

Input 350 ± 3.5 ohms or 700 ± 7 ohms resistive
Output 350 ± 5.0 ohms or 700 ± 10 ohms resistive

b. Bridge Excitation: 10 VDC (each axis)

c. Full range output: 2 ± 1 MV/V (each axis)

d. Shunt calibration resistor: 100% full range (each axis)

e. Ground isolation: Minimum 10^9 ohms - all terminals in parallel to ground. (each axis individually)

3.2 Mechanical

The transducer shall mount on a 4 1/2 inch bolt circle containing (5) 1/2" - 20 lugs. The mating rim to be supplied by the offerer shall be a 14" x 5.5" JJ type. Details of methods for rim interchangeability shall be included with the offerers response. The transducer shall be mountable on either the front or rear axle of a vehicle.

The design of the transducer/rim assembly shall be such that the track dimension of a vehicle with the transducer installed is unchanged from the manufacturers designated value.

3.3 Environmental

The transducer, slip ring assembly and each mating connector shall be designed or specified to provide maximum protection against moisture contamination of the transducer elements. The transducer will be mounted on vehicles performing maneuvers on wet pavement. Hence, no degradation of transducer performance shall occur as a result of such testing.

In addition to splash protection, the transducer shall be designed to operate within the performance requirements given in section 2.0 in the presence of 90% relative humidity at 90°F.

4. OPTIONAL ACCESSORIES

The offerer shall submit in the form of separate cost additions the following accessory items. If any of the following items are standard components furnished with the transducer, the offerer shall so state in his response.

a. Transducer angular reference indicator

Transducers having sensitive axes rotating with the vehicle wheel shall be furnished with a device that provides a suitable high level pulse signal occurring at a predetermined angular position of a given sensitive axis relative to a vehicle fixed reference.

b. Transducer internal temperature sensor

Since the heat generated during vehicle braking maneuvers may produce elevated temperatures in the strain gaged elements of the transducer, it is desirable to have a temperature sensor located in close proximity to the strain gages. A suitable thermocouple or resistive film temperature sensor (Micro-Measurements ETG Series or equivalent) shall be mounted in an appropriate position within the transducer.